

AD-A128 046

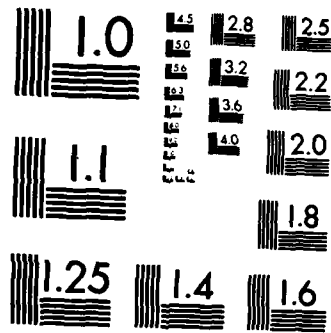
ALFVEN WAVES IN THE SOLAR WIND IN ASSOCIATION WITH
SOLAR ENERGETIC PARTIC. (U) FRANKLIN INST NEWARK DE
BARTOL RESEARCH FOUNDATION D J MULLAN ET AL. 04 FEB 83
AFGL-TR-83-0028 F19628-81-K-0004 F/G 3/2

1/1

UNCLASSIFIED

F/G 3/2

NL



MICROCOPY RESOLUTION TEST CHART
NATIONAL BUREAU OF STANDARDS-1963-A

AFGL-TR-83-0028

ALFVEN WAVES IN THE SOLAR WIND IN
ASSOCIATION WITH SOLAR ENERGETIC
PARTICLES: SUNSPOT UMBRAL ORIGIN

D.J. Mullan
A.J. Owens

Bartol Research Foundation
of The Franklin Institute
University of Delaware
Newark, Delaware 19711

Final Report for Period 1 August 1980 - 31 March 1983

4 February 1983

Approved for public release; distribution unlimited

AIR FORCE GEOPHYSICS LABORATORY
AIR FORCE SYSTEMS COMMAND
UNITED STATES AIR FORCE
HANSCOM AFB, MASSACHUSETTS 01731

DTIC

MAY 10 1983

H

DTIC FILE COPY

83 05 10 008

Qualified requestors may obtain additional copies from the Defense Technical Information Center. All others should apply to the National Technical Information Service.

Unclassified

SECURITY CLASSIFICATION OF THIS PAGE (When Data Entered)

REPORT DOCUMENTATION PAGE		READ INSTRUCTIONS BEFORE COMPLETING FORM
1. REPORT NUMBER AFGL-TR-83-0028	2. GOVT ACCESSION NO. AD-A128 048	3. RECIPIENT'S CATALOG NUMBER
4. TITLE (and Subtitle) ALFVEN WAVES IN THE SOLAR WIND IN ASSOCIATION WITH SOLAR ENERGETIC PARTICLES: SUNSPOT UMBRAL ORIGIN?		5. TYPE OF REPORT & PERIOD COVERED Final Report 1 Oct 1980 - 31 March 1983
7. AUTHOR(s) D.J. Mullan A.J. Owens		6. PERFORMING ORG. REPORT NUMBER
9. PERFORMING ORGANIZATION NAME AND ADDRESS Bartol Research Foundation of The Franklin Inst. University of Delaware Newark, Delaware 19711		8. CONTRACT OR GRANT NUMBER(s) F19628-81-K-0004
11. CONTROLLING OFFICE NAME AND ADDRESS Air Force Geophysics Laboratory Hanscom AFB, Massachusetts 01731 Monitor/Donald F. Neidig/PHS		10. PROGRAM ELEMENT, PROJECT, TASK AREA & WORK UNIT NUMBERS 61102F 2311G3CB
14. MONITORING AGENCY NAME & ADDRESS (if different from Controlling Office)		12. REPORT DATE 4 February 1983
		13. NUMBER OF PAGES 87
		15. SECURITY CLASS. (of this report) Unclassified
		15a. DECLASSIFICATION/DOWNGRADING SCHEDULE
16. DISTRIBUTION STATEMENT (of this Report) Approved for public release; distribution unlimited		
17. DISTRIBUTION STATEMENT (of the abstract entered in Block 20, if different from Report)		
18. SUPPLEMENTARY NOTES		
19. KEY WORDS (Continue on reverse side if necessary and identify by block number) Alfven Waves Particle Propagation Solar Wind Solar Proton Flares		
20. ABSTRACT (Continue on reverse side if necessary and identify by block number) We report on a search for Alfven waves in the solar wind during solar particle events. During the period June 6-8, 1979, we find clear signatures of outgoing Alfven waves which could have been released from the sun simultaneously with the initial release of energetic particles. The waves are soliton-like, with durations of 200-900 seconds. An isolated square Alfven soliton is also seen when the first particles (with $E \approx 57$ MeV) are detected: the width of this soliton is ~ 950 seconds. A series of five small amplitude "spikes" in the magnetic field are also seen, preceding the arrival		

DD FORM 1473

1 JAN 73

EDITION OF 1 NOV 65 IS OBSOLETE

Unclassified

SECURITY CLASSIFICATION OF THIS PAGE (When Data Entered)

Unclassified

SECURITY CLASSIFICATION OF THIS PAGE(When Data Entered)

of the first particles by a few hours. The spikes are separated by intervals of 854 ± 20 seconds. We suggest that these periodicities are determined by conditions at the sun. The features which we have detected are consistent with Alfven waves released from the umbra of a sunspot during a flare.

DTIC
COPY
INSPECTED
2

Accession For	
NTIS GRA&I	
DTIC TAB	
Unannounced	
Justification	
By	
Distribution/	
Availability Codes	
Dist	Avail and/or Special
A	

Unclassified

SECURITY CLASSIFICATION OF THIS PAGE(When Data Entered)

I. INTRODUCTION

Alfven wave like fluctuations have been known for many years to be common features in the interplanetary magnetic field (Belcher and Davis, 1971). Typical periods of such waves are of order hours. Several studies have been devoted to analyzing the properties of Alfven waves in the "general" solar wind (e.g. Burlaga and Turner, 1976; Parker, 1980a,b). However, there seems to have been less attention paid to the possibility that the Alfven waves might take on a special character during certain periods. Specifically, in this paper, we ask: what are the properties of Alfven waves which accompany the arrival of solar energetic particles. For example, if the particles were accelerated at the sun by a magnetic process of some kind, Alfven waves might also be emitted by the process, with characteristics which might contain signatures of the acceleration process itself. It was the possibility that a solar particle flare might allow escape of Alfven waves from the umbra of a sunspot (Mullan, 1981) that prompted us to undertake the study reported here.

II. DATA

In this paper, we use data from the ISEE-C satellite. First, the data pool tapes were searched for periods when the energetic particle flux was above background. The particle detector which we used was sensitive to particles with energies of 4-57 MeV/nucleon. Plots of the particle fluxes for the first two years of operation were provided to us by Dr. T. Von Rosenvinge, and these were also scanned to help in identifying favorable time intervals for our search. Four intervals of three days each were selected on the basis of the particle data. For these intervals, magnetometer data were provided to us by the JPL group (Dr. E.J. Smith, Principal Investigator), and solar wind data by the Los Alamos group (Dr. S. Bame, Principal Investigator).

The magnetometer data consist of three components of the interplanetary magnetic field, with x-axis pointing towards the sun, and z-axis pointing toward the north ecliptic pole. Data were taken at a rate of six times per second. For our purposes, we averaged sets of 48 consecutive data points. Thus, our discussion will be in terms of ~ 8 -second averages of the original data.

The solar wind data consist of measurements of the velocity, the density, the ecliptic flow angle, and temperatures parallel and perpendicular to the magnetic field lines. The flow angle is measured outward from the sun. Thus, the x and y components of the magnetic field have to be reversed in order to bring them into the solar wind coordinate system. The solar wind measurements were made every 24 seconds.

In what follows, we shall deal mainly with one of the three-day intervals which we selected, namely, days 157-159 in 1979 (June 6-8, 1979). The particle fluxes during these three days are shown in Fig. 1. The first particles to arrive in the detector have energies of 57 MeV/nuc, i.e. speeds of about 10^5 km/s. Such particles therefore require 0.4 hours to travel radially (in a scatter-free mode) from the sun to the earth, or about 0.6 hours if they travel (scatter-free) along the average archimeadean spiral field lines. We note that the particle flux in this detector first began to rise above background at about 6 hours UT on DOY 157. Hence, these first particles were released from the sun at ~ 5.4 -5.6 hours UT on DOY 157. Below, we shall find that some Alfvén waves were also released from the sun at almost the same time as these particles. We shall also see that Alfvén waves appear to arrive at the satellite simultaneously with the first particles.

The interval of time on which we concentrate here (June 6-8, 1979) has also been studied in some detail by another experiment on (ISEE-C: the ULEZEQ detector has determined the charge states of various elements, averaged over the entire event (Gloeckler et al., 1981). These authors ascribed the particles to a flare of importance 2B at longitude east 18. According to solar geophysical data (SGD), two flares of importance 2B occurred on June 5, 1979 at N18E14 and N18E12 in McMath Region 16051. These flares started at 0455 UT and 0600 UT respectively, and lasted for more than two hours each (SGD #419, Part 1, p. 15). The active region where these flares occurred was very rich in sunspots: there were 64 spots in the region on June 5 (SGD #420, Part 1, p. 111), with total area of 630 millionths of the solar atmosphere. The areas of the two 2B flares were 990 and 1074 millionths, respectively. Thus, the two flares had a good chance of covering one or more umbrae in the active region. This is a necessary condition which must be satisfied if umbral Alfvén waves are to become detectable in interplanetary space (Mullan, 1981). In the spots in this region, the magnetic field strength was recorded as 4 kilogauss. Hence, the total magnetic flux through the sunspots in this region was 7.6×10^{22} maxwells. For future reference, we note that if this flux were spread out over a square of dimension 0.5 solar radii, the mean field strength passing through the square would be 63 gauss.

We note that when a flare occurs at a longitude of East 18, it may take as long as 20-30 hours for particles with energies of tens of MeV to reach the base of the Sun-Earth field line (Reinhard and Wibberenz, 1974). Thus, particles from two 2B flares which occurred early on June 5 may not have begun their propagation to the Earth until early on June 6 (DOY 157). This is consistent with the estimate above.

III. CROSS-POWER SPECTRA OF THE MAGNETIC FIELD

If we had no velocity information, it would be possible to identify Alfvén waves from the cross-power matrix of the magnetic field vector. The technique has been described by Owens (1975). We can summarize the technique as follows.

Consider a coordinate system in which the mean field is directed along the z-axis. During an interval of time T, let the mean value of the i-th component of the field be $\langle B_i \rangle$. Then the field variance matrix for the interval of time T is defined as $M_{ij} = \langle B_i B_j \rangle - \langle B_i \rangle \langle B_j \rangle$. In the presence of linear Alfvén waves, the characteristic signature of Alfvén waves is that the field variance matrix should take on the form

$$\overset{\leftrightarrow}{M} = \begin{pmatrix} M_{xx} & 0 & 0 \\ 0 & M_{yy} & 0 \\ 0 & 0 & M_{zz} \end{pmatrix}$$

where $M_{zz} < M_{xx}, M_{yy}$. Thus, the field fluctuations have minimum variance along z.

In the present case, we have chosen $T = 1$ hour. From our 8-second averages, we first derive the mean values of B_x, B_y, B_z for each hourly interval. For our purposes, we assume that it is an acceptable approximation to neglect $\langle B_z \rangle$. Thus, we consider the mean field during the hour to lie in the ecliptic plane and to be given by the vector $(\langle B_x \rangle, \langle B_y \rangle, 0)$. For each hour, we define a new coordinate system (ξ, η, ζ) such that the ζ -axis points along the mean field direction. We choose the ξ -axis to point along the z-axis (see Figure 2).

The variance matrix is evaluated for each hour in terms of its own (ξ, η, ζ) coordinate system. Fourier analysis allows us to obtain power spectra of the field components, as well as coherence spectra for the various

cross-terms in the matrix. The spectra which we have obtained cover a frequency range from $1/16 \text{ sec}^{-1}$ to $1/400 \text{ sec}^{-1}$. In each hourly interval, we have 35 degrees of freedom. If the data we were examining were purely random noise, the spectral coherence should have a "bias" of $(2/35)^{1/2} \sim 0.24$. We can therefore consider the coherence to be essentially zero if its value falls to 0.24 (or below) in our sample. In principle, the technique of Owens (1975) requires the off-diagonal elements of the variance matrix to fall to zero, but in our case, falling to a value of 0.24 or smaller is tantamount to zero cross-correlation.

In Figure 3, we show coherence spectra for two separate intervals (each of 1 hour duration). We show the coherences for the cross-terms (B_{ξ}, B_{η}) and (B_{ξ}, B_{ζ}) . (To avoid confusion in the figures, we have omitted the third cross-coherence, (B_{η}, B_{ζ}) .) The major difference between the values plotted in Fig. 3a and those in Fig. 3b is that in the former, the coherences are in general larger. Thus, of the 26 points plotted in Fig. 3a, none falls at or below the "noise" level, whereas in Fig. 3b, 15 of the 26 points lie below the "noise", and can therefore be considered to be essentially zero. As an alternative way to state this conclusion, we can evaluate a crude measure of a "mean" coherence for the entire spectrum by averaging the 13 values in each spectrum. (We have used a geometric average in what follows.) In Fig. 3a, the "mean" coherences in (B_{ξ}, B_{η}) and in (B_{ξ}, B_{ζ}) are found to be 0.49 and 0.55, i.e. both larger than the "noise" level by factors of 2-3. On the other hand, in Fig. 3b, the "mean" coherences in the (B_{ξ}, B_{η}) and (B_{ξ}, B_{ζ}) spectra are found to be 0.24 and 0.20 respectively, i.e. both at or below the "noise" level.

According to the criteria of Owens (1975), the data in Fig. 3a would not be consistent with the presence of Alfvén waves during hour=15 (i.e. from 15

hours UT to 16 hours UT) on DOY 157, 1979. On the other hand, the results in Fig. 3b are suggestive of the presence of Alfvén waves during hour=12 on DOY 159, 1979.

In Figure 4, we show the "mean" coherences for the (B_ξ, B_η) and (B_ξ, B_ζ) components for each hour during the entire three-day interval for which we had data (62 hours in all). In Fig. 4, the "mean" coherence in each hour is defined in the same crude way as mentioned above. In principle, the technique of Owens (1975) would require that the coherences in both (B_ξ, B_η) and (B_ξ, B_ζ) should be "small" (i.e. at or below "noise" level) if Alfvén waves are present. Of the 62 hours, 6 satisfy this requirement. They are circled in Fig. 4. It is also necessary that the (B_η, B_ζ) coherence be "small" (i.e. < 0.24), and that $M_{\zeta\zeta} < M_{\xi\xi}, M_{\eta\eta}$. Near each of the circle points in Fig. 4, we have written the values which we have found for the "mean" $(B_\eta - B_\zeta)$ coherence during the hour interval. We see that during none of the 6 circled hours does the $(B_\eta - B_\zeta)$ coherence fall below the "noise" level. Moreover, of the 6 circled points, only two correspond to hours when the field variance is minimum along the ζ -axis: these are labelled $<$ in Fig. 4. Thus, it would appear that according to Owens' criteria, Alfvén waves have not been identified at any time during the 3-day interval.

However, our definition of a "mean" coherence is so simple that it must be considered as only a very crude characterization of the cross-power spectrum: a more realistic definition of a "mean" may yield a more profitable diagnostic. Moreover, Owens' criteria are strictly valid only for small amplitude waves. If the Alfvén waves are non-linear, the minimum variance direction can no longer be used for unambiguous identification of the waves (Barnes, 1976). We shall see below that when we take advantage of velocity

information, Alfvén wave-like features do seem to be present during certain hours in Figure 4, especially hour 6 on DOY 157, and hours 1,4,6, and 12 on DOY 159. The features which we will label as Alfvén waves are not at all sinusoidal in shape, and so they might not qualify as linear waves of the ideal kind which entered into Owens' discussion. This would help to explain why Owens' criteria have not permitted us at this stage to identify waves in our data. Nevertheless, it is striking that of the 5 hours just mentioned as containing Alfvén waves on the basis of velocity information, three are circled in Figure 4. This suggests that Owens' criteria may in fact be useful for identifying Alfvén waves if one can find a better definition of a "mean" coherence than the crude definition used in plotting Figure 4.

Finally, we note that in the case of ISEE-C, velocity data were obtained once every 24 seconds. Thus, if waves are present in the solar wind with periods shorter than, say, one minute, ISEE-C data cannot be used to search for velocity-field correlations of the type which are the most unambiguous identifier of Alfvén waves. For such short-period Alfvén waves, the Owens criteria may be the only method of confirming the presence of the waves.

IV. VELOCITY-MAGNETIC FIELD CORRELATIONS

The clearest signature of Alfvén waves (whether linear or non-linear) is a high correlation, ρ , between the fluctuations in the velocity vector and the fluctuations in the magnetic vector. Since the plasma detector on ISEE-C measured both x and y components of the wind velocity in the ecliptic plane, and the magnetometer also provided magnetic field measurements in the same directions, we can evaluate separately the correlations between V_x and B_x (ρ_x) and between V_y and B_y (ρ_y). The direction of the waves can be determined from the sign of the product $\rho_x \langle B_x \rangle$: if this product is

negative, the waves are propagating outward from the Sun (Burlaga and Turner, 1976).

For purposes of computing a correlation coefficient, we again grouped the data into intervals of one hour duration. During each hour, we interpolated the 8-second averages of magnetometer data and the 24-second measurements of plasma data onto a set of points separated by about 50 seconds in time. This would then allow us to identify waves with periods as short as about 100 seconds, if such periods were present in the solar wind. (The models of convection in sunspot umbrae, (see Mullan, 1974) had led us to believe that the possible periods of Alfvén waves would lie between about 100 seconds and about 1000 seconds.) Thus, in each hourly interval, some 70-80 points were used in determining the velocity-field correlations.

During each hour, we first obtain the mean values of $\langle V_x \rangle$, $\langle V_y \rangle$, $\langle B_x \rangle$, and $\langle B_y \rangle$. Then we calculate the linear correlation coefficient according to

$$\rho_i = \frac{\sum (v_i - \langle v_i \rangle)(B_i - \langle B_i \rangle)}{(\sum (v_i - \langle v_i \rangle)^2)^{1/2} (\sum (B_i - \langle B_i \rangle)^2)^{1/2}}, \quad (i = x, y)$$

In order to take maximum advantage of the information contained in both x and y components of V and B, we define a quantity ρ'' according to

$$\rho'' = \rho_x^2 \rho_y^2$$

This can be considered as a sort of "super-correlation" coefficient for the hour. Note that we are not defining a cross-correlation between x and y components by the above relation: it is simply a convenient definition. For an ideal Alfvén wave, where $\rho_x = 1$ and $\rho_y = 1$, the "super-correlation" coefficient is also equal to unity.

In Figure 5, we show the values we have obtained for the supercorrelation coefficient for each of the hourly intervals during 1979 DOY 157-159 for which we had the requisite data. During certain hours, there were partial or total dropouts in one or other data set, and so, lower weight should be ascribed to the supercorrelation coefficient at such times. These lower weight points are denoted by parentheses in Figure 5.

With the directional information which is available from $\rho_X \langle B_X \rangle$, we have plotted the supercorrelation index as positive in Figure 5 for outgoing waves, and negative for ingoing waves for purposes of display.

Results in Figure 5 suggest that we can divide the 3-day interval into three periods.

First, hours 0-9, DOY 157. Here, the correlations are not zero, but they are also not particularly high: note especially hours 0, 1, 5, and 7. (In the present paper, the hour interval between 0 hours UT and 1 hour UT is labelled hour = 0) Thus, Alfven waves are in general not prominent in the data, except possibly during hour = 6. Whatever waves are present during this period are outgoing. We will return to hour = 6 below (Section VI).

Second, from hour = 10 on DOY 157 to essentially the end of DOY 158. Here, the correlations are in almost all cases very small, and no definite direction of propagation is apparent. Thus, during this period, there is no evidence for significant fluxes of Alfven waves in the data. We note that the beginning of this period coincides with the passage of a sector boundary. Such a boundary prevents Alfven waves from penetrating it (see, e.g. Steinolfson and Mullan, 1980). This may help in understanding why Alfven waves which may have been present in the vicinity of ISEE-C during the earlier period can no longer reach the detectors. The sector boundary swept the space

around ISEE-C "clean" of Alfvén waves for a time interval of 30-40 hours. In passing we note that one of the hours during period two seems to have a high value of the supercorrelation (see hour = 20). However, this hour coincided with complete dropout of plasma data, and so the "data" which entered into our calculation of the supercorrelation were actually interpolated. In view of the data dropout, the statistical significance of the supercorrelation coefficient at hour = 20 is essentially zero.

Third, DOY 159. Here, the waves are entirely outgoing, and at times the supercorrelation coefficient becomes very large. The maximum value of the supercorrelation occurs at hour = 12, when $\rho_x = 0.95$ and $\rho_y = 0.97$. Since the velocity data and the magnetic field data were measured by two independent instruments, it is very difficult to imagine how such high correlations in both x and y could be due to chance. Moreover, we recall that the data we have used for the correlation calculations were interpolated onto 50-second intervals from time strings which are different for magnetic field from those which were used for the velocity data. Now, the interpolation cannot be expected to yield highly precise values of either variable. Hence, even if the true correlation between V and B were exactly unity in the interplanetary medium at some time, it seems unlikely that our method of calculating the correlation would yield a coefficient of exactly unity. In view of this, we regard the V-B correlation during hour = 12 on DOY 159 as nearly perfect.

V. TIME BEHAVIOR OF MAGNETIC FIELDS AND PLASMA

(a) Descriptive

The details of the variation of solar wind quantities during hour = 12 on DOY 159 are shown in Figure 6. In the different panels, we have plotted B_x , B_y , B_z , $|B|$, (the magnitude of the magnetic field), velocity, ecliptic

flow angle, (PHI), density, temperatures parallel and perpendicular to the field lines, and the temperature flow angle. In each panel, we plot 10,000 seconds of real time, centered on hour = 12. Thus, most of hour = 11 and hour = 13 also appear in each panel. Note that since PHI is small, $V_x = V \cos \phi$ is essentially equal to V , while $V_y = V \sin \phi \approx V\phi$ is essentially proportional to ϕ .

A visual examination of the V_x and B_x panels confirms the striking correlation during this hour. A visual examination of ϕ and B_y leads to the same conclusion. At the same time, there are no obvious features in the density curve, or in the temperature curves, corresponding to, say the prominent feature labelled "B" in the velocity panel. Furthermore, we note that in the panel labelled BMAG, the magnitude of the magnetic field remains essentially unchanged (within $\pm 5\%$) during hour = 12 despite the fact that B_x varies from $+1\gamma$ to -5γ , B_y varies from -4γ to $+4\gamma$ and B_z varies from $+4\gamma$ to -3γ . Thus, the features which occur during hour = 12 are non-compressive, non-dissipative structures with constant total field, although the separate components of the field are quite variable.

Moreover, consider the feature labelled "B" in the velocity panel. This peak has two dips (labelled $\beta\beta$) on either side. We can characterize the velocity amplitude of this feature δV_x by the difference of velocity between the peak B and the two dips $\beta\beta$. We find $\delta V_x = 65-73$ km/sec. In this feature, the amplitude δB_x can be read off: 5-6 gammas. Hence, in this feature, the ratio $\delta V_x / \delta B_x$ has the value $(1.1-1.5) \times 10^{11}$ cgs. Between the dips labelled $\beta\beta$, there are 41 density measurements. The density values do not vary much with time, and it is meaningful to consider an average value throughout the period of time which spans feature "B". The arithmetic mean

of the 41 measurements is 1.66 cm^{-3} . If we assume that 10 of the measured ions by number are helium, we find that the mean value of $(4\pi\rho)^{-1/2}$ in the feature labelled "B" is 1.5×10^{11} cgs. Hence, in this feature, the velocity and field amplitudes seem to satisfy the relation $\delta V_x = \delta B_x / (4\pi\rho)^{1/2}$ rather well.

All of these properties suggest that feature "B" during hour = 12 is an Alfven wave. Clearly, the wave is far from sinusoidal. It might be better to refer to the feature as a soliton. We shall use the terms soliton and wave interchangeably for the prominent peaks in Fig. 6 and subsequent similar figures.

Further examples of features which have obvious similarities in both V_x and B_x , and also in ϕ and B_y can be found in Figures 7, 8, and 9. Again, each panel in these figures spans a time range of 10,000 seconds. For future reference, we have denoted the most prominent peaks in Figures 6-9 by letters (A-K) on the velocity curves.

By way of contrast, we present in Figure 10 the variations of plasma and fields during an interval when the supercorrelation index is so small that there are almost certainly no Alfven waves present. These data refer to hours 2, 3, and 4 on DOY 158, when $\rho'' = 0.00012$, 0.000004 , and 0.029 respectively.

By way of further contrast, we show in Figure 11 an example of a feature which, if one had access to only information on B_x and velocity, might look like an Alfven wave. This feature is labelled P' in the figure, and the correlation coefficient between V_x and B_x is quite high ($\rho_x \approx 0.90$) during the hour that this event occurred (hour = 8, DOY 157). However, in the plots of density, temperature, and field magnitude, the feature labelled P' is seen to be compressive and dissipative, and certainly does not conserve the

magnitude of the magnetic field. On these counts, therefore, feature P' could not be considered as an Alfvén wave.

(b) Duration of Alfvén Waves

If the waves were sinusoidal, periods could be defined with little difficulty. In the present case, however, there is no unambiguous measure of the period or duration of a feature. For working purposes, we propose to use the following definition. For each hour, we draw a horizontal line at the average velocity for that hour. Then, in the vicinity of a peak, the actual velocity lies above (or below, depending on the sign of B_x) that horizontal line for a time period Δt_0 . This period is a rough measure of the full width of the soliton at its base. Our proposal certainly underestimates the full width at the base. Hence, the periods to be discussed here should be considered as lower limits on the true width of the soliton at its base. Using the plasma data, we have extracted values for Δt_0 for each of the 11 features labelled A-K in the above figures. Results are in Table 1. The values of Δt_0 are plotted as a function of time in Figure 12. The abscissa axis in Fig. 12 extends from about hour = 9 to about hour = 17 on DOY 159. The hour with the largest supercorrelation (hour = 12) is marked.

We note that the values of Δt_0 range from about 200 seconds to about 860 seconds. We recall that these are lower limits to the true widths of the solitons: the true widths therefore probably range in value up to 900-1000 seconds. (The dashed numbered lines in the Figure will be discussed below.) With such periods, the spectral analysis reported in Section III above would have been only marginally sensitive to the features under discussion here: these features would have contributed power only at the two lowest frequency points (if at all), where the spectrum is already rising steeply.

It will be readily appreciated that we have selected what we consider subjectively to be the most prominent peaks in Figs. 6-9 for inclusion in Table 1. Other peaks will undoubtedly catch the reader's eye, where the durations are shorter than the values plotted in Fig. 12. Hence, we do not claim that in Fig. 11, there is a lower boundary on the permissible values of the wave durations. However, it is of some interest to raise the related point: is there perhaps an upper limit on the wave durations in Fig. 12? This is an important point in terms of interpreting our data. Our impression, after visually scanning the magnetic field plots for the entire three day interval, is that prominent features in the field (or in the velocity) with Δt_0 greater than 860 seconds are in fact rare, if not altogether absent.

For example, each panel in Figs. 6-10 spans 10,000 seconds. Hence, if there were features with base widths of, say, 2-3 thousand seconds, they should be readily identifiable visually. But we have been able to find no clear evidence for structures with such long periods.

This leads us to the tentative conclusion that the Alfvén solitons coming from the sun appear to have "true" widths no greater than 900-1000 seconds. This time-scale will emerge again below as a significant characteristic of certain other features in the data.

(c) Wave Transit Time From The Sun

The time required for Alfvén waves to propagate from the sun to the Earth is

$$\tau(r_s - r_E) = \int_{r_s}^{r_E} \frac{dr}{V_w + V_A}$$

where r_s is the radius of the release point at the Sun, r_E is the radius

of the Earth's orbit, and V_w and V_A are solar wind speed and Alfvén speed. In order to use this expression, we need to know the radial variations of both V_w and V_A between the Sun and the Earth. Neither of these can be known precisely, and we must approximate in both cases.

For the solar speed, we may refer to Figure 13, where we show the hourly averages of solar wind speed at ISEE-C during the 3-day period. (The solid line joins the velocity averages.) We note that by the time the waves in which we are interested arrive at ISEE-C on Hour = 12 on DOY 159, the solar wind has been almost constant (600 km/sec) for about 40 hours. This suggests that this high speed material is quite uniform in its properties. Note also the density (dashed curve), which is also almost constant for about 40 hours prior to wave arrival at hour = 12 on DOY 159. (The plotted densities are not averages over an hour, but simply "snapshots" extracted from the data at certain instants of time.) We will assume therefore that as the waves propagate from Sun to Earth, the solar wind properties remain constant, with a flow speed of 600 km/sec, and a density variation which depends on radial distance as r^{-2} .

We note in Figure 13 that the high speed stream which reaches ISEE-C at 18-19 hours on DOY 157 is preceded by a very short-lived density spike (duration = 13 minutes). This is presumably ambient material which has been swept up by the leading edge of the high speed stream. However, in the high speed stream itself, the density of the wind is definitely lower than it was before the stream arrived. Thus one cannot identify the velocity jump in Fig. 13 with a shock front, at least not with a forward shock. It is possible that we are seeing a reverse shock.

Clearly, the interplanetary flows around the time of the particle event which we are discussing are quite complex: there is a sector boundary, followed by a broad density rise (lasting 3-4 hours), followed by a sharp density spike, and finally the high speed stream arrives. What effects might this complex flow pattern have on the energetic particles which we are using as a signature of a solar flare? Could some of the particles be accelerated at the velocity jump, assuming that the latter is in fact due to a reverse shock? This seems unlikely, since the event profile (Fig. 1) does not display the typical shock-acceleration character of a rapid rise prior to shock passage, followed by an equally rapid (or even more rapid) decline once the shock has passed (Armstrong and Decker, 1979). Moreover, a shock would have to be rather strong to accelerate interplanetary particles to energies as high as 57 MeV/nuc. On the other hand, the event profile has the appearance of a "classical" solar event, with a rapid rise followed by a slower, exponential decay: the time constant during decay is 0.6 days, quite comparable to other solar events: see e.g. Fichtel and MacDonald (1967).

For these reasons, we will assume that the particles detected by ISEE-C on DOY 157-159, 1979, are solar in origin. It just happened that their path from the sun to the Earth was almost entirely inside a high speed stream where conditions remained to a good approximation uniform. Moreover, the sector boundary, which passed by on DOY 157 helped to "sweep clean" the interplanetary medium of Alfvén waves for 30-40 hours, so that when the flare-related Alfvén waves arrived, they could be easily distinguished.

Parenthetically, we note that in the interaction region between the high speed stream and the slower ambient wind, the ISEE-C data indicate that the temperature rises to a value of $(1-2) \times 10^6$ K at 19.5 hours on DOY 157. Such

heating can be produced in the interaction if the velocity difference between high and low speed streams is 310-440 km/sec. (To obtain this result, we have used the work of Steinitz and Eyni (1977)). Now, it is clear from Fig. 13 that the velocity jump from low to high speed streams is indeed in this range: even in the hourly averaged data (plotted in Figure 13), the jump in velocity is ~340 km/sec. When we examine the detailed measurements, we find that, just prior to the density spike, the velocity of the wind was ~ 300 km/sec, whereas in the high speed stream, the highest measured value of the velocity was 946 km/sec (at 21.3 hours). With a velocity jump of 646 km/sec, the temperature in the interaction region could be as high as 4.3×10^6 K.

The radial dependence of the Alfvén speed v_A can be derived as follows. In a cylindrical coordinate system, the components of the field B_r and B_ϕ are given by

$$B_r = B_0 (r_0/r)^2, \quad B_\phi = (r\Omega/v_w)(r_0/r)^2$$

(Parker, 1963). Here r_0 is a reference radius, where $B_r = B_0$, and Ω is the angular velocity of the Sun's rotation. Hence, the magnitude of the magnetic field is

$$|B| = B_0 \left(\frac{r_0}{r}\right) \left[1 + \frac{r^2 \Omega^2}{v_w^2}\right]^{1/2}$$

Choosing $r_0 = 1$ A.U., expressing r in units of AU, and setting $\Omega = 2.7 \times 10^{-6} \text{ sec}^{-1}$, and $V = 600 \text{ km sec}^{-1}$, we have

$$B = (B_0/r^2)(1 + 0.46r^2)^{1/2}$$

with density varying as r^{-2} . The Alfvén speed at radius r can be related to the value at the Earth's orbit, V_{A_0} , by

$$\frac{V_A}{V_{A_0}} = \frac{1}{1.21r} (1 + 0.46r^2)^{1/2}$$

To evaluate V_{A_0} we note that throughout DOY 159, the magnitude of the magnetic field measured by ISEE-C remained essentially constant at 4.5γ ($\pm 0.2\gamma$); N was also almost constant, $N \approx 1.6 \text{ cm}^{-3}$. Hence, if we again assume that helium is present in the plasma to the extent of 10% by number, we find $V_{A_0} \approx 70 \text{ km sec}^{-1}$.

Numerical integration from 0.1 to 1.0 AU gives $\tau(0.1-1.0) \approx 2.10$ days. At distances closer to the Sun than 0.1 AU, $V_A > 600 \text{ km sec}^{-1}$, i.e. $V_A > V_w$. Hence, we can obtain an upper limit on the time to propagate from the Sun to 0.1 AU if we neglect the solar wind velocity relative to V_A . Then we find $\tau(0.0 - 0.1) < 0.15$ days. More realistically, we note that at 0.1 AU, with the parameters we have adopted, $V_w/V_A \sim 1$. If we therefore assume that the ratio of V_w/V_A remains constant (and equal to unity) between 0.1 AU and the Sun, we would obtain a lower limit on the propagation time there. We find, in this way, $\tau(0.0-0.1) \geq 0.075$ days. Hence, we estimate that the propagation time from Sun to Earth is 2.175 - 2.25 days.

Consider the feature labelled "B" in Fig. 6, which arrived at ISEE-C at 12.0 hours on DOY 159, and which has all the characteristics of an Alfvén wave propagating outwards from the Sun. Applying the above estimates to propagation time, feature "B" must have left the Sun between 6 hours UT and 7.8 hours UT on DOY 157.

Now, we remarked above that the first particles to reach ISEE-C during this event left the Sun at 5.4-5.6 hours UT on DOY 157. This is quite close to the estimated time of departure of the Alfven waves. In fact, the time of propagation of the Alfven waves from Sun to Earth which we estimated above needs to be increased by only 1-4% to make the two times of departures from the Sun (i.e. waves and particles) identical. Given the errors which entered into our approximate estimate of the wave propagation time, it is certainly not implausible for our estimated propagation time to be in error by such amounts (or more).

We conclude that the feature in our data which looks most like an Alfven wave of solar origin (in the sense that it occurred during the hour when the conditions for outgoing Alfven waves are most completely satisfied, hour = 12 on DOY 159) could indeed have been released from the sun at the same time as the first 57-MeV protons were released. If this conclusion is correct, the properties of the Alfven waves may contain information on the process which was involved in the flare particle acceleration.

The other Alfven wave-like features which we have labelled in Figures 8-10 may have been released from the Sun within a few hours of the initial particle release. When we recall that the two 2B flares which may have been ultimately responsible for the particles we are discussing both lasted for 2-3 hours, it would not be improbable for Alfven waves to be emitted by the Sun for periods of that order. Moreover, some dispersion of the waves must have occurred in interplanetary space, since different wave packets, which followed somewhat different paths along the disturbed field lines, would arrive at somewhat different times.

VI. ALFVEN SOLITON ARRIVING WITH THE FIRST PARTICLES

In Section IV above, we mentioned that on DOY 157 the supercorrelation coefficient rose to its highest value during hour = 6. During this hour, the correlation coefficient between V_x and B_x is found to be 0.93; the Y components have a correlation coefficient of 0.90. The sign of the correlation is such that outgoing waves are indicated. From Figure 5, we also note that although the supercorrelation coefficient is high during hour = 6, it is low during the hour immediately preceding, and also during the hour immediately following. Thus, whatever is causing the high correlation lasts for only about one hour.

In Figure 14, we show the time variations of solar wind parameters and magnetic field for hour = 6. As before, each panel covers 10,000 seconds of real time, extending over not only hour = 6, but also roughly one hour on either side as well. The most prominent feature is the large square wave labelled "S" which appears most clearly in the magnetic data as a steep-sided feature. The velocity feature is not quite so steep-sided, but the occurrence of such a prominent large feature in both B_x and V_x explains the large correlation during hour = 6. And as before, the feature in V_y correlates well with a feature in PHI, the ecliptic flow angle. The magnitude of the magnetic field remains constant during the square wave, to better than $\pm 1\%$. The density remains unchanged within a few percent as the square wave passes by (apart from a very narrow spike in density towards the end of the square wave). The temperatures parallel and perpendicular to the field show almost no alteration as the square wave passes. Thus, as for feature "B" in Figure 6, the square wave in Fig. 14 shares many of the properties of Alfvén waves: it is incompressive, non-dissipative, leaving the magnitude of the field

unchanged, despite substantial changes in the three components of the field. Moreover, the direction of propagation is outward. Finally the amplitude of the wave in B_x is $\delta B_x = 3-4\gamma$, while in velocity, the amplitude is $\delta V_x = 16 \text{ km sec}^{-1}$. Hence, the ratio $\delta V_x / \delta B_x$ for this square wave is $(4.0-5.3) \times 10^{11} \text{ cgs}$. This compares favorably with the value of $(4\pi\rho)^{-1/2}$: with a mean density of 18 cm^{-3} and again assuming 10 helium by number, this quantity has a value of 4.6×10^{11} .

We are therefore led to conclude that the square wave in Fig. 14 is an Alfvén wave propagating outward from the Sun.

To estimate the width of the wave, we apply the same criterion we applied above to estimate roughly the "full width at base". We find, from the velocity data, that $\Delta t_0 = 964 \text{ seconds}$. If, instead of using velocity data, we use magnetic data, for example, B_y , where the square wave has the sharpest edges, we can estimate the width of the wave from the time interval between the rising side of the square and the falling side: this gives a width of 944 seconds. Thus a value of $\Delta t_0 \sim 950 \text{ sec}$ is representative of the true width of this Alfvén wave.

The feature labelled "S" in the figure is the most prominent square wave which we have seen throughout the three-day interval. It is also more steep-sided than any other feature in the three days. The question naturally arises: is it merely a coincidence that this prominent feature occurs during the hour when the first 57-MeV protons arrive from the Sun? If the answer to this question is yes, then we would simply identify the square wave with an Alfvén wave which departed from the Sun some (4-5) days earlier. (Note the wind speed prior to hour = 6 on DOY 157 is lower by a factor of ~ 2 than was

used in estimating the propagation time $\tau(r_S - r_E)$ for the waves which arrived on DOY 159).

If, on the other hand, there is no coincidence, what relation do the Alfven waves in the square soliton have with the arriving particles? If the waves were emitted by the Sun simultaneously with the 57-MeV particles, then the waves must have propagated with the same speed as the particles, i.e. 10^5 km sec^{-1} . Could the waves have been excited by the particles? It is known that streaming particles can excite Alfven waves (Wentzel, 1975). We consider this as unlikely; with the particle fluxes which were present in interplanetary space at the time of arrival of the first particles, the growth time for Alfven waves associated with the streaming particles turns out to be long, of order tens or hundreds of days. Neither could the waves have come from the magnetosphere: they are propagating in the wrong direction for that interpretation and the field at ISEE-C, when extrapolated to Earth, does not intersect the magnetosphere. We shall consider a possible interpretation of this square wave below, when we consider possible field strengths in the solar corona at the source of the waves.

In either case, we note that the width of the soliton in this case (and now this is the "true" width, in view of the very steep sides of the feature), turns out to lie close to the upper limit of the "true" widths which were found for the Alfven solitons on DOY 159 (labelled A-K in Figures 6-9). In the next section, we shall refer to another set of magnetic features in our data which are characterized also by a well-defined time scale of 800-900 seconds. A time-scale of just under 1000 seconds seems to be important as far as the Alfven waves are concerned during DOY 157-159 in 1979. Again, we stress that this range of periods appears to play the role of an upper limit

on "permitted" periods. Either the source of the waves, or the medium through which the waves propagate, constrains the periods to be no greater than 900-1000 seconds.

VII. SHOCK TRAIN IN THE SOLAR WIND ?

In the course of plotting the magnetic field components during the three day interval, we noticed a series of "spikes" in the field during hour = 3 on DOY 157, i.e. some three hours before the first particles arrived. This series of spikes is shown in Figure 15. The spikes are most clearly visible in the plot of B_y . They are labelled A-E in the Figure. High resolution magnetometer data are plotted in Fig. 16 for intervals of ± 120 sec around each "spike". These spikes have half-widths of less than 100 seconds each, and as a result, they would be barely noticeable in plots of one-minute averages of the field. When we recall that the plasma data on ISEE-C are recorded once every 24 seconds, sometimes with gaps of about 150 seconds, it will be appreciated that it is very difficult to calculate an accurate correlation coefficient for the "spikes". Thus, we cannot tell the direction of propagation of the "spikes".

The most noticeable property of the "spikes" is the quasi-regular spacing between them. The time intervals between the five spikes are 816, 872, 887 and 840 seconds. The average of these is 854 ± 28 seconds. The total duration of the train is somewhat greater than one hour. Apparently the source of the spikes was open to the solar wind for only an hour or so.

The shape of the spikes is reminiscent of the shape to which a train of switch-on shocks evolves as it propagates in the wind (Hollweg, 1982), i.e. with a sharp leading edge, followed by a more gently sloping wake. As the

evolution proceeds, the wake becomes shorter and shorter, until eventually, the wake is almost as abrupt as the leading edge. As regards the origin of such a train of shocks, Hollweg (1982) suggests that they might arise when a train of Alfvén waves propagates up through the solar atmosphere: then the time spacing between individual shocks in the train would be determined by the period of the original train of Alfvén waves in the solar atmosphere. If that interpretation is correct, then the series of "spikes" was created by solar Alfvén waves with a rather narrowly defined period: 854 ± 28 seconds.

The questions arises: where did the Alfvén waves originate which gave rise to the train of shocks? The train, after all, occurs during a time when there are essentially no energetic particles in interplanetary space (see Figure 1). Thus they are not obviously related to solar particles. If the shocks have propagated at about the Alfvén wave speed in the wind since their origin, then they must have departed from the Sun some 4-5 days previously, on June 1-2. Even if we could identify a flare from which the train of shocks emerged (there were 5 flares of Importance 1B on June 1-2), we would have to conclude from the lack of detectable particles that the flare might not fit into the category of "particle flares". It would therefore not be a good candidate for searching for Alfvén waves from sunspot umbrae, unless of course the ISEE particle detector was simply not sensitive enough to detect the particles.

Nevertheless, it is striking that the preferred period in this train of shocks is almost identical to the maximum period associated with the Alfvén waves which accompany the particles during DOY 157 and 159. If we can identify the mechanism which constrained the maximum permissible period of Alfvén waves emitted in association with the particles to be no greater than

800-1000 seconds, we might conclude that the same mechanism was operative when the train of shocks left the Sun 4-5 days previously. A mechanism which is inherent to the solar atmosphere would be a natural candidate to seek as a source of explanation for the preferred periodicities in the two cases.

VIII. ORIGIN OF PREFERRED PERIODS FOR ALFVEN WAVES

The Alfven waves which we have detected are apparently coming from the direction of the Sun. Thus, they could be generated in interplanetary space or at the Sun. If they are created in interplanetary space, we have not been able to think of a mechanism which would select certain periods for preference. However, if they arise at the Sun, there appears to be a possible cause for preferring certain periods. Although we cannot be sure that this mechanism (to be discussed in this section) is the only source of preferred periods, it is at least a viable mechanism which should be considered, even if other mechanisms are also discovered.

Hollweg (1972, 1978) has considered the propagation of Alfven waves of various periods from the surface of the Sun upwards through the chromosphere and corona. He finds that the transmission coefficient of Alfven waves upwards is not a monotonic function of period. Instead, there are certain peaks in the transmission at preferred periods. The peaks occur as a result of resonances in the atmosphere, where reflection of Alfven waves depends on the time required for a wave to transit a characteristic scale height in the atmosphere. Hollweg finds that there is a well-defined longest period which can be resonantly transmitted upwards through the atmosphere. The period turns out to be ~ 1.6 hours if the field pervading the solar atmosphere is uniform, and equal to 10.5 gauss. In a uniform field, the longest resonant

period scales inversely with the field strength. Thus, in a uniform field of, say, 60-76 gauss, the longest resonant periods would lie in the range 800-1000 seconds. In more recent work, Hollweg (1978) has considered the effect of a field which varies with height in the atmosphere. Here, the main intent was to model Alfven wave emission from the highly localized bundles of magnetic field which have been discovered during the last several years in many different parts of the solar surface. Such features may be as small as a few hundred kilometers in diameter at the photosphere, with field strengths of almost 2 kilogauss, but they spread out quickly, so that by the time they reach coronal heights, the mean field strength has fallen off to a few gauss. Hollweg found that the resonant peaks were still present in the transmission coefficient, but now shifted to considerably shorter periods.

Clearly, the approximation of a strictly uniform field pervading the entire solar atmosphere above a source of Alfven waves is overly simplified. However, it is equally to be stressed that the great divergence of field which entered into Hollweg's later calculations is likely to be more representative of the small bundles of field, rather than large sunspots. Above spots, the field certainly must diverge to some extent with height, but it is likely to be less divergent than over the small bundles. Hence, we believe that the approximation of a uniform field will be most likely to be realistic in the case of the field which emerges from a sunspot, especially a large spot, or group of spots, where the flux is already spread out over a significant area at the photosphere.

We therefore consider the uniform field results of Hollweg as providing upper limits on the resonant periods of Alfven waves leaking up from sunspot umbrae. By the same token, preferred periods of 800-1000 seconds are created

by fields which are certainly no greater than 60-76 gauss: if we were to allow for the effects of divergent magnetic fields above the umbra. such periods could be selected out for resonant transmission in the presence of weaker coronal fields.

Clearly, we cannot here derive accurately what the transmission characteristics over a spot would be, since there is at present no accurate knowledge of how the field over a sunspot penetrates upwards into the corona. The point of the present discussion, however, is simply to point out that, since the Sun's atmosphere itself acts as a narrow band filter for Alfvén waves, the Sun itself will select certain periods for preferential transmission into interplanetary space, even if a broad spectrum of waves is inserted at the solar surface.

One of the features which persists in the various treatments of the transmission problem by Hollweg is that the resonant periods bear certain ratios to each other; they occur in a sequence which is inversely proportional to the roots of the zeroth order Bessel function. Thus, in all cases considered by Hollweg (both uniform and divergent fields), the longest resonant period is a factor 2.3 larger than the second longest resonant period, and a factor of 3.6 longer than the third longest resonant period. In Figure 12 above, we have shown where the second and third preferred periods would lie if the longest preferred period were to lie at 864 seconds (group of first 5 points), or at 664 seconds (remaining group). (In the latter case, we have averaged the three highest values to obtain a mean value for what might be the longest preferred periods at those times.) There is perhaps a tendency for the soliton widths to cluster around the dashed lines. More data will be needed to evaluate the reality of this tendency.

However, as we mentioned above, Hollweg's treatment does lead to a well-defined longest resonant period, P_0 . At periods longer than P_0 , the transmission coefficient of the atmosphere falls off to negligible values. Hence, even if waves of periods $P > P_0$ were present at the solar surface, they would rarely be able to leak through to interplanetary space with detectable fluxes. This point is clearly of some interest in view of our discussion of an upper limit on the soliton widths in Figure 12.

IX. ARE THE ALFVEN WAVES COMING FROM SUNSPOT UMBRAE?

Mullan (1974) constructed a model of a sunspot umbra in which the missing flux was carried by Alfven waves. In this model, a vertical magnetic field reduces the efficiency of convective energy transfer, but does not impede convection altogether. (The electrical conductivity is allowed to have a finite value.) The residual convection is considered to interact with the magnetic field, emitting Alfven waves of sufficient flux to conserve the total energy flux (i.e., the sum of the energy fluxes carried by radiation, convection plus waves equals the undisturbed solar flux). The Alfven waves which are created in this model have periods which are equal to convective turnover times. In the models computed by Mullan (1974), these times are typically several hundred seconds. Now, in the conditions which pertain to solar convection, a high degree of turbulence is expected: the Rayleigh and Reynolds numbers are extremely large. Hence, it is inevitable that a spectrum of convective time-scales exists in the convection zone in an umbra. (Similarly, in the non-magnetic solar atmosphere, convective cell lifetimes span a rather broad range around the mean value of 6-7 minutes: changes are noticeable in the granulation pattern after only 2-3 minutes, whereas some

granules live as long as 20 minutes (Bray and Loughhead, 1967). We expect that the range 100-1000 seconds should cover most of the power in umbral convection. Hence, Alfven waves from umbrae should have periods in that range.

Under normal conditions, the Alfven waves are efficiently reflected at the strong density gradient in the visible layers. As a result, the waves are normally trapped beneath the visible layer of the spot. (We call this trapping the Alfven "valve" effect.) The fact that the missing sunspot flux is indeed trapped inside the sun has been established by the solar maximum mission (Willson et al., 1981). The point which was central to the paper by Mullan (1981) was the following: conditions over an umbra during a proton flare are far from normal and this could affect the "valve" so as to allow the Alfven waves to leak out of the umbra upwards into the corona with greatly enhanced efficiency. It was estimated that the "valve" would stay open as long as the flare emission covered the umbra of the spot. In particle flares, this is typically about one hour. Thus, a burst of Alfven waves, of duration about an hour or so, might leak into the corona during particle flares.

If Alfven waves are to reach interplanetary space, the magnetic fields rooted in the umbra must become open. The same condition is also imposed on the field lines in order to allow the particles to escape. The escape of solar particles from the corona can be described by a coronal "bottle" model (Schatten and Mullan, 1977; Mullan and Schatten, 1979). In this model, field lines in the vicinity of the flare which were originally closed, become distended up into the corona by the pressure of the flare ejecta. The fields remain closed (trapping particles and waves in a "bottle") for a finite time, until some process occurs to open the bottle. The process identified by Schatten and Mullan for bottle opening was the Rayleigh Taylor instability,

followed by reconnection. (For a recent summary of how this scenario agrees with a variety of solar particle and radio data, see Mullan, 1983).

The point we wish to stress here is that when the bottle opens, allowing Alfven waves to escape, the top of the bottle has reached altitudes of order 0.3-1 solar radius above the Sun's surface, and the transverse dimension of the bottle as it opens up is also comparable to 0.3-1 solar radii. For a pictorial representation of the bottle at its opening, see the sketch in Fig. 17. Note that when the bottle opens, field lines from the base of the bottle (i.e. from sunspots down there) are spread out over a length scale of 0.3-1 solar radii.

Now we can revert to the estimate made above concerning mean field strength which would obtain if we were to distribute the magnetic flux in active region 16051 over an area whose typical dimension was 0.5 solar radii. (See Section II above): the estimated field strength was 63 gauss.

In this regard, we point out that if the solar atmosphere were pervaded by a uniform field of 63 gauss, the longest preferred period for Alfven wave transmission would be $P_0 = 960$ seconds. This agrees with the upper limit of 800-1000 seconds which we derived from the interplanetary data above. (In particular, it coincides almost exactly with the duration of the remarkable Alfven soliton which arrives simultaneously with the first particles at hour = 6 on DOY 157.) It seems consistent with our data to claim the following: during the flares associated with the particle event we are studying, Alfven waves with a range of periods (possibly from 100 to 1000 seconds) leaked into the low corona because of the flares (which enhanced the transmission coefficients out of the umbra to much higher than normal values). This broad spectrum of Alfven waves then propagated upwards through the solar corona.

However, only those waves whose periods matched the resonance peaks of the corona at that time were successful in reaching interplanetary space in detectable fluxes. The resonance peaks occur at periods which are determined by the roots of the zeroth order Bessel function. If the longest period was 864 seconds, say, then the next two longest periods which would be transmitted to interplanetary space would be 377 and 240 seconds. There is some evidence that such periods are indeed preferred in our data (see Figure 12).

Finally, we note the following point. At altitudes of order 1 solar radius above the solar surface, the local density is of order $3 \times 10^6 \text{ cm}^{-3}$ (Newkirk, 1967). If a magnetic field of strength 60-76 gauss permeated material of such density, the Alfven speed would be of order 10^5 km sec^{-1} . Under normal conditions, as the field expanded into interplanetary space, the Alfven speed would decrease rapidly, falling off roughly as r^{-1} and reaching values of a few hundred km/sec at the Earth's orbit. However, we are not considering "normal" conditions. On the contrary, we are considering a time when particles whose speeds are $\sim 10^5 \text{ km sec}^{-1}$ are also beginning to stream away from the Sun as soon as the bottle opens up. It is a matter of some interest to consider what will happen to the Alfven waves which begin to stream away from the open bottle at a speed which is initially as high as the fastest particles. The equality of wave speed and particle speed suggest the possibility of coupling between the waves and the particles. It will be recalled that a prominent square Alfven wave arrived at ISEE-C at precisely the same time as the first 57-MeV particles. We speculate that the square wave became coupled to the particles at the Sun (under some favorable conditions), and "rode the particles" to the Earth. We notice that the supercorrelation between velocity and magnetic field was at a high level only

during hour = 6, but not during hours 5 or 7. Thus, if our speculation is correct, the conditions for wave-particle coupling were favorable for a period of only an hour or so. This interval is comparable to the period during which umbral Alfvén waves could leak out of the umbra, before the "valve" closed once more (see Mullan, 1981).

The remainder of the Alfvén waves, which did not satisfy the conditions for coupling to the particles, behave like "normal" Alfvén waves, propagating at the local Alfvén speed relative to the solar wind, and arriving at the orbit of the Earth after a delay of $\tau(r_s - r_E) = 2-3$ days.

In all cases, even if an Alfvén wave starts off at the sun as a sinusoid of a certain period, it seems likely that non-linear processes in the interplanetary medium will cause the shape to alter. By the time the wave reaches the Earth's orbit, this may cause the shape to have evolved to the soliton-like shapes which we have observed in our data. The duration of the soliton would be expected to be related to the period of the original sinusoid.

The conclusion we draw from this discussion is that we may be seeing Alfvén waves from the umbrae of sunspots in association with solar energetic particles. Several features of the waves are consistent with this hypothesis.

If this hypothesis can be confirmed in other events, it would constitute circumstantial evidence that the missing flux in the umbra of a sunspot is indeed being carried by Alfvén waves.

X. CONCLUSION

Using magnetometer and plasma data from the ISEE-C spacecraft, we have found evidence for outward-propagating features in the solar wind in association with a solar energetic particle event. The features which we have

observed fulfil the conditions for Alfvén waves, but they are not sinusoidal. Instead, they are soliton-like. The widths of the solitons are in the range from about 200 seconds to almost 1000 seconds. Longer periods do not appear to be present in the data. We argue that the existence of an upper limit on the wave periods, and the possible existence of preferred periods for the solitons, is due to processes in the solar atmosphere. One such process is associated with the filtering properties of the atmosphere: Alfvén waves are transmitted resonantly through the atmosphere only at certain preferred periods below a certain maximum period.

We have considered the hypothesis that the Alfvén waves which we have detected in the solar wind originate in sunspots. If the missing flux in spots is carried by Alfvén waves, the waves would normally not be detectable in interplanetary space: the stratified atmosphere acts like a firmly closed "valve" which normally allows only a negligible fraction (of order 10^{-5}) of the Alfvén waves to leak up into the corona. However, conditions during a particle flare (such as we are examining in this paper) are far from normal: hot flare plasma lies over the umbrae of spots and helps to open the "valve". In the conditions which obtain in the vicinity of a "particle flare", umbral Alfvén waves have a greatly enhanced probability of leaking up into the corona. Once there, the waves need to escape into interplanetary space if we are to detect them. In this regard, we note that, as a matter of definition, in order for a flare to be classified as a "particle flare", the magnetic fields at the sun must have (somehow) opened up to interplanetary space. The same open field lines which allow solar particles to escape also ensure that solar Alfvén waves (if they exist) escape from the corona. However only

certain periods escape efficiently. The properties of the Alfven-like solitons which we have detected are consistent with the umbral hypothesis.

Since Alfven waves and charged particles may undergo coupling processes in favorable circumstances, the possibility that Alfven waves may contribute to stochastic particle acceleration has already been considered by some authors (Lacombe, 1979; Barbosa, 1979). This raises the question as to whether or not the Alfven solitons which we have detected here are themselves responsible to any extent for accelerating the particles in the event which we are studying. No definite answer can be given to this question at present. However, we have pointed out that wave-particle coupling may help to explain an Alfven-like soliton which arrived simultaneously with the first particles.

Acknowledgements

This work has been supported by Air Force Geophysics Laboratory under Contract.F19628-81-K-0004. We thank Drs. T. von Rosenvinge, B. Tsurutani, and R. Zwickl for data tapes, and Bob Schaffer and Suzanne Goodrich for assistance with the data reduction.

References

- Armstrong, T.P. and Decker, R.B. 1979, in Particle Acceleration Mechanisms in Astrophysics (AIP Conf. Proc. 56), eds. J. Arons, C. McKee, and C. Max, p. 101.
- Barbosa, D.D. 1979, Ap. J. 233, 383.
- Barnes, A. 1976, J. Geophys. Res. 81, 281.
- Belcher, J.W. and Davis, L. 1971, J. Geophys. Res. 76, 3534.
- Bray, R.J. and Loughhead, R.E. 1967, The Solar Granulation, (London: Chapman and Hall), p. 26.
- Burlaga, L. and Turner, J. 1976, J. Geophys. Res. 81, 73.
- Fichtel, C. and McDonald, F.B. 1967, Ann. Rev. Astron. Ap. 5, 351.
- Gloeckler, G. et al. 1981, Proc. XVII Int. Conf. Cosmic Rays (Paris), Vol. 3, p. 136.
- Hollweg, J.V. 1972, Cosmic Electrodynamics, 2, 423.
- Hollweg, J.V. 1978, Solar Phys. 56, 305.
- Hollweg, J.V. 1982, Ap. J. 254, 806.
- Lacombe, C. 1979, Astron. Ap. 71, 169.
- Mullan, D.J. 1974, Ap. J. 187, 621.
- Mullan, D.J. 1981, Solar Phys. 70, 381.
- Mullan, D.J. 1983, Ap. J. (in press, June 15 issue).
- Mullan, D.J. and Schatten, K.H. 1979, Solar Phys. 62, 153.
- Newkirk, G. 1967, Ann. Rev. Astr. Ap. 5, 213.
- Owens, A.J. 1975, Astrophys. Space Sci. 38, 469.
- Parker, G.D. 1980, J. Geophys. Res. 85, 4275 and 4283.
- Reinhard, R. and Wibberenz, G. 1974, Solar Phys. 36, 473.
- Schatten, K.H. and Mullan, D.J. 1977, J. Geophys. Res. 82, 5609.

Steinitz, R. and Eyni, M. 1977, Proc. COSPAR Symp. B (Study of Travelling Interplanetary Phenomena), eds. M.A. Shea, D.R. Smart, S.T. Wu (AFGL-TR-77-0309), p. 101.

Steinolfson, R.S. and Mullan, D.J. ____Ap. J. 241, 1186.

Wentzel, D.G. 1974, Ann. Rev. Astron. Ap. 12, 71.

Willson, R.C. et al. 1981, Science 211, 700.

Table 1

Feature	Hour	$\langle v_w \rangle$	V_{\max}	t_{\max}	Δt_0
A	11	572	594	40777	207
B	12	573	620	43428	864
C	12	573	599	45742	266
D	10	589	632	36318	242
E	10	589	665	38126	360
F	14	581	642	54081	775
G	15	598	634	54877	634
H	16	513	605	59143	583
I	16	573	597	60348	181
J	17	578	613	61722	377
K	17	528	609	63240	354

FIGURE CAPTIONS

- Figure 1. Particle fluxes in ISEE-C detector (energy range 4-57 MeV/nucleon). Data courtesy of Dr. T. von Rosenvinge (Project Scientist, ISEE-3). The study reported here concentrates on June 6-8, i.e. DOY 157-159.
- Figure 2. ISEE-C magnetometer measures three components of field in xyz system shown here. During each hour interval, we derive the mean field $\langle B \rangle$. Its projection onto the xy-plane (the ecliptic) is used to define the ζ -axis of a new triad. This new triad is used for purposes of cross-correlation studies on the magnetic variance matrix.
- Figure 3. Spectral coherence for two different hourly intervals. (a) Hour = 15, DOY 157; (b) Hour = 12, DOY 159. Only two of the three off-diagonal terms in the cross-correlation matrix are plotted here (to avoid confusion). Filled circles are $\xi\eta$ coherences; open circles are $\xi\zeta$ coherences. The "noise" level is determined by our sampling rate (35 degrees of freedom). Notice that in (a), all points lie above the "noise" level, whereas this is not true in (b).
- Figure 4. Mean coherences for each hour throughout the three-day interval. These means are geometric averages of 13 points in the spectral plots for each hour. Circled data refer to hours during which both coherences plotted here fall below "noise". Numbers near circles in lower panel refer to mean coherences in the third off-diagonal component ($\eta\zeta$). Signs < denote hours during which the minimum variance is along the ζ -axis.

Figure 5. Supercorrelation coefficient between velocity and magnetic field vectors: $\rho'' = \rho_x^2 \rho_y^2$. Outward going waves are plotted above the zero line, inward going waves are plotted below.

(a) DOY 157, when first particles arrive at 57 MeV/nuc. Notice sector boundary passage at 9-10 hours UT.

(b) DOY 158. Supercorrelation is low most of the day. Points where significant data dropouts occurred are in parentheses.

(c) DOY 159. All waves outward. Notice particularly high supercorrelation during Hour = 12.

Figure 6. Magnetic and plasma data during Hour = 12 on DOY 159. Each panel spans almost 3 hours of real time. Start time and end time of each panel (in seconds) are labelled. Magnetic field data are 8-second averages. Plasma data are 24-second averages.

Figure 7. Magnetic and plasma data around Hour = 10 on DOY 159. Features labelled with capital letters in Figs. 6-9 correspond to features in Table 1.

Figure 8. Magnetic and plasma data around hours = 14 and 15, DOY 159.

Figure 9. Magnetic and plasma data around hour = 16 on DOY 159.

Figure 10. Radial component of magnetic field and wind velocity during interval when velocity-field correlation is very small (DOY 158, hours = 2,3,4).

Figure 11. Magnetic and plasma data around hour = 8 on DOY 157. The correlation between V_x and B_x is high during the feature labelled P', but this is not an unambiguous signature of an Alfvén wave: note the density and temperatures alter in the "wave", and the magnitude of the magnetic field varies by a large amount (factor 3).

Figure 12. Widths of solitons observed in solar wind at various time during DOY 159. For definition of "width" see text. Dashed lines labelled 1,2,3 are discussed in Section IX.

Figure 13. Solid curve joins hourly average values of solar wins speed throughout the 3-day interval of our study. Open circles denote instantaneous measurements of solar wind density. The density shows a very narrow spike (13 minutes) when the high speed stream arrives, but the density is definitely much lower in the high speed stream than it was in the slow wind (cf. hours 0-5, DOY 157).

Figure 14. Magnetic and plasma data during the hour when particles first arrive at ISEE-C (at $E=57$ MeV/nuc) on DOY 157. Notice the square wave which is most prominent in BY.

Figure 15. Possible train of shocks in the solar wind (labelled E-E in BY panel. Notice the quasi-regular spacing between the "spikes". Plotted here are 8-second averages of the magnetic field. At his resolution, the "spikes" are present in the data, but not clearly resolved.

Figure 16. High resolution magnetometer data of the five "spikes" in Fig. 15. Each panel now spans 240 seconds of real time, with plotted points every $1/6$ second.

Figure 17. Sketch of release of Alfven waves from sunspots SS into solar wind during a solar flare. Initially (a), fields are closed and waves cannot escape. Particles are also trapped at this stage. As flare proceeds, bottle expands (b) but still remains closed for a finite time. Eventually, (c), fields must open to release particles (if the flare is to be classified as a "particle" flare. When fields open, Alfven waves can also escape. Notice when fields open, sunspot fields are spread out over a large area of the corona at altitudes of order 0.3-1 solar radii above the photosphere. (See Schatten and Mullan, 1977).

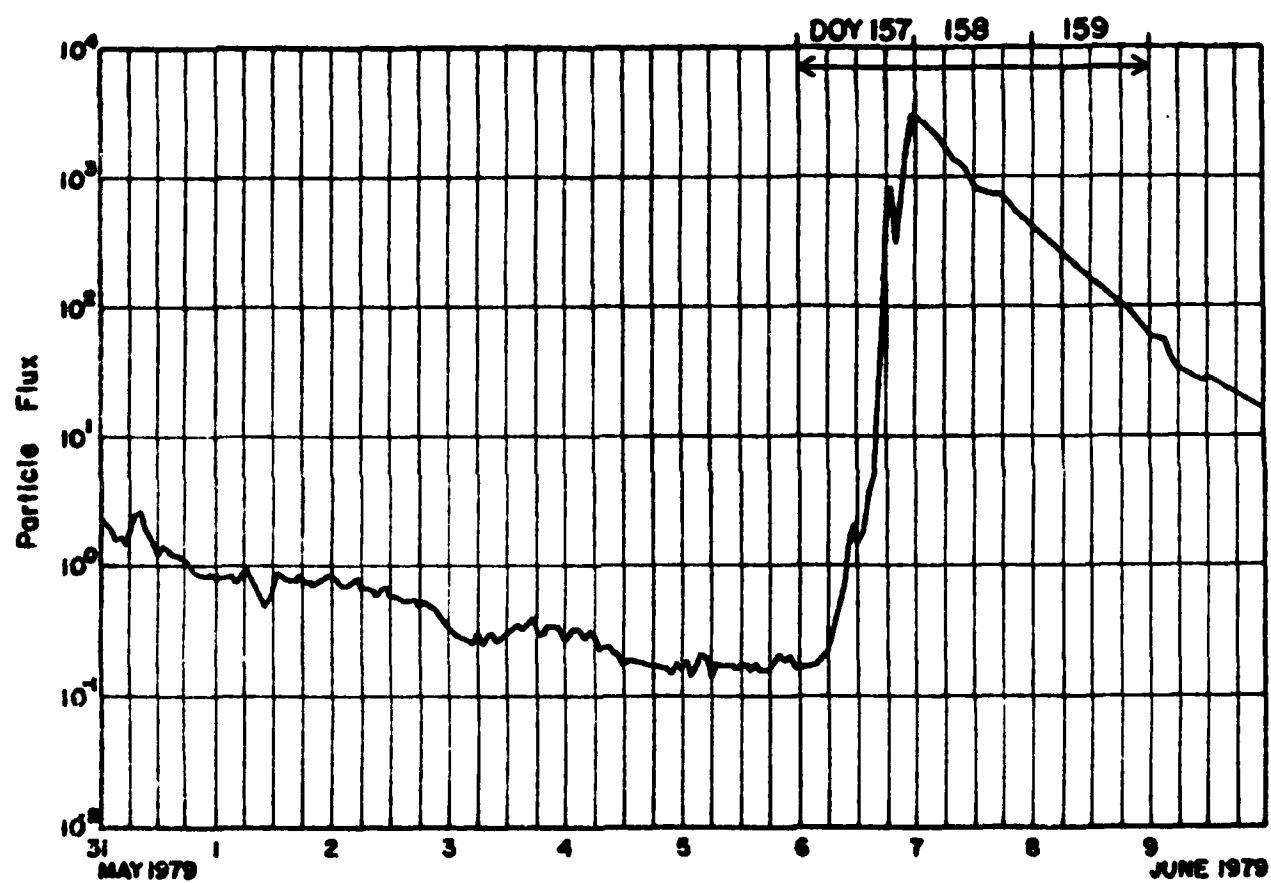


Fig. 1

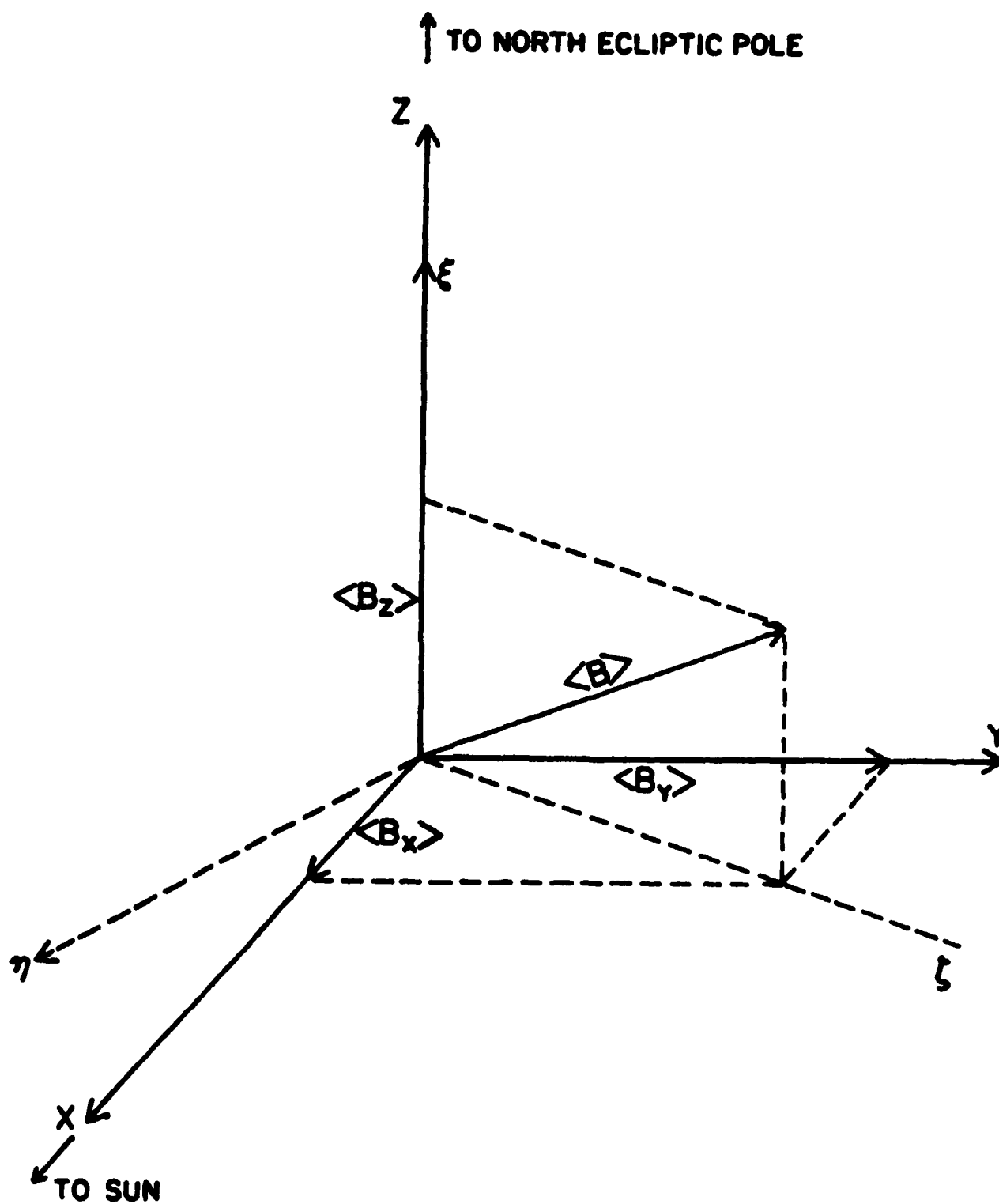


Fig. 2

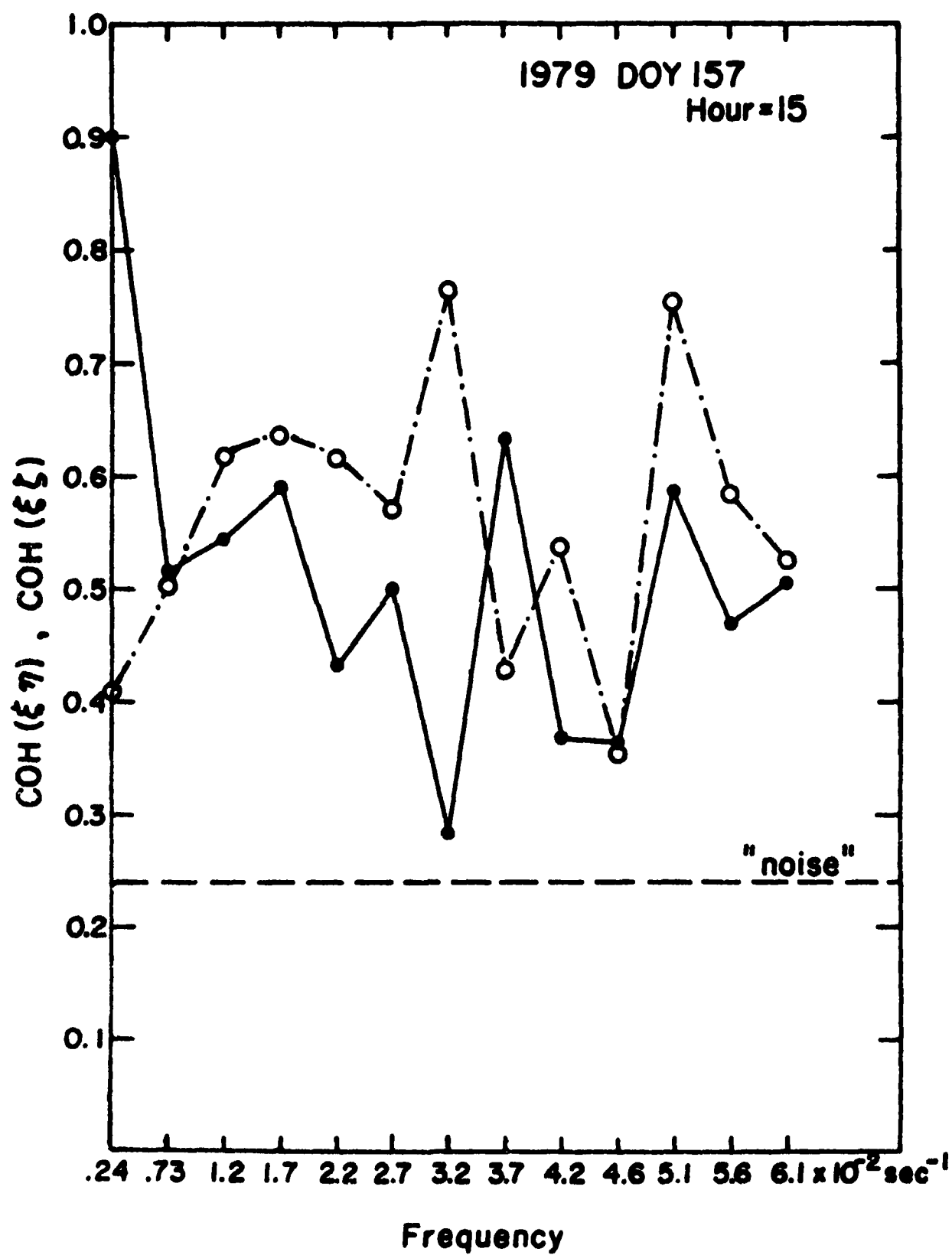


Fig. 3(a)

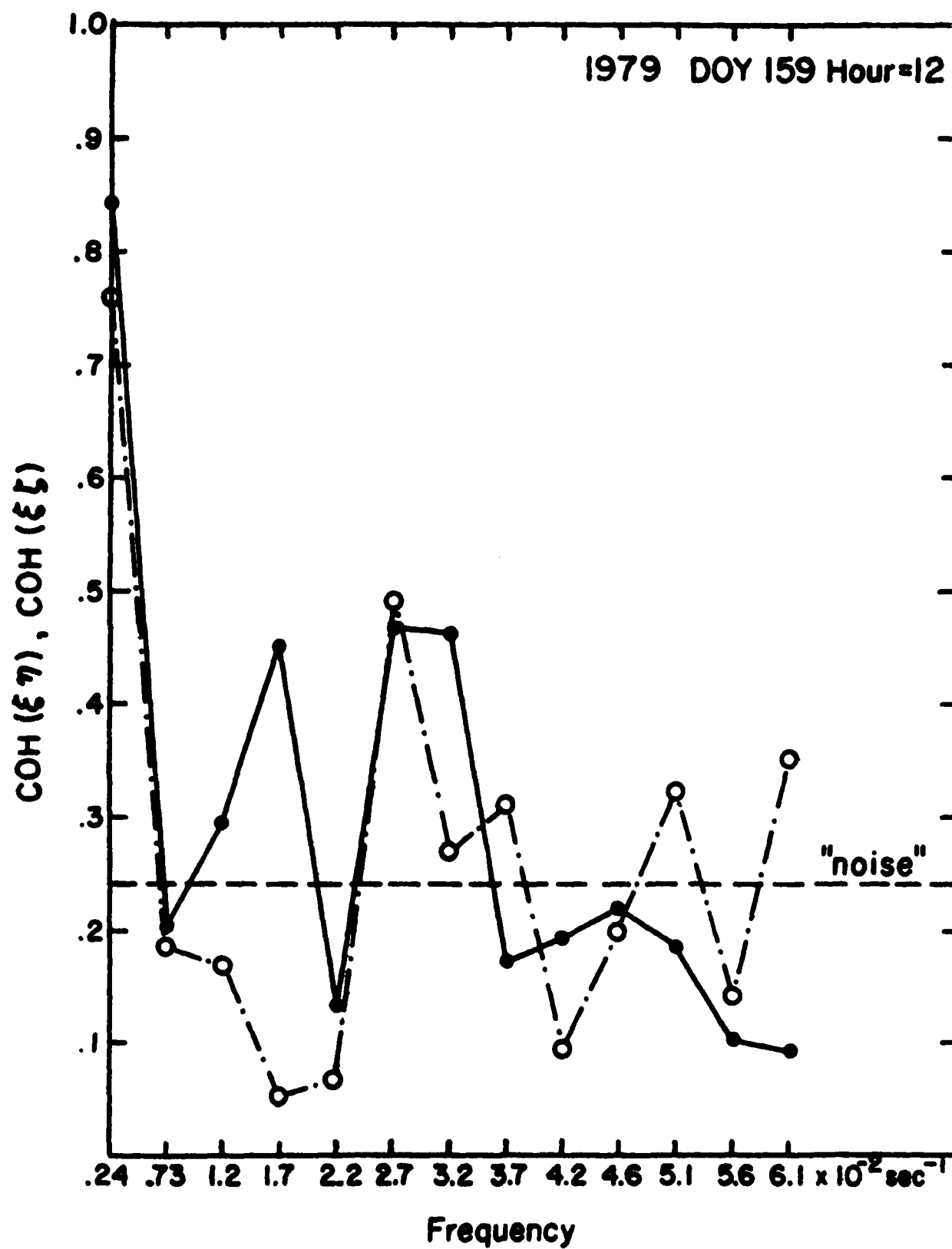


Fig. 3(b)

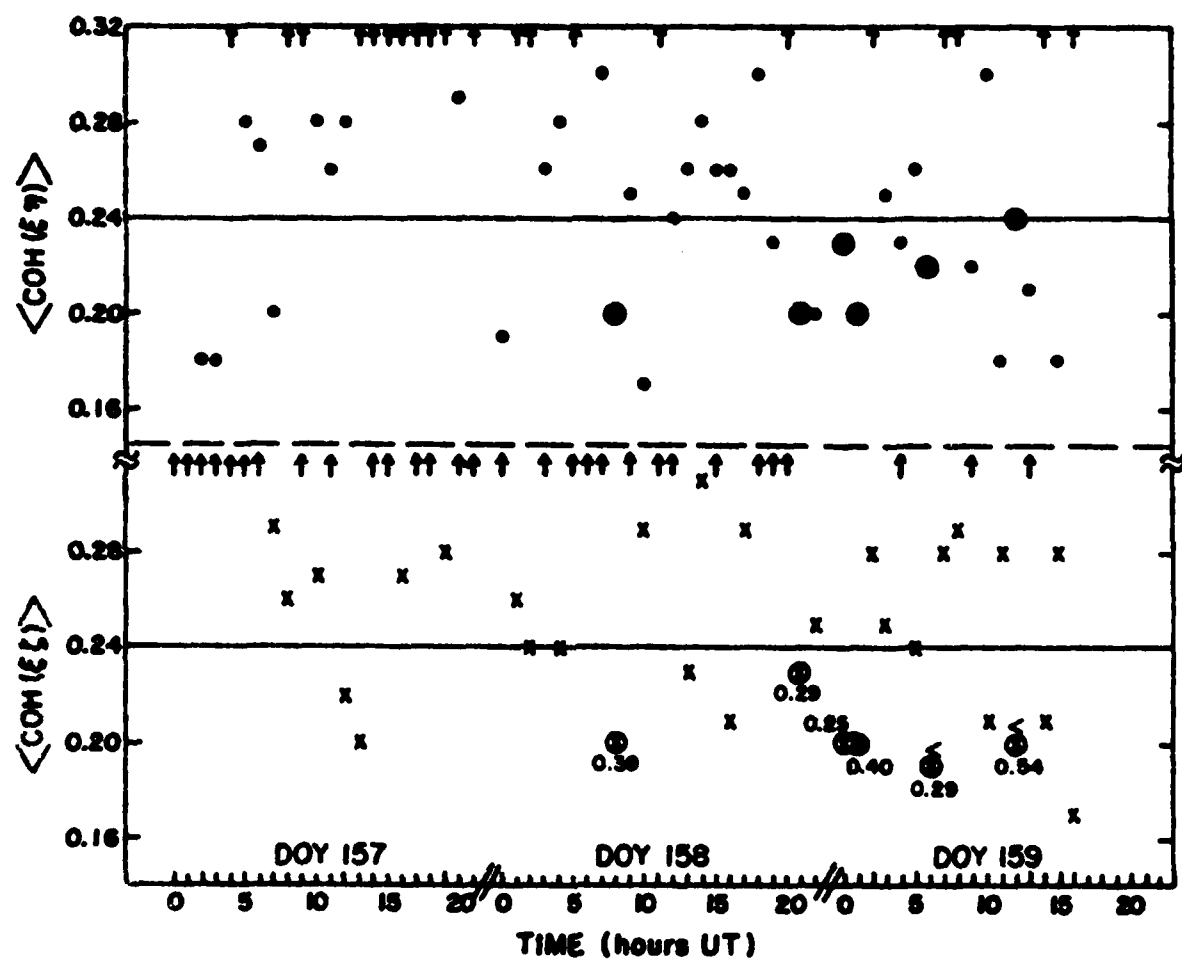


Fig. 4

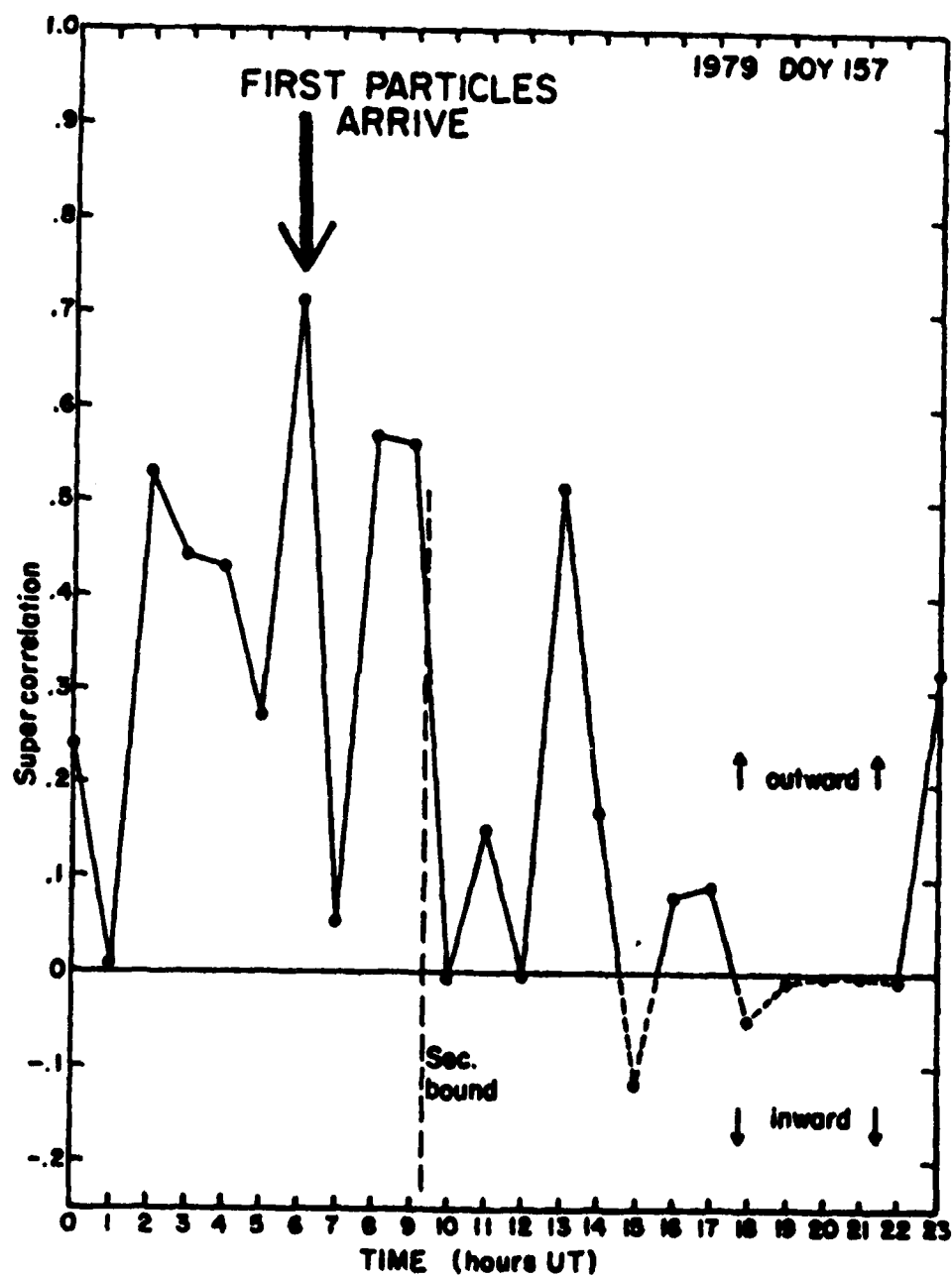


Fig. 5(a)

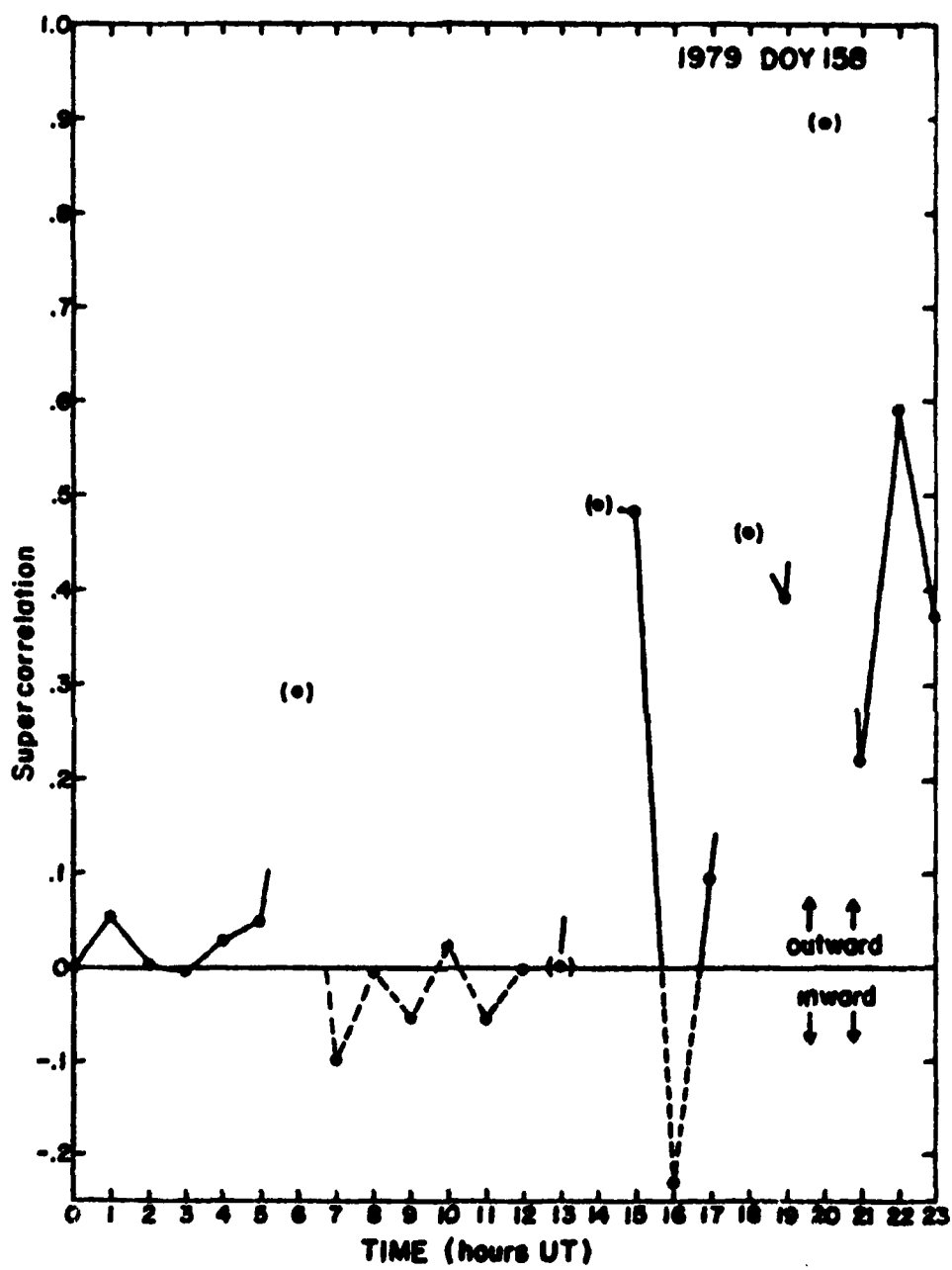


Fig. 5(b)

1979 DOY 159

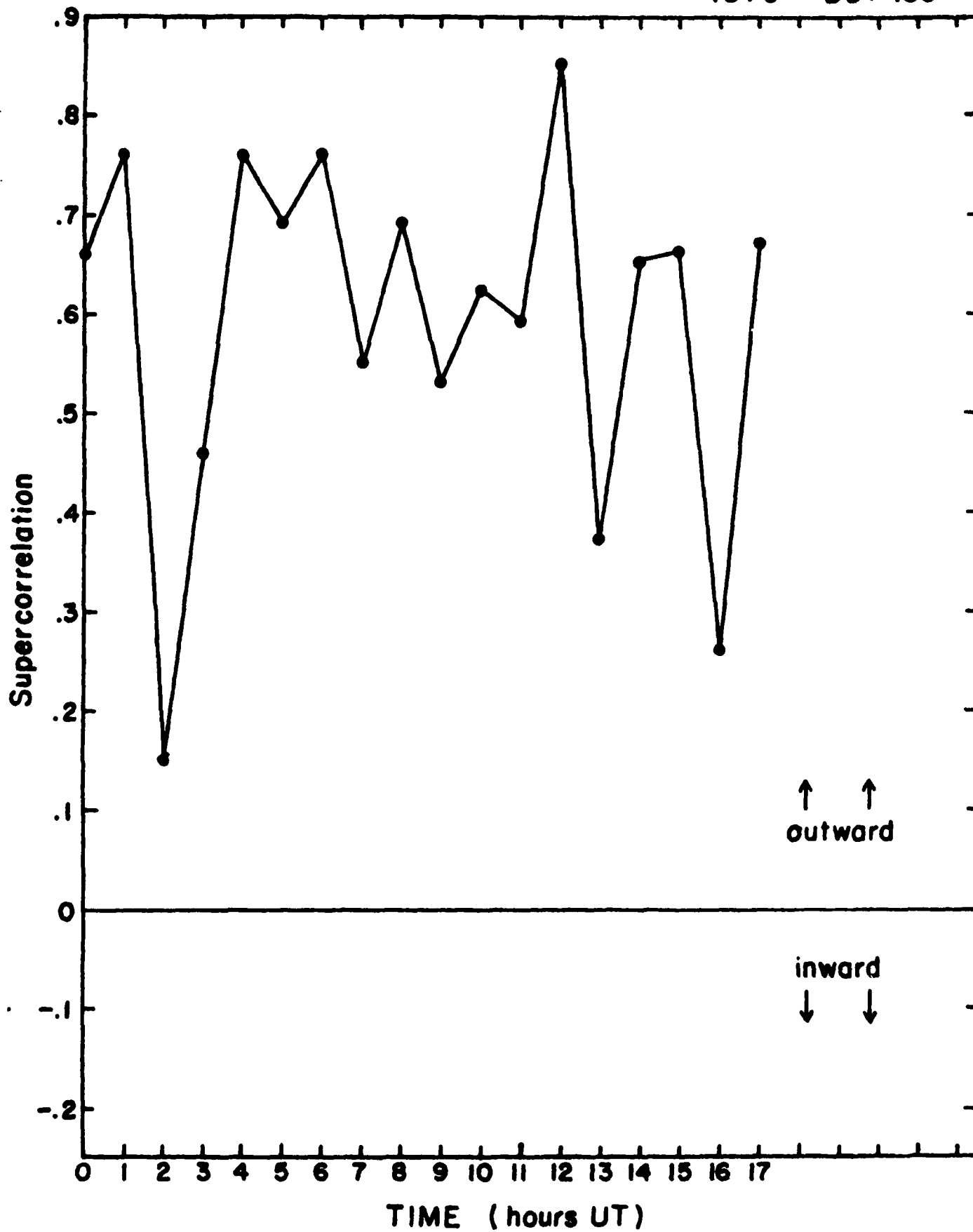


Fig. 5(c)

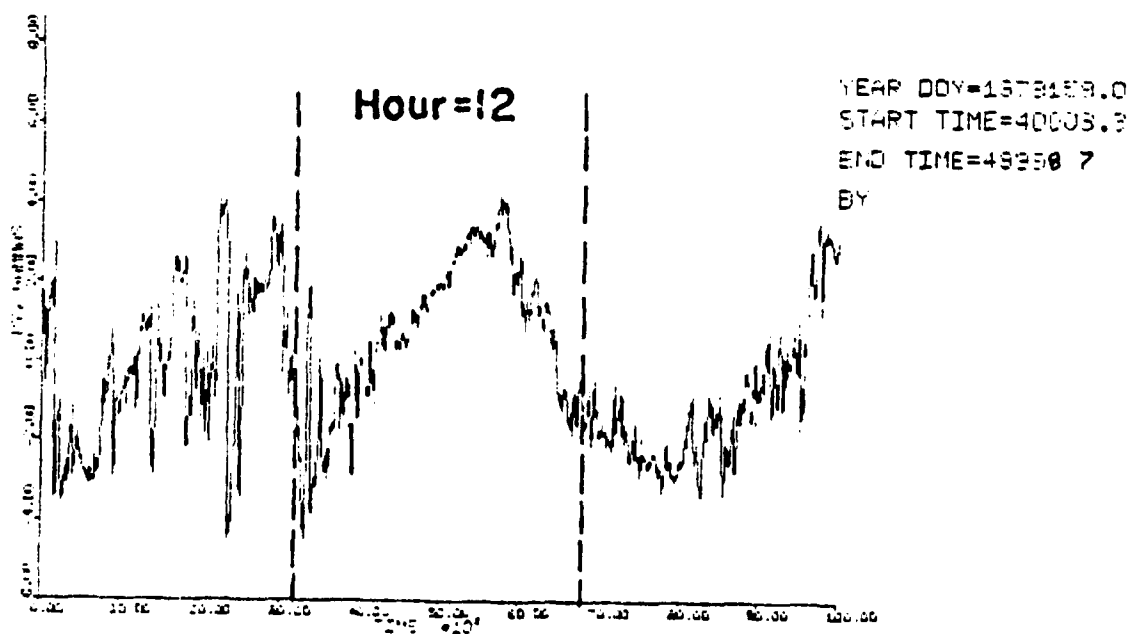
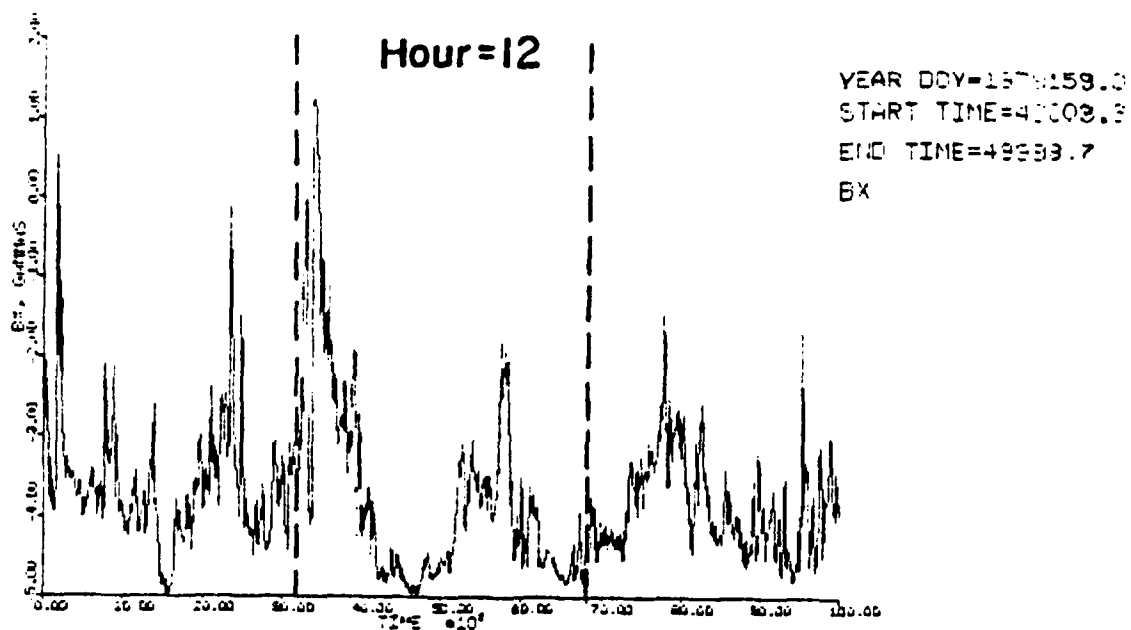


Fig 6 (a)

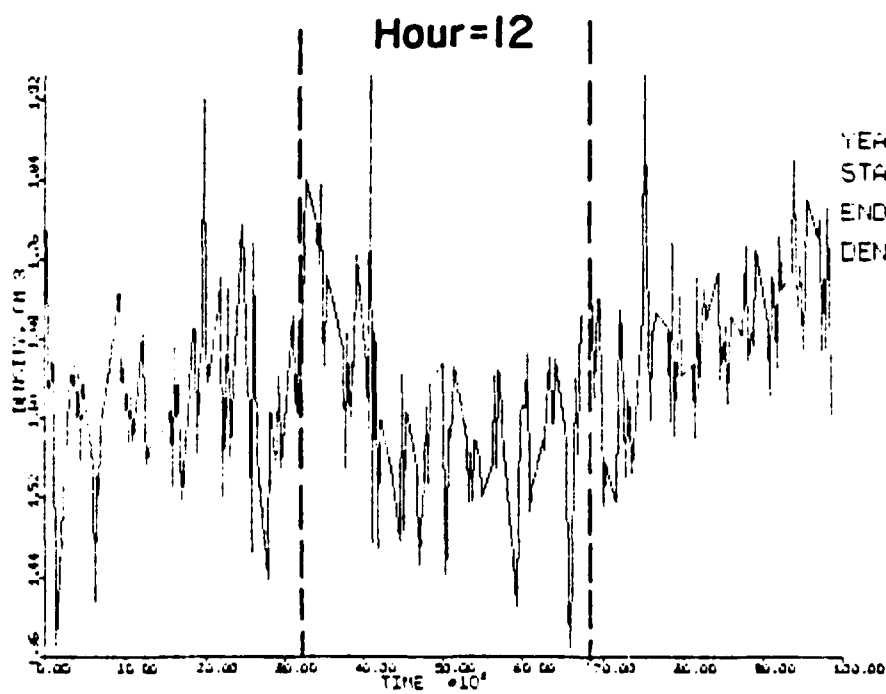
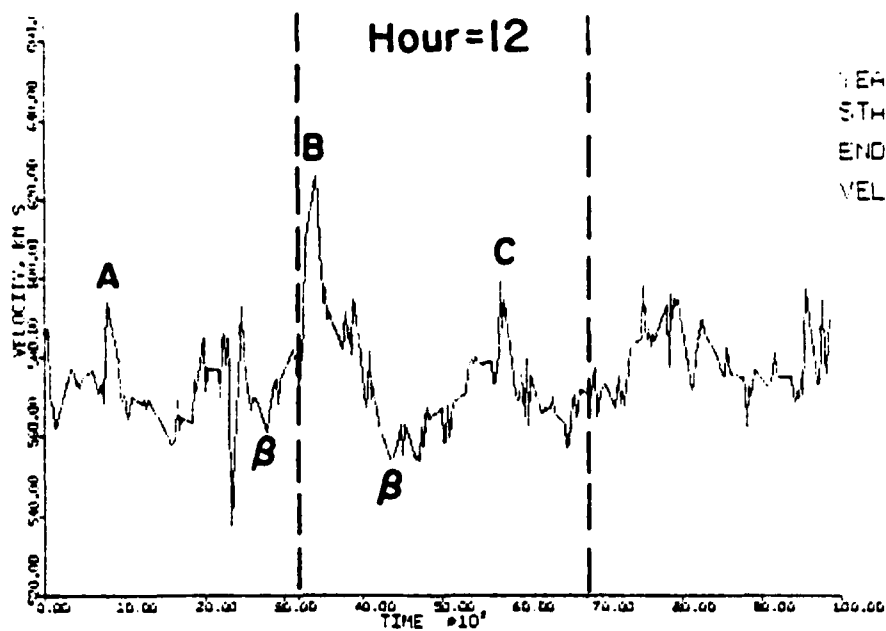


Fig. 6 (b)

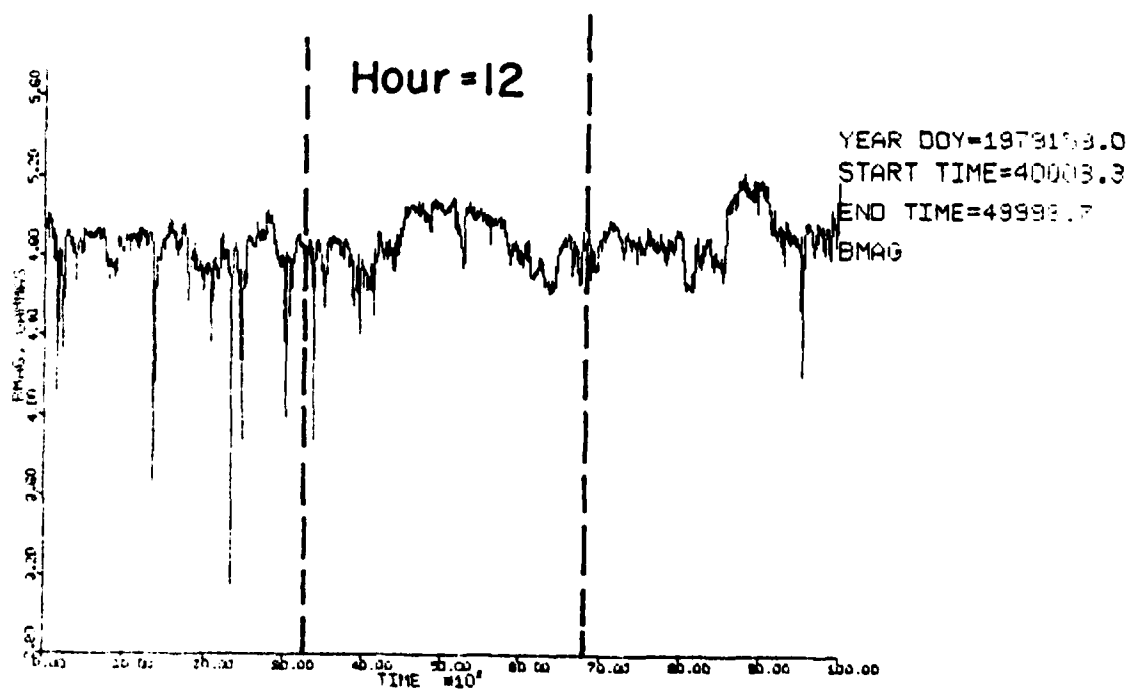
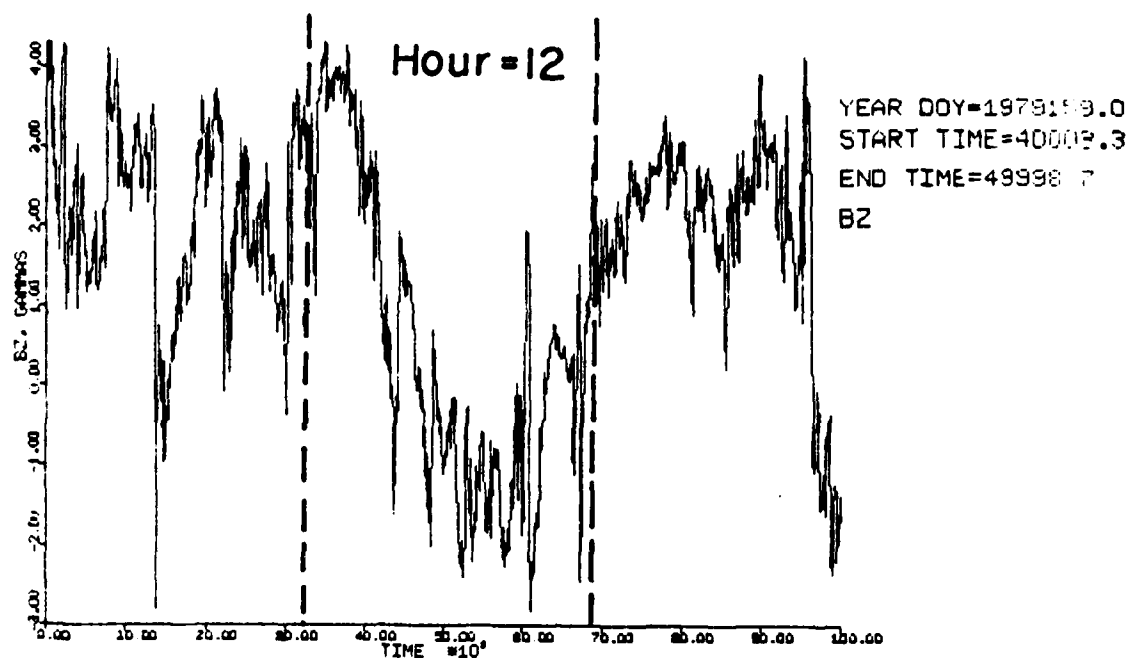


Fig. 6 (c)

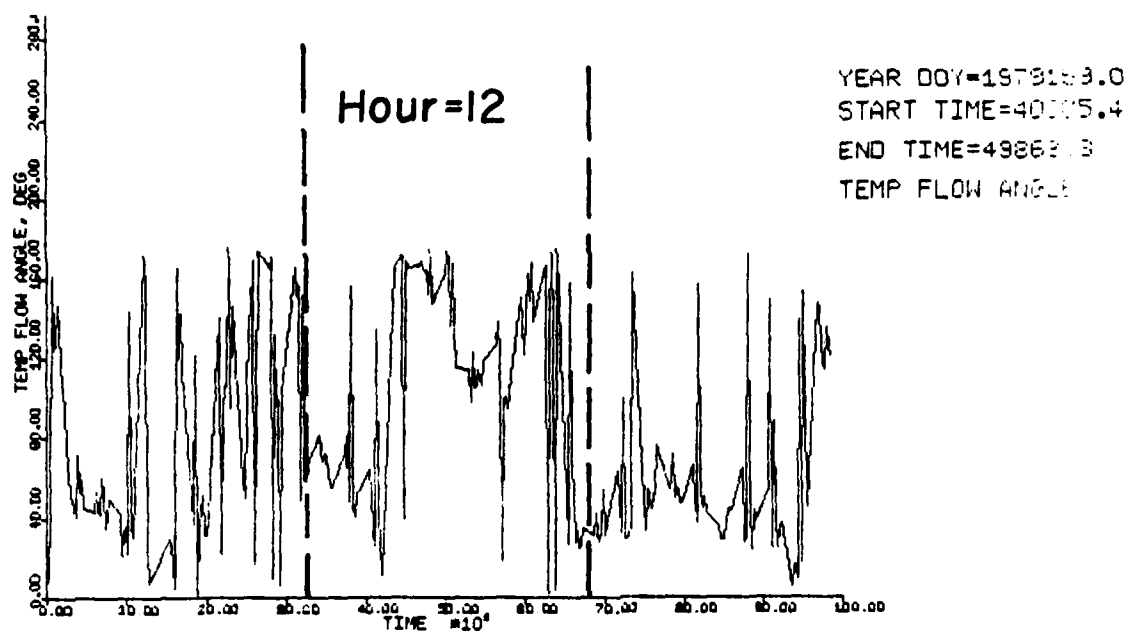
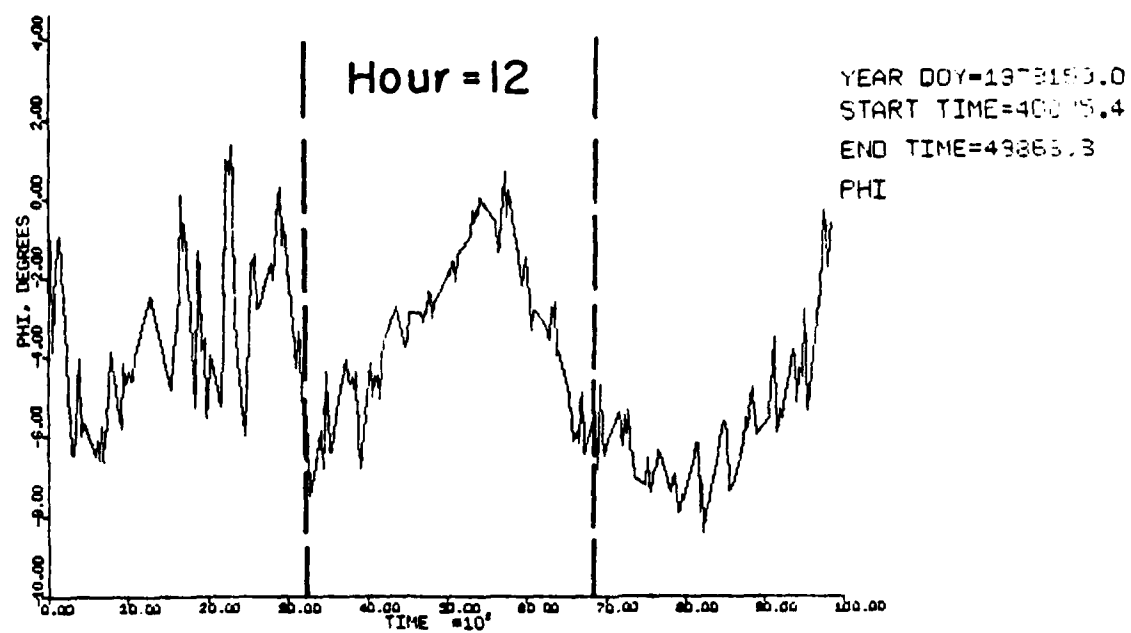


Fig. 6 (d)

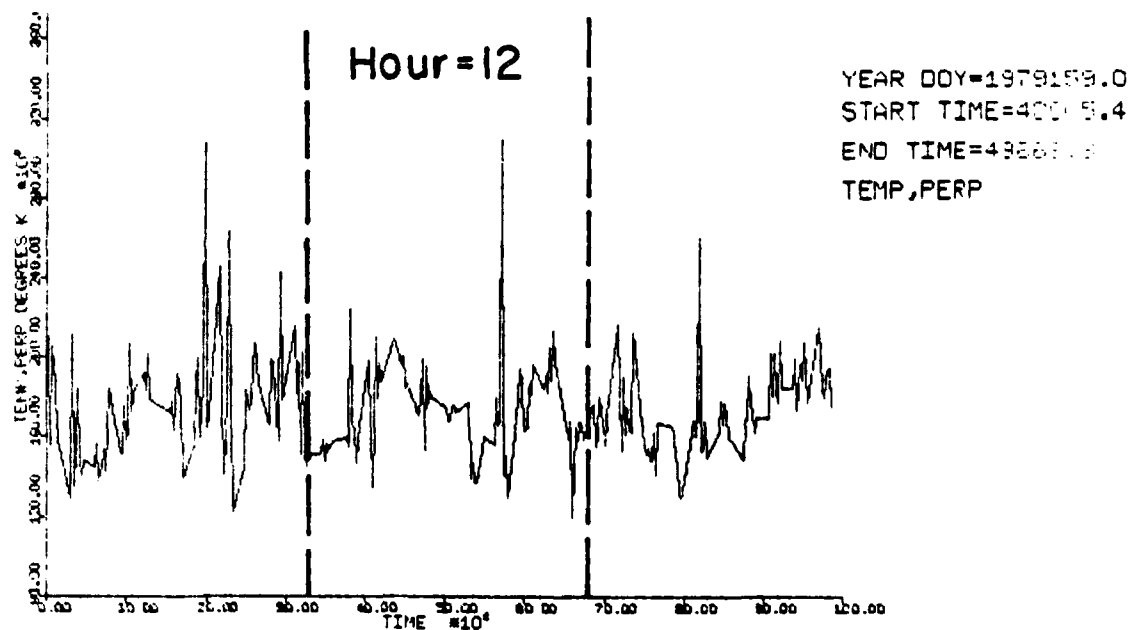
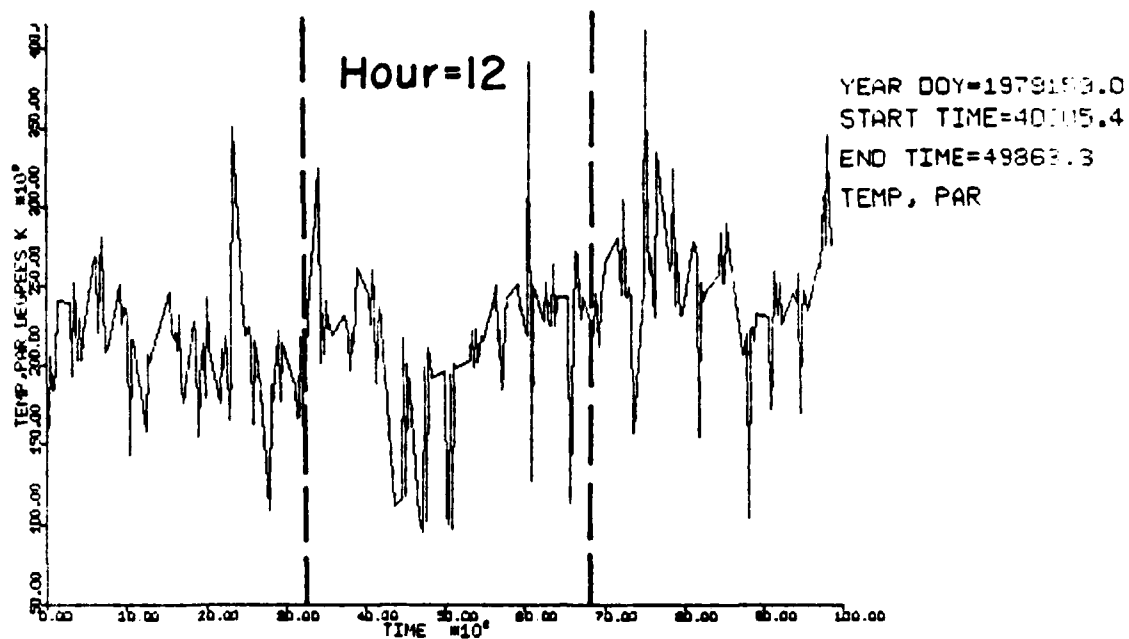


Fig. 6 (e)

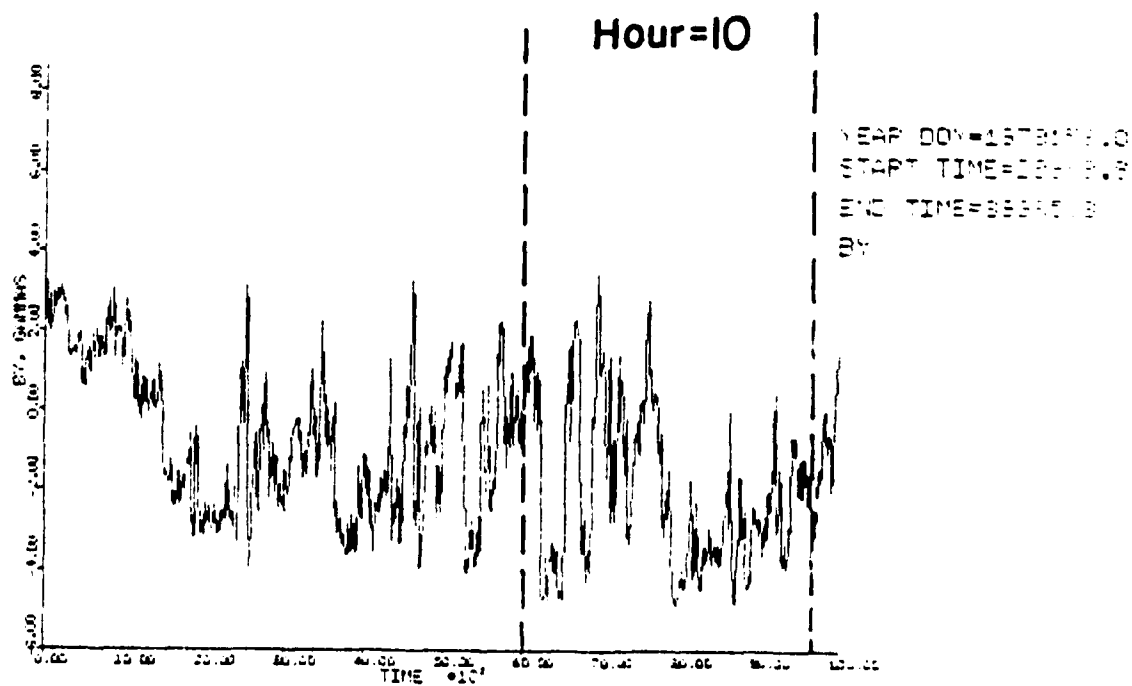
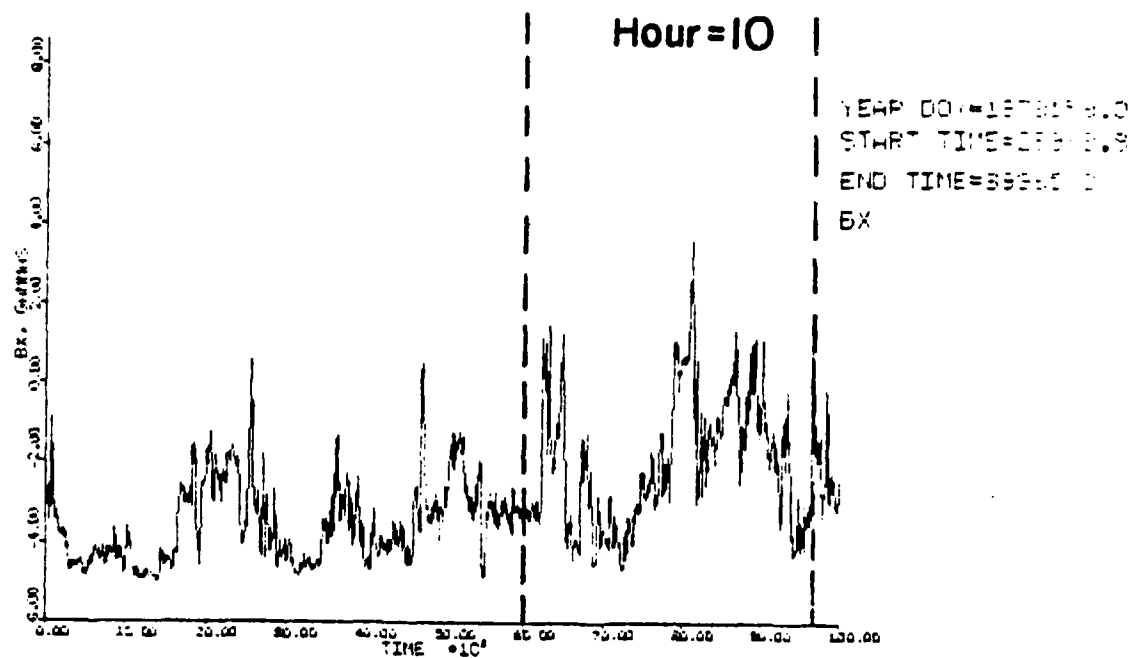


Fig. 7 (a)

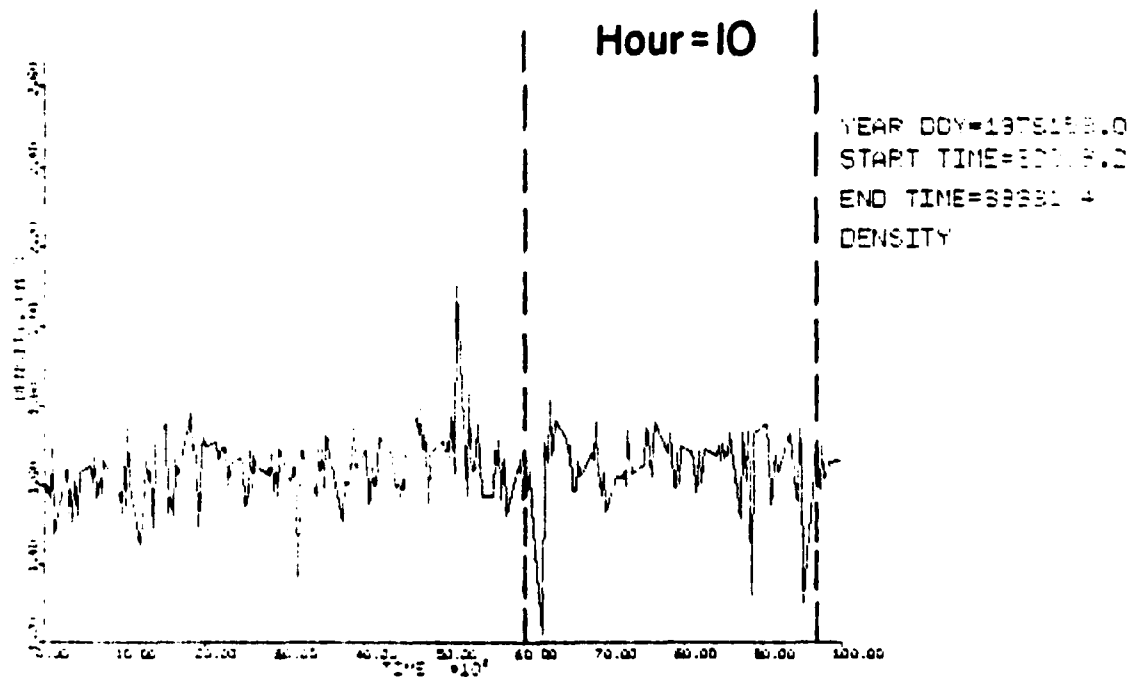
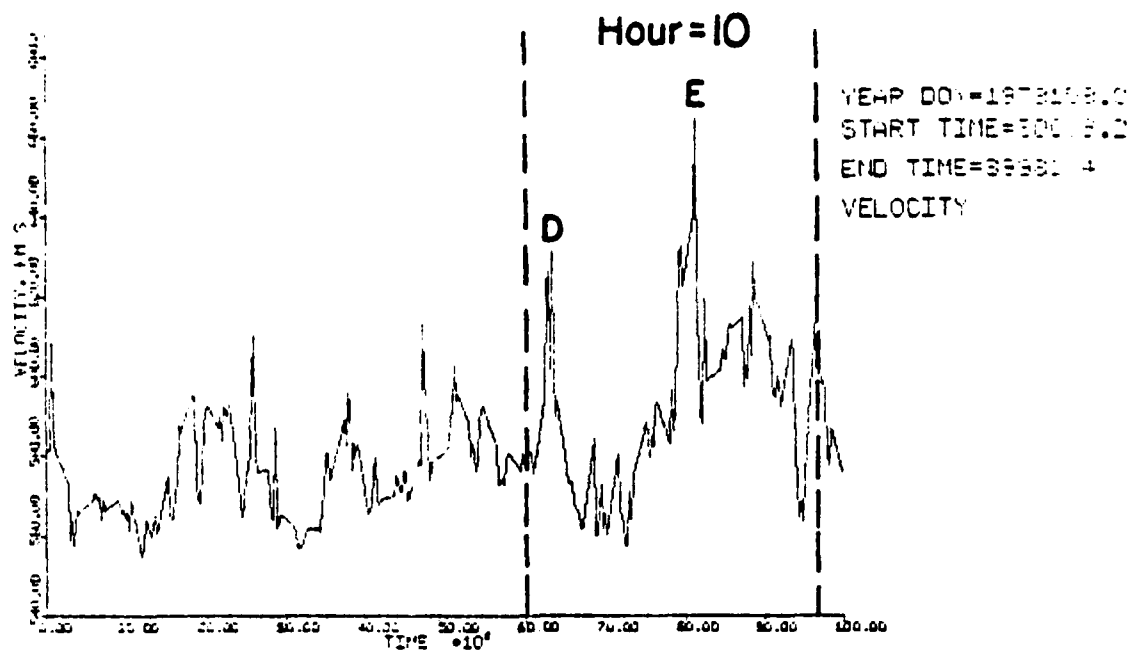


Fig. 7 (b)

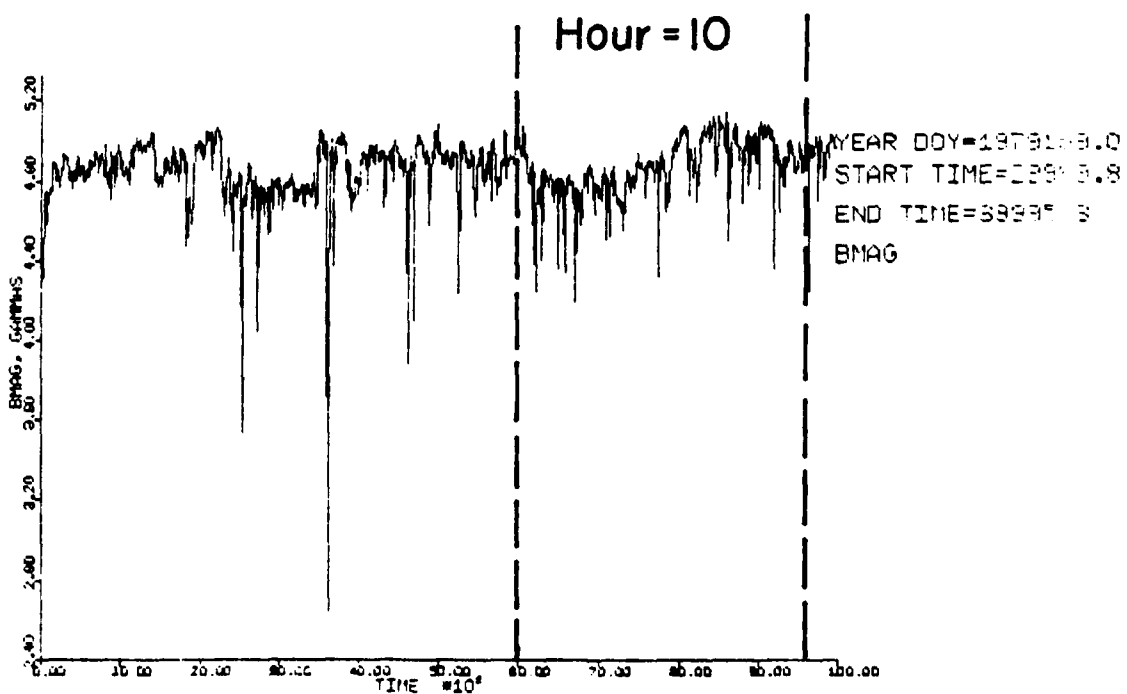
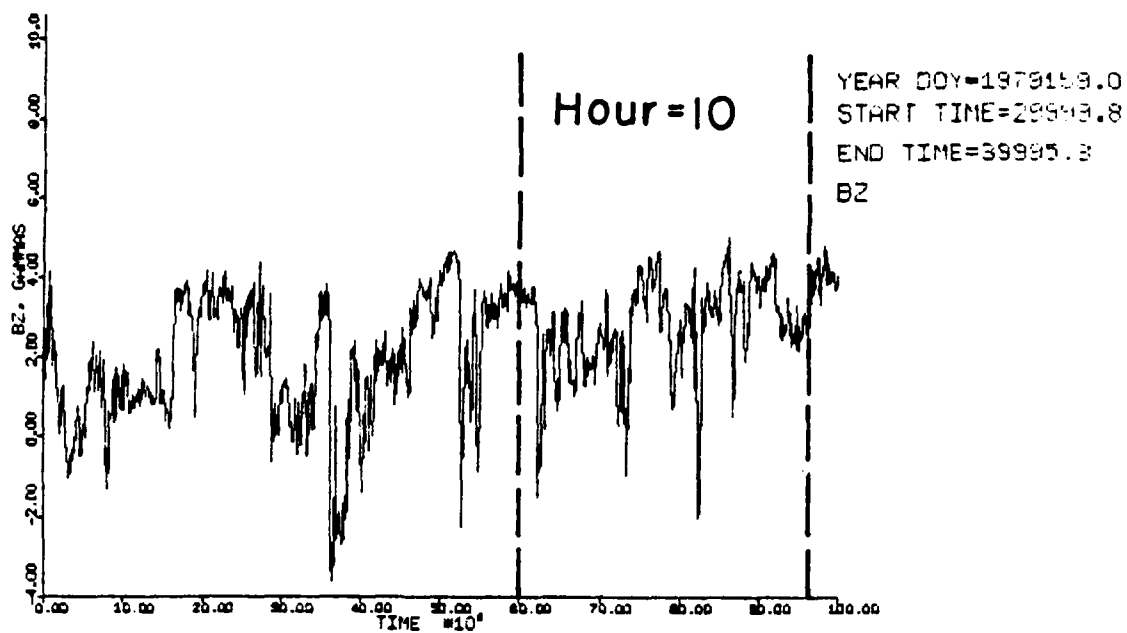


Fig. 7 (c)

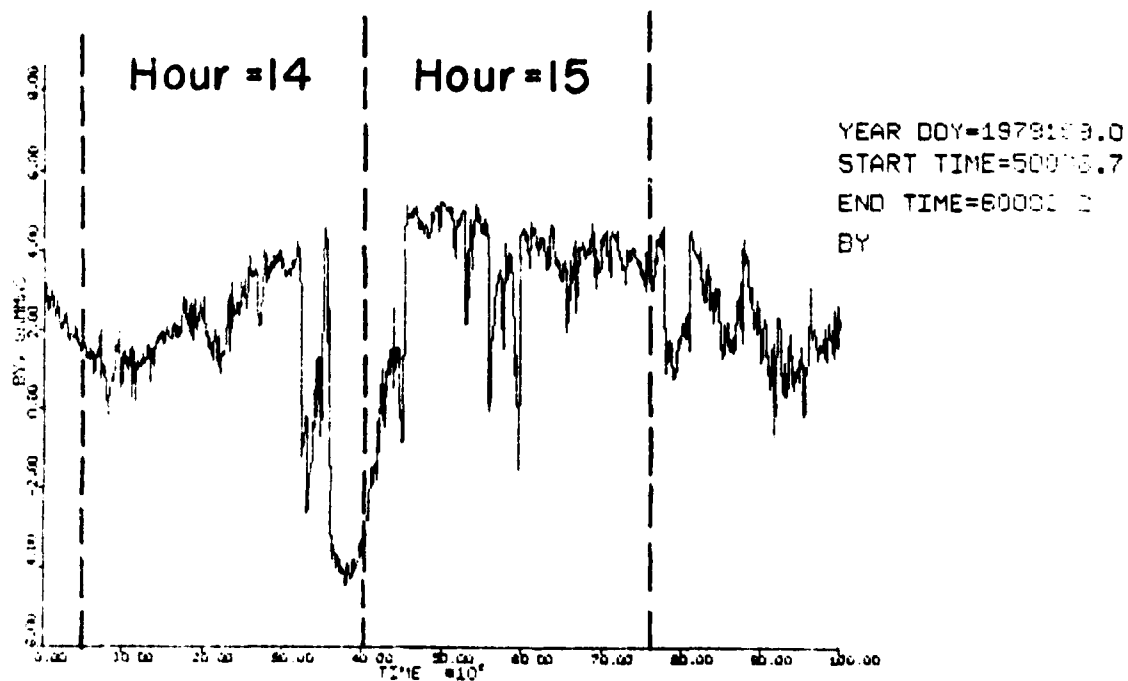
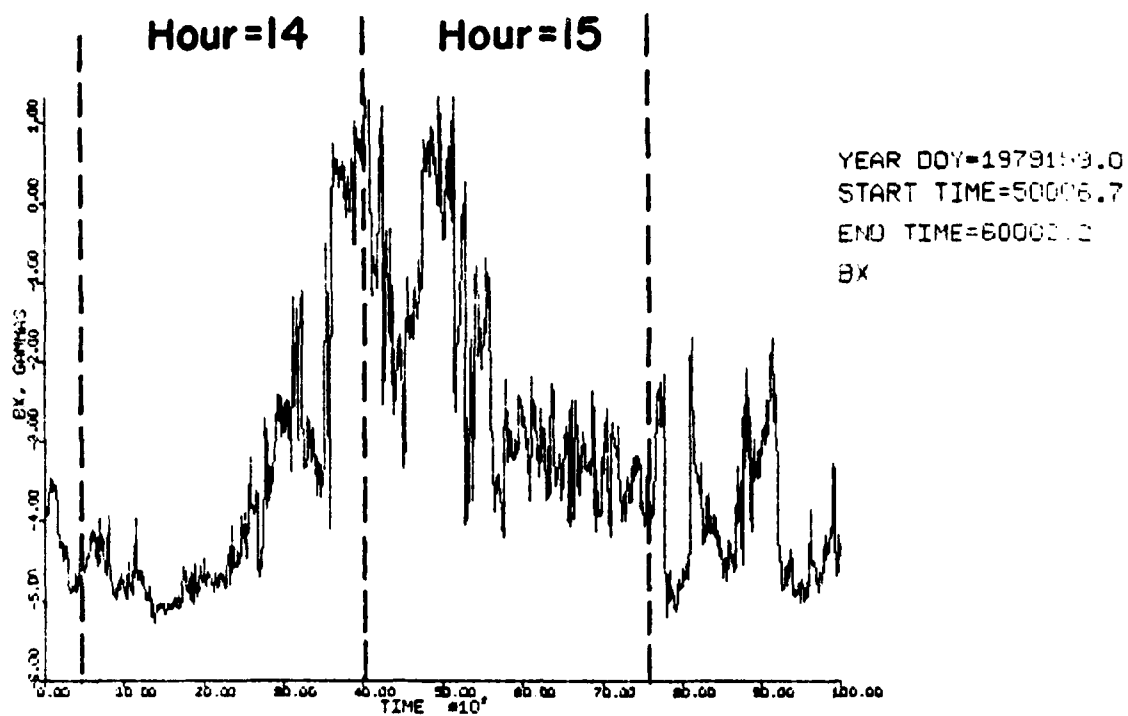


Fig. 8 (a)

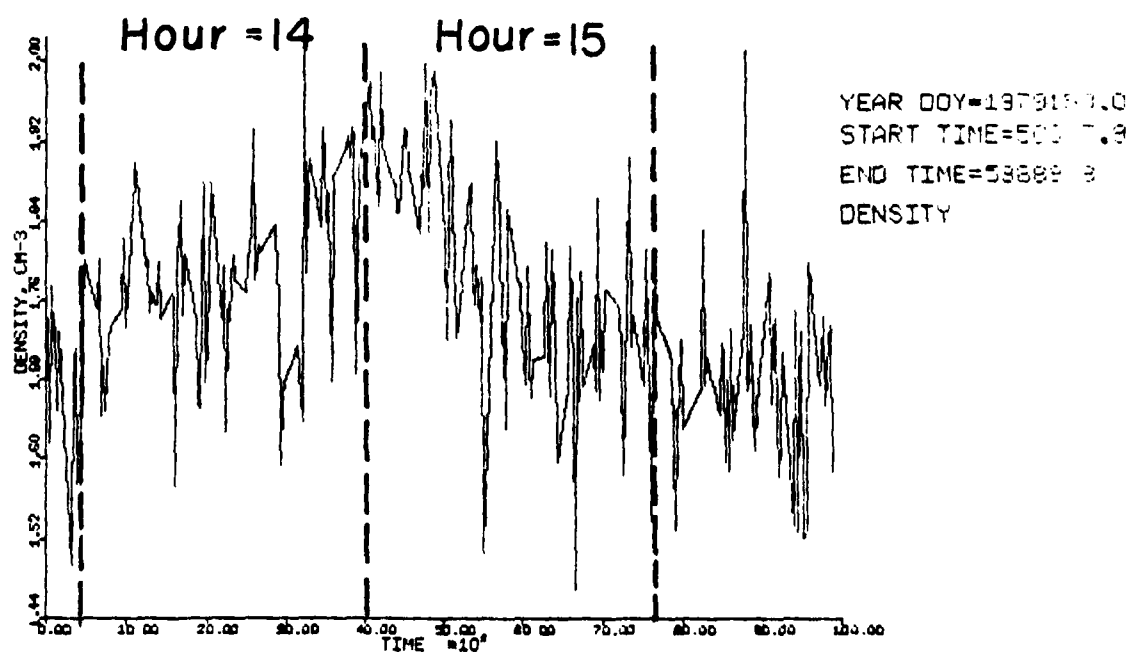
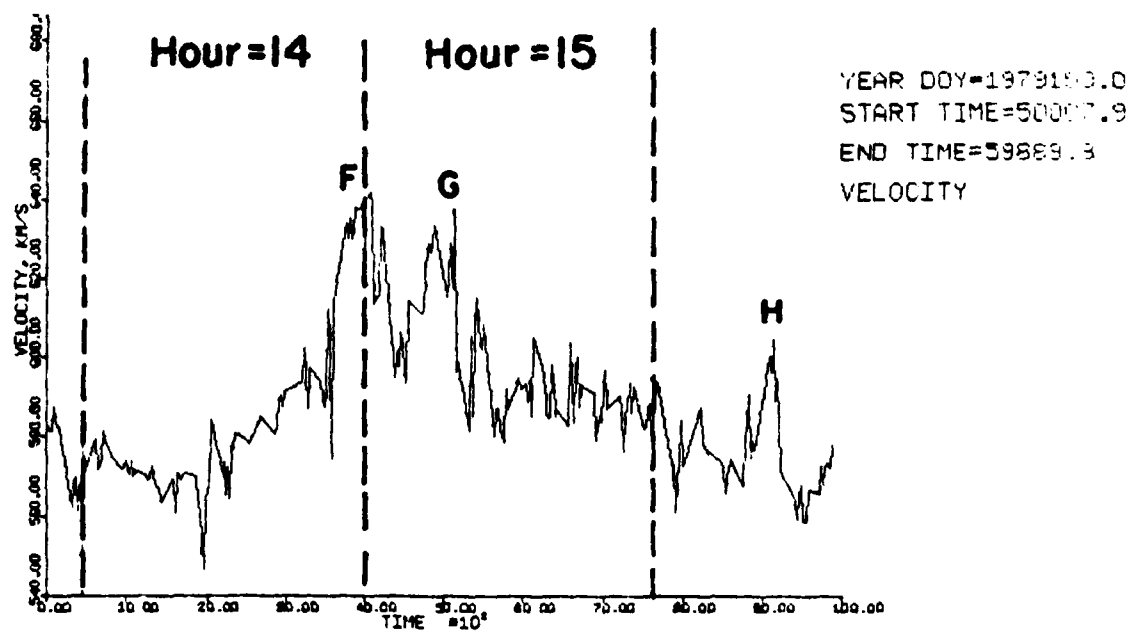


Fig. 8 (b)

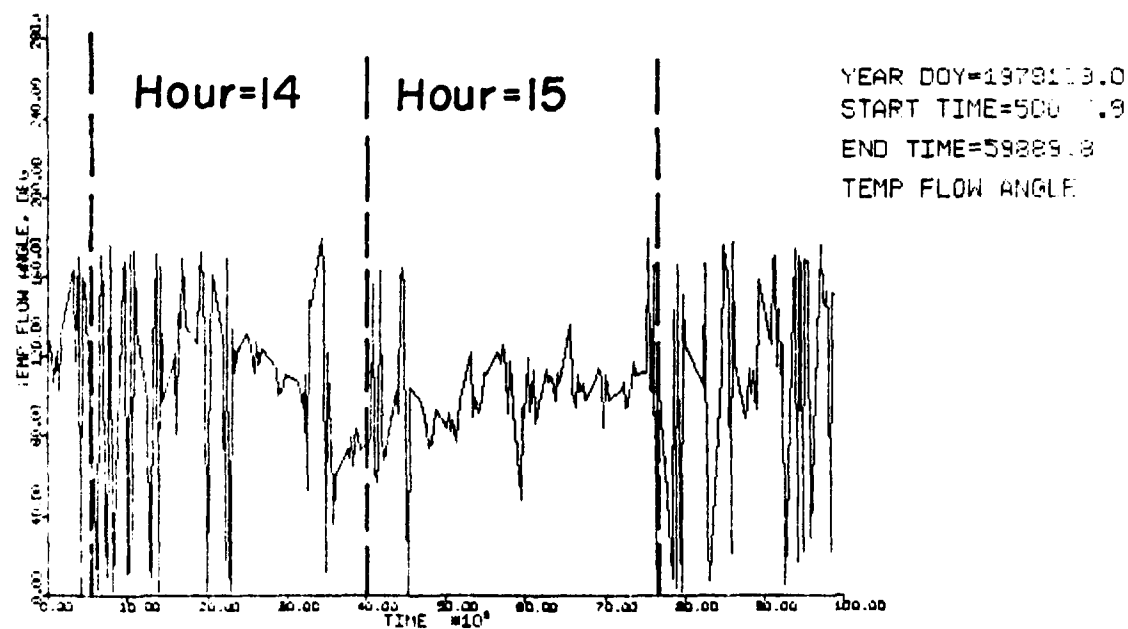
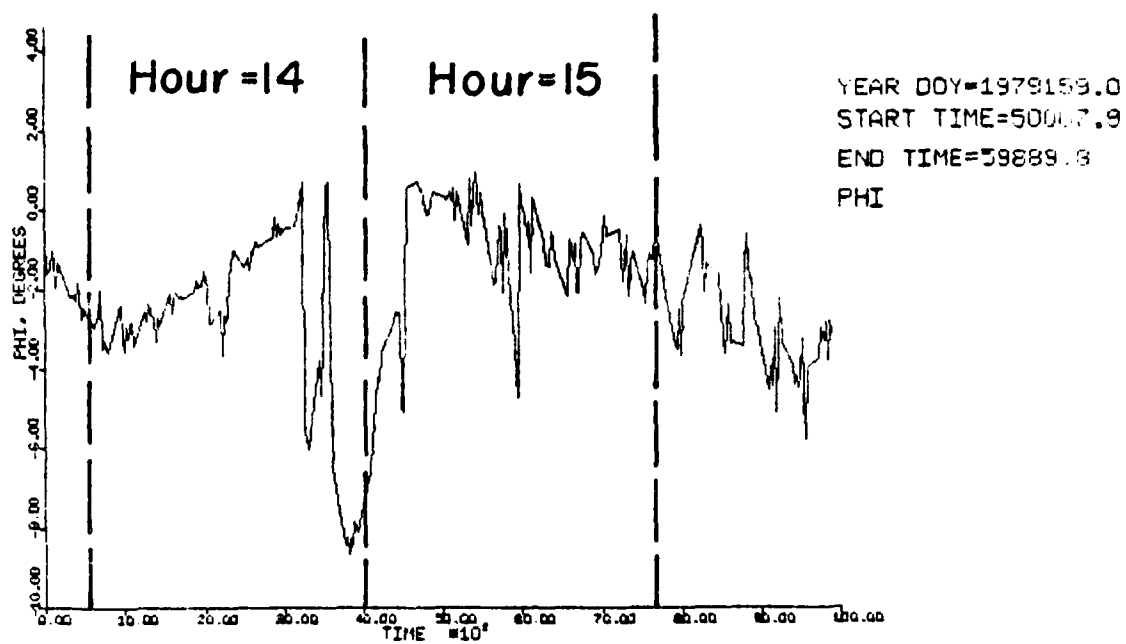


Fig. 8 9c)

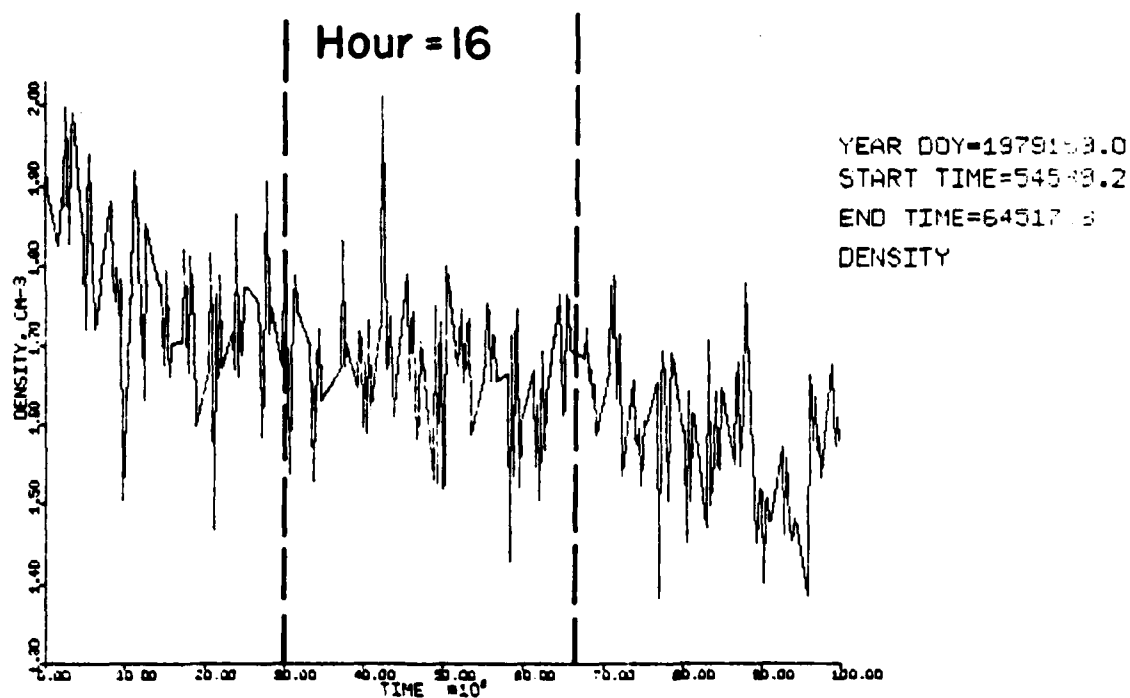
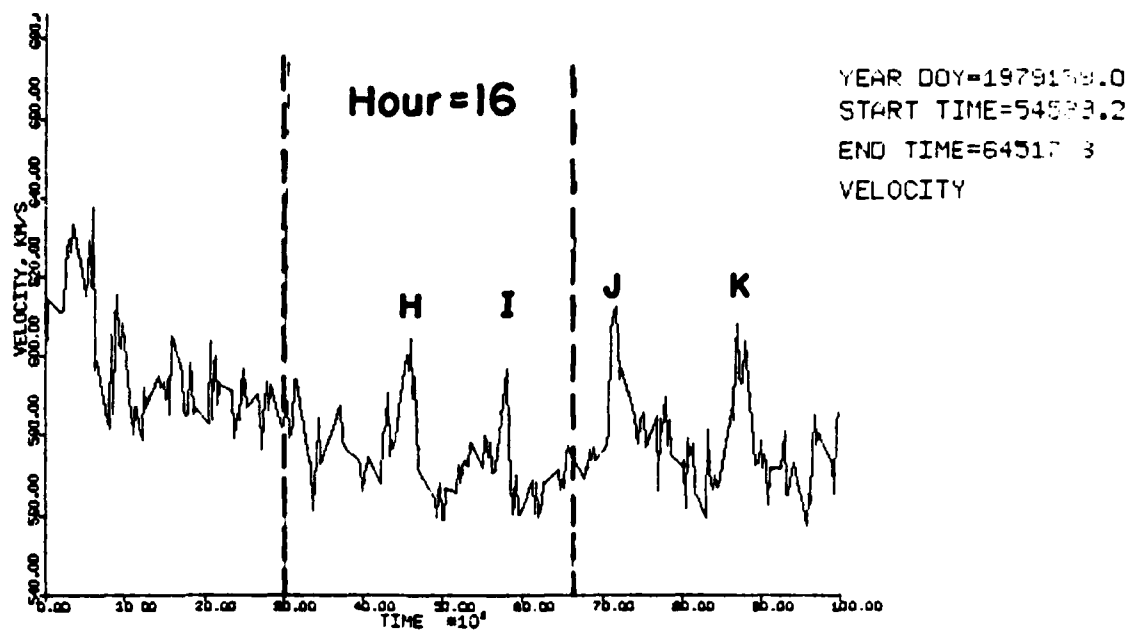


Fig. 9 (a)

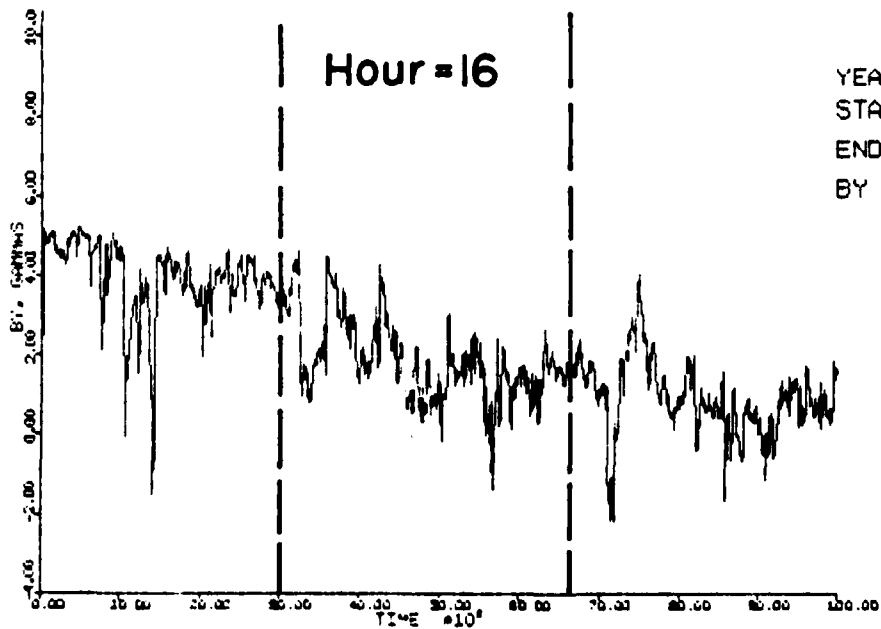
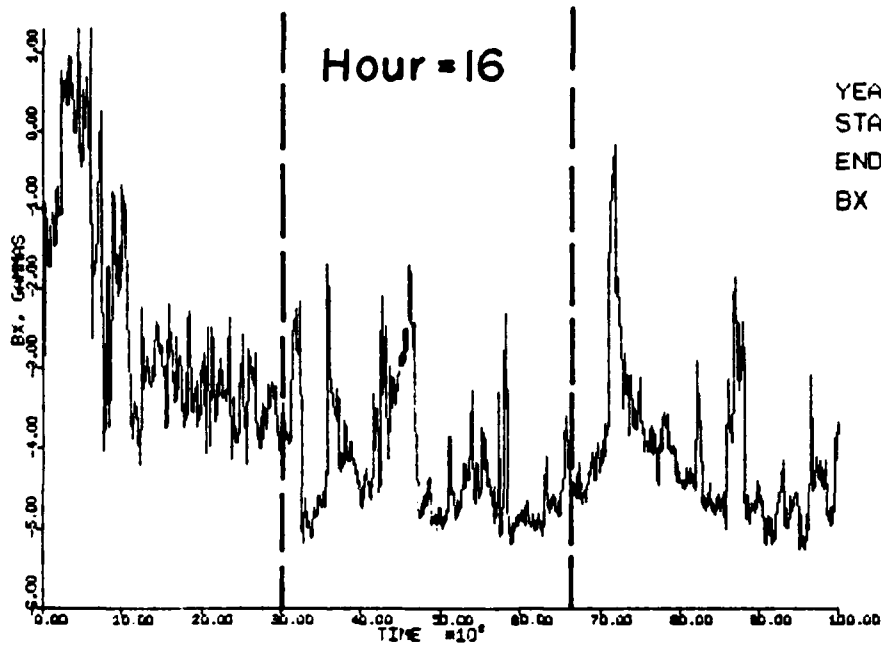


Fig. 9 (b)

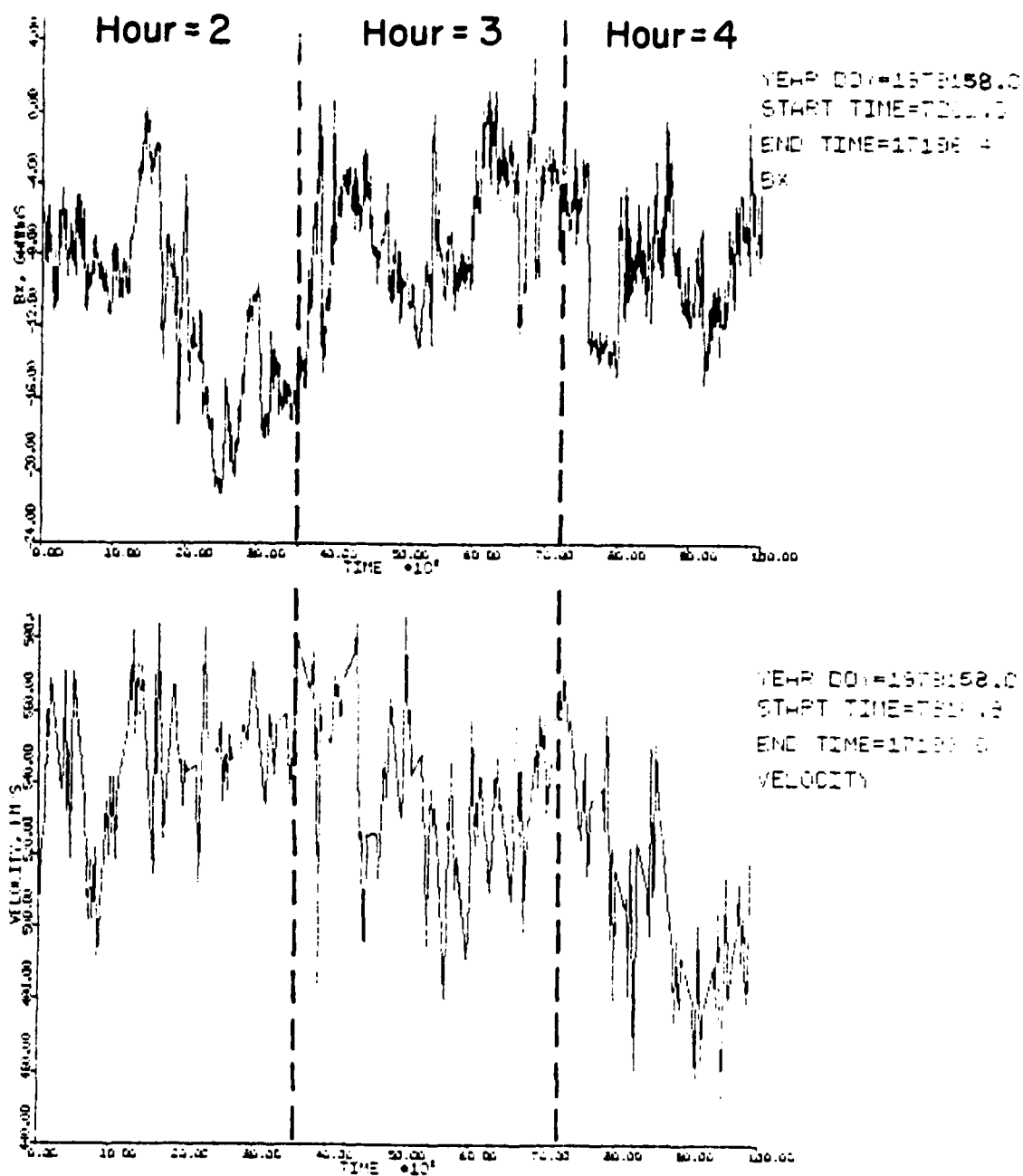


Fig. 10

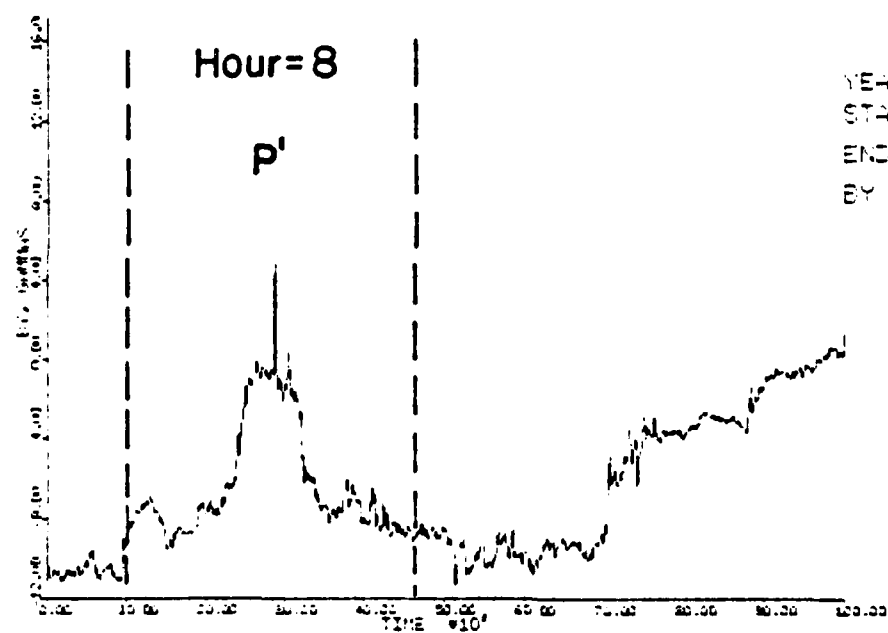
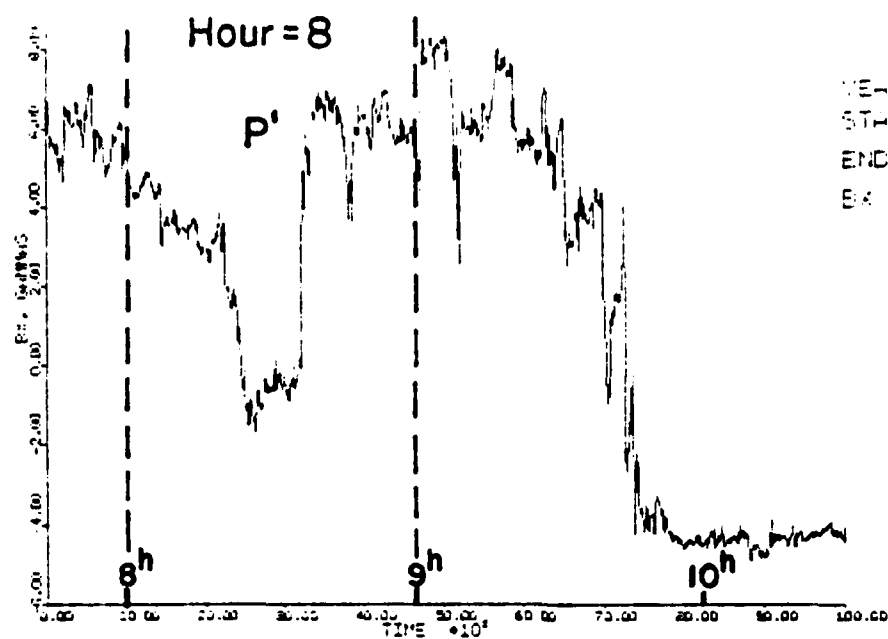


Fig. 11 (a)

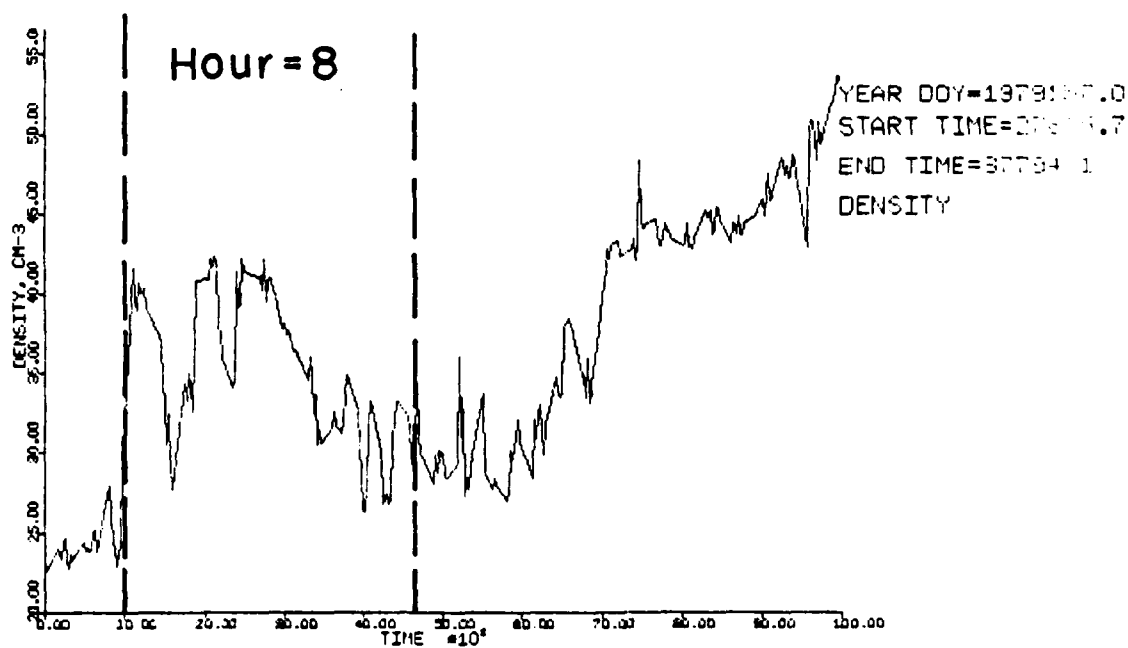
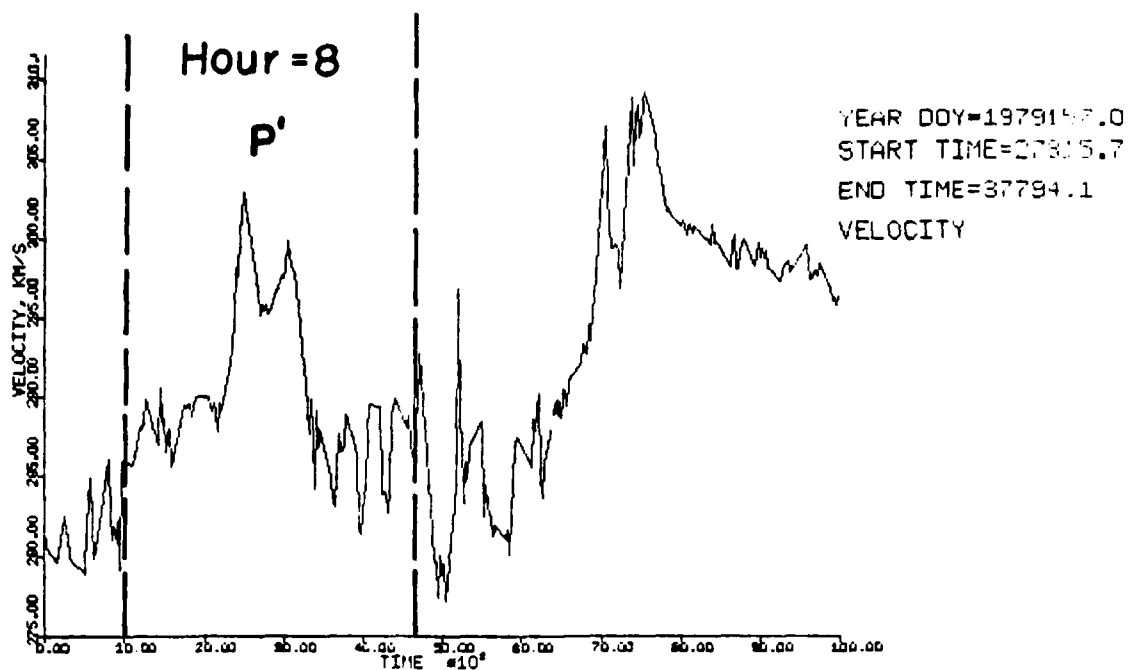


Fig. 11 (b)

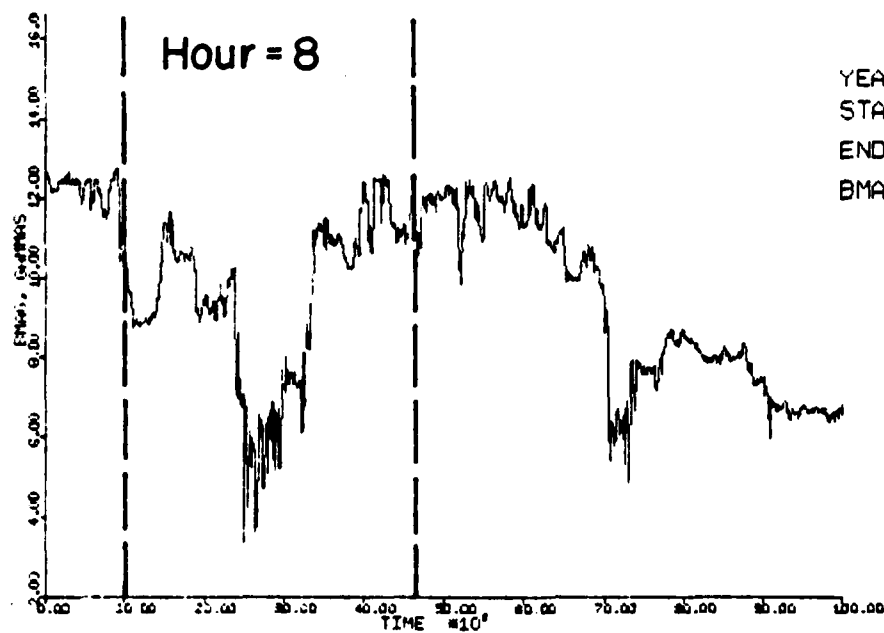
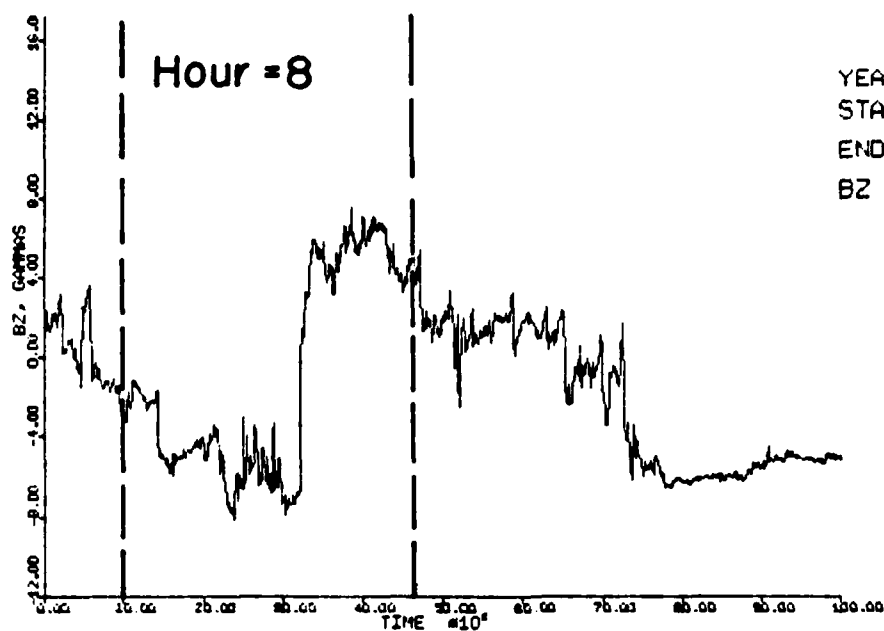


Fig. 11 (c)

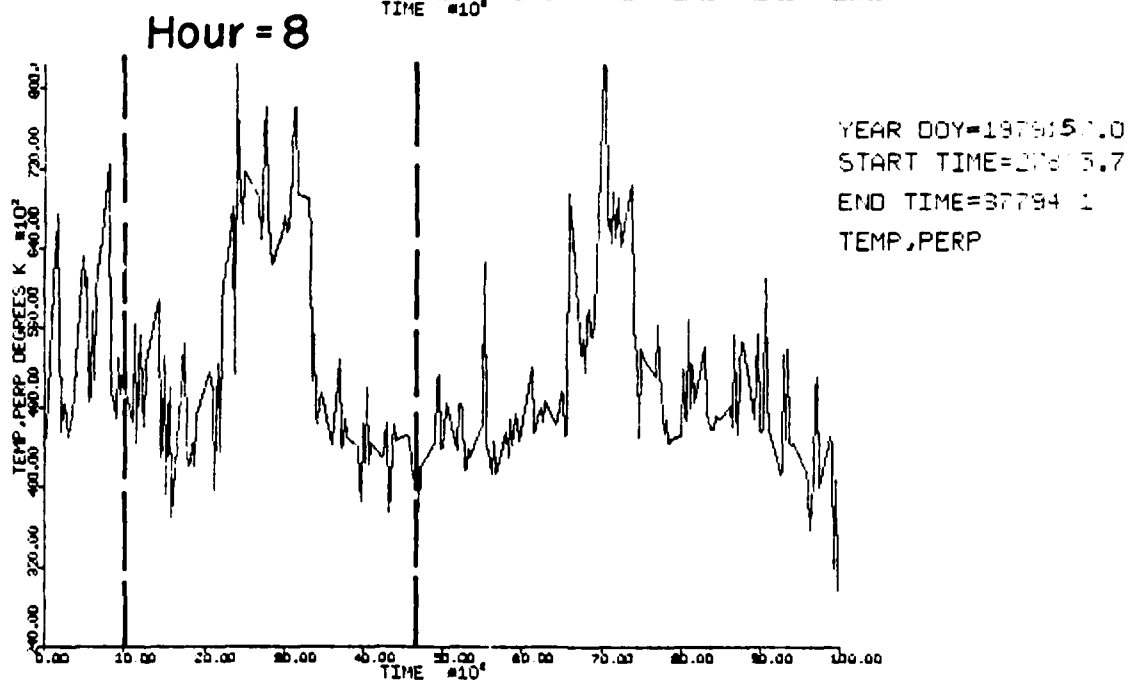
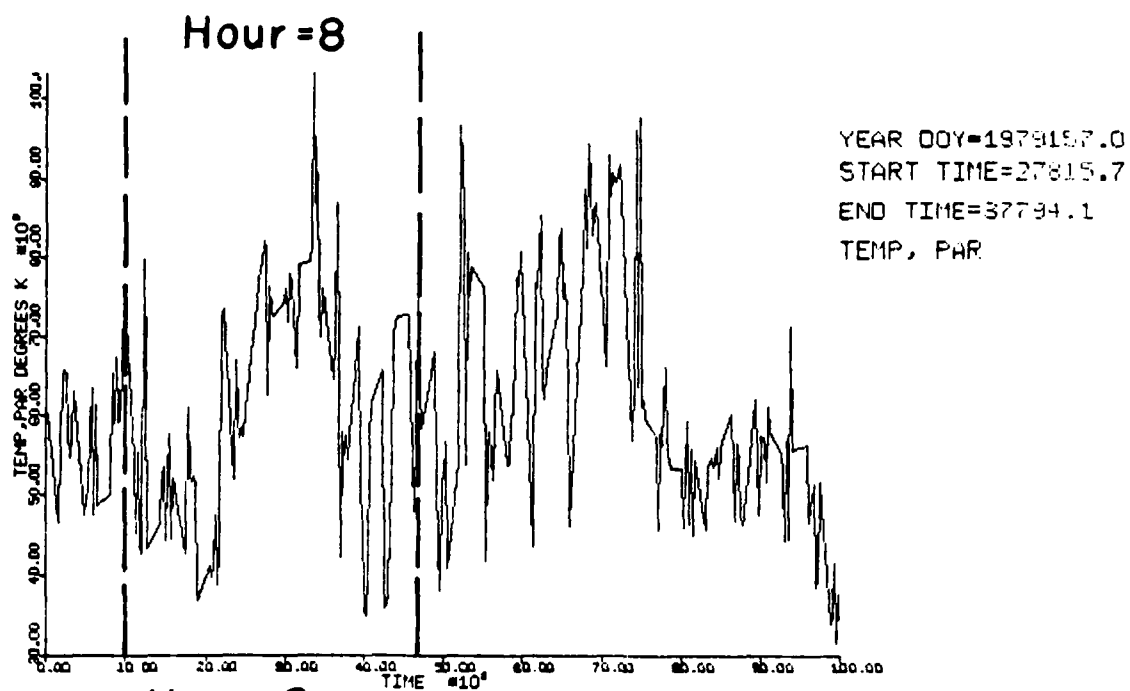


Fig. 11 (d)

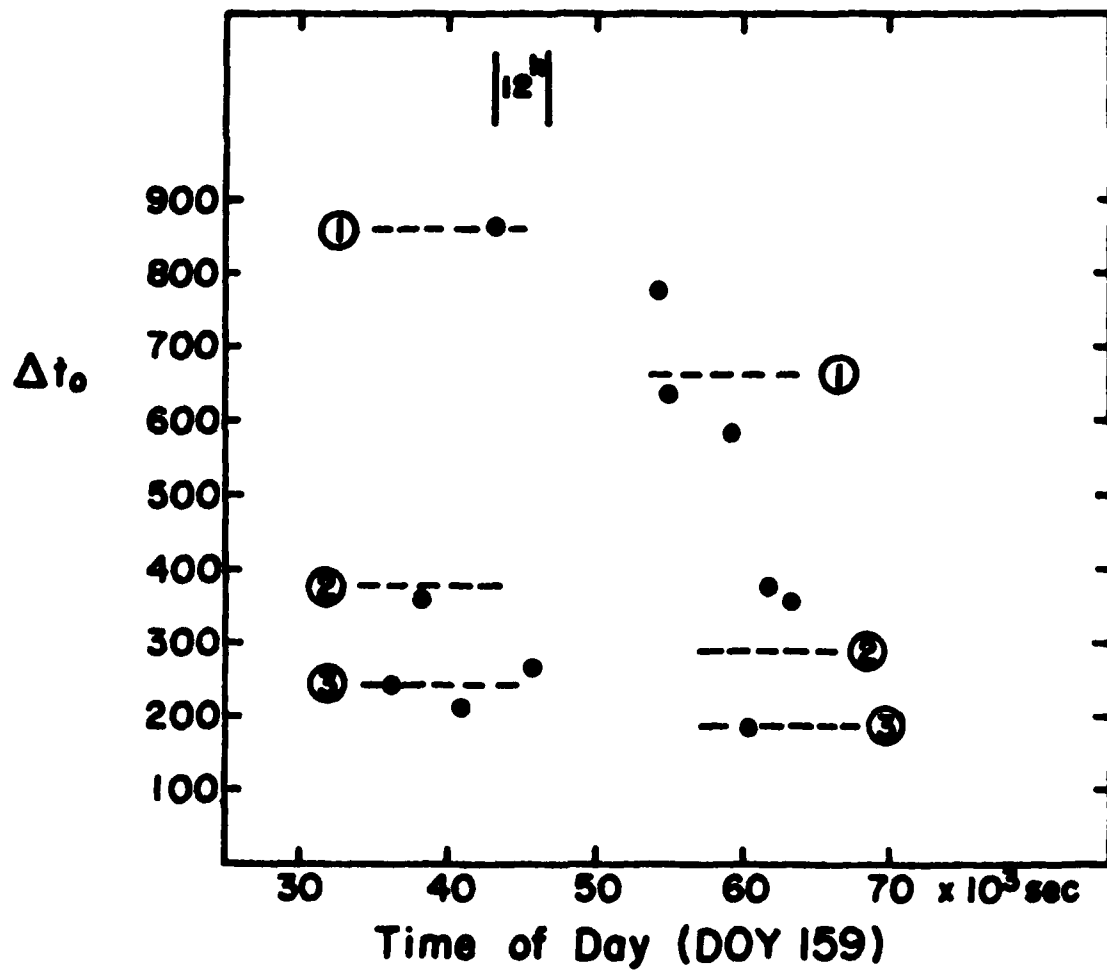


Fig. 12

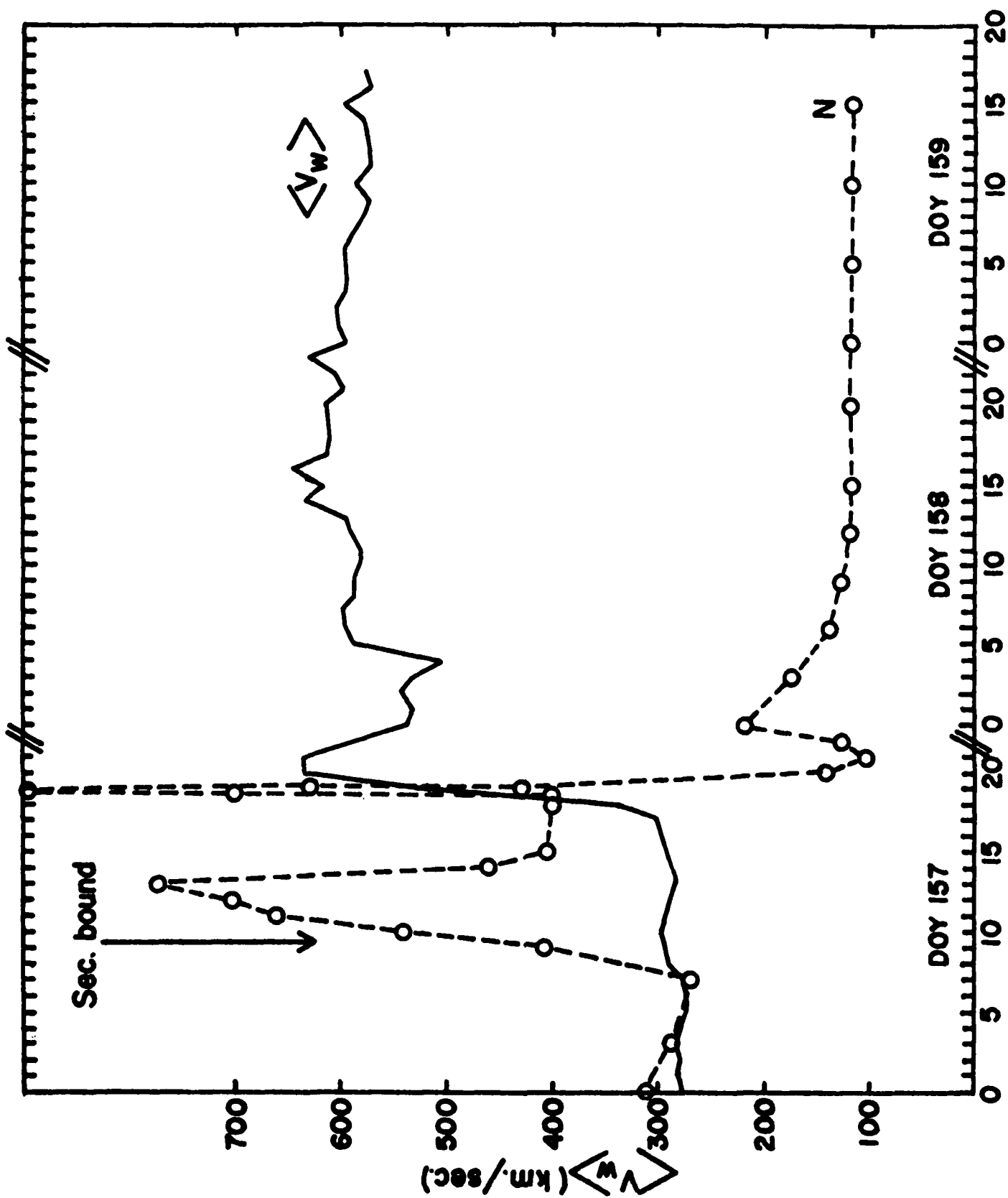


Fig. 13

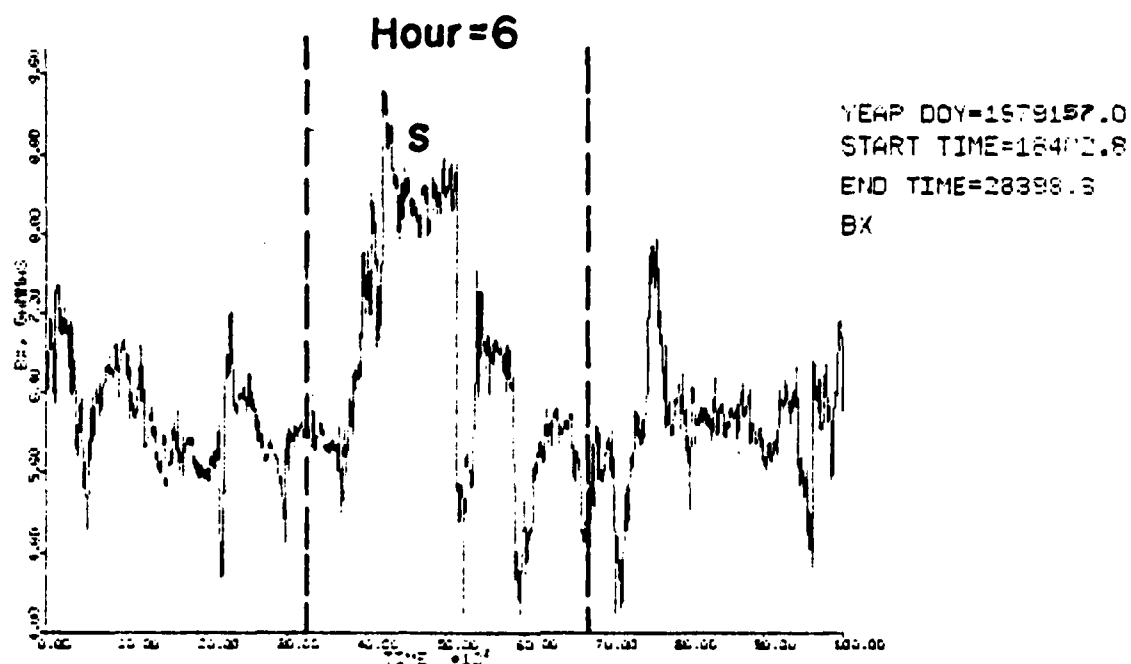


Fig. 14 (a)

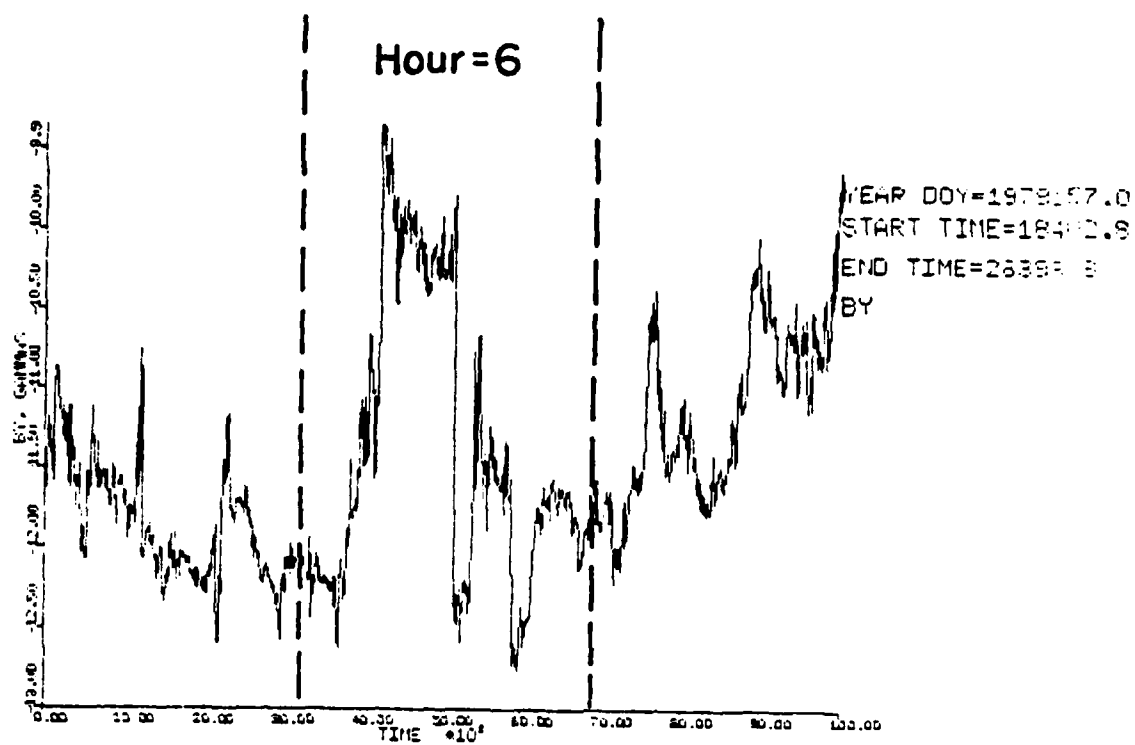


Fig. 14 (b)

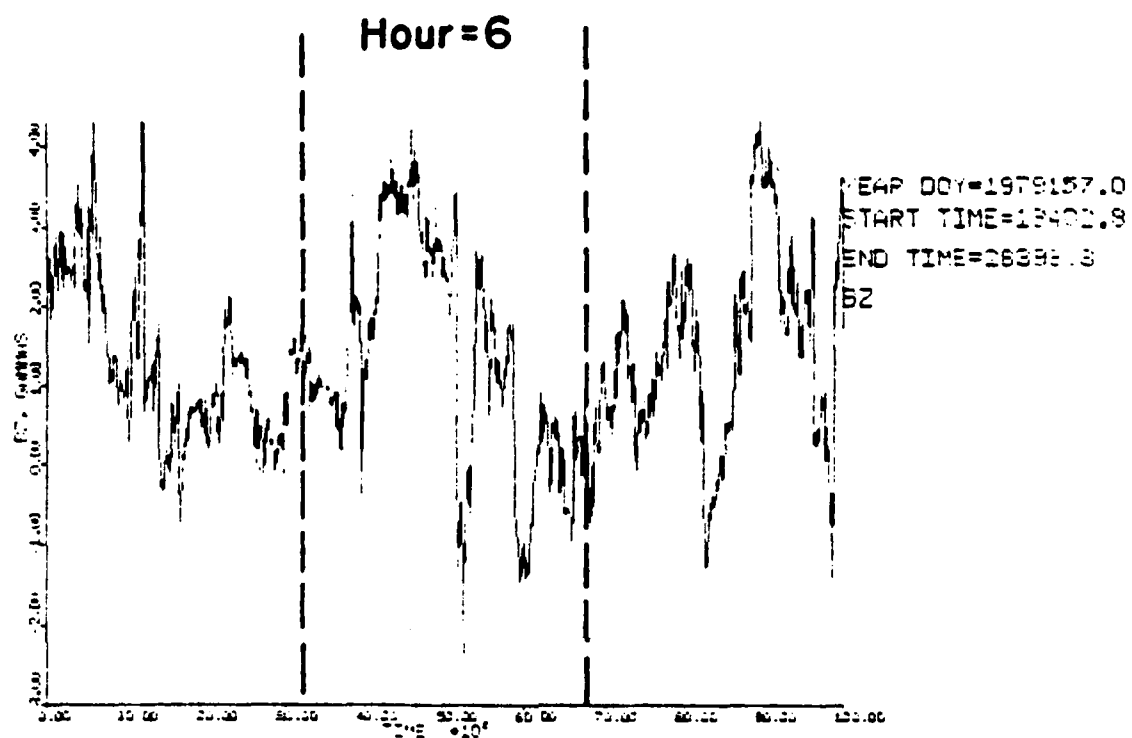


Fig. 14 (c)

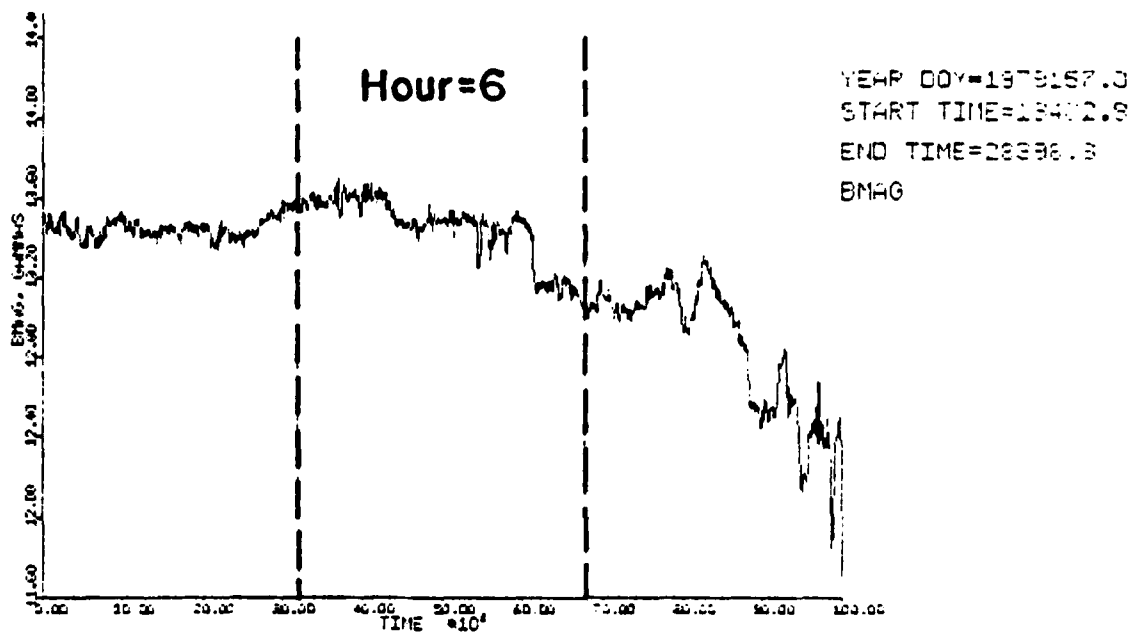


Fig. 14 (d)

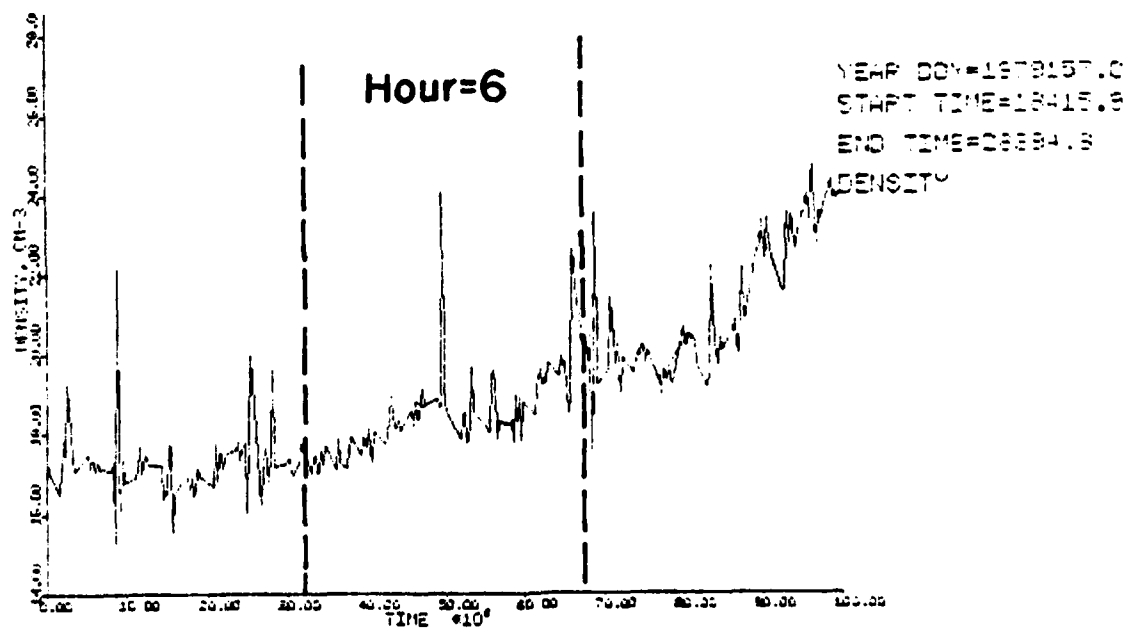
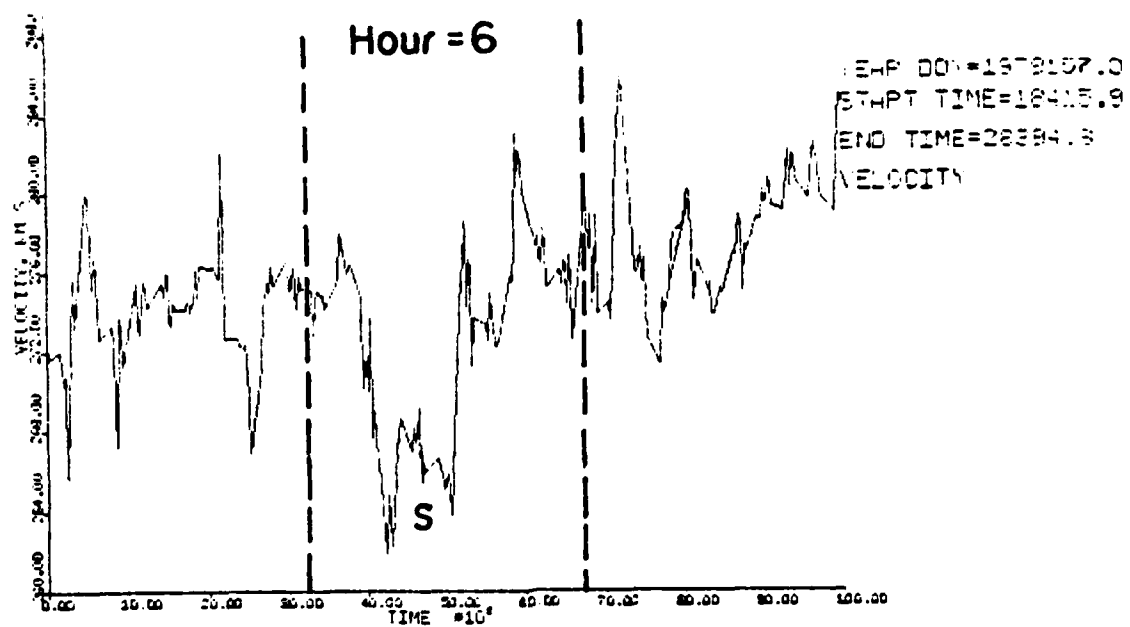


Fig. 14 (e)

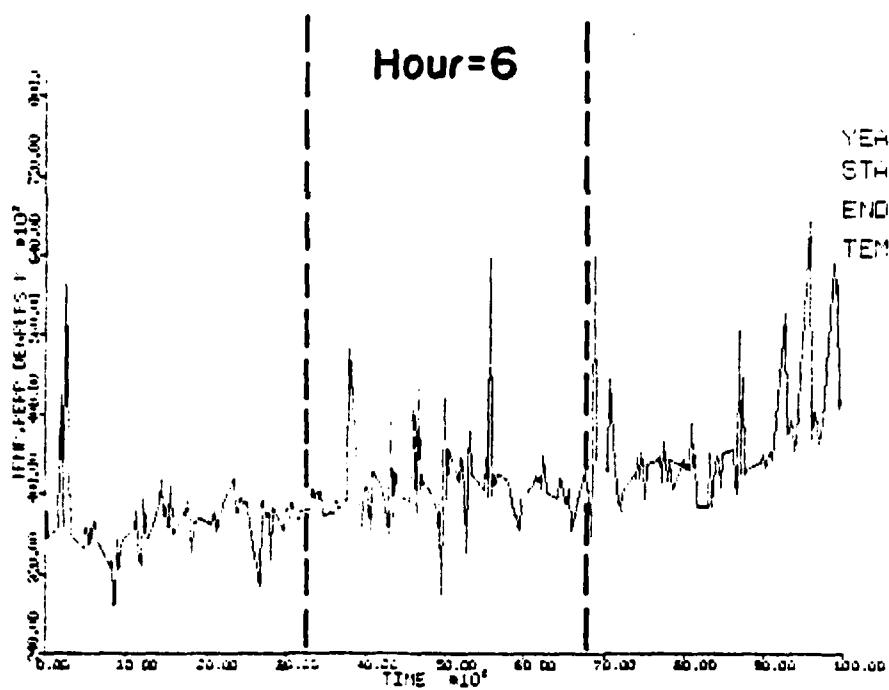
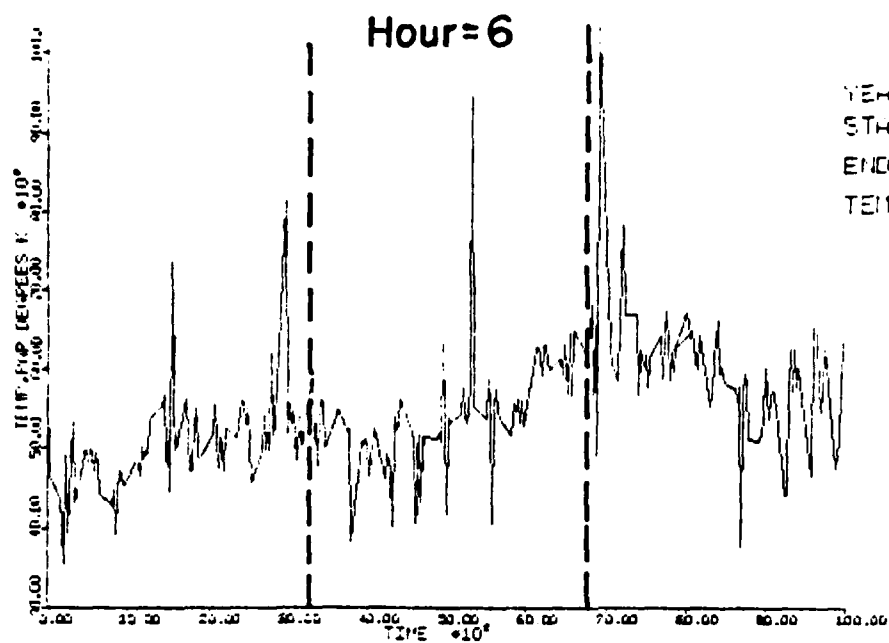


Fig. 14 (f)

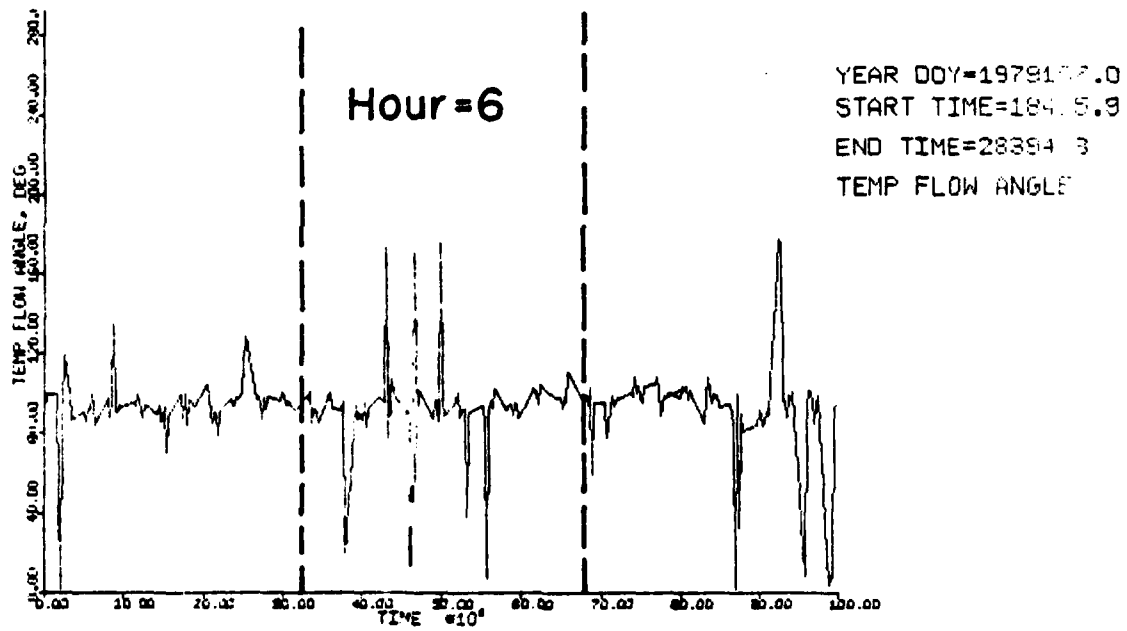
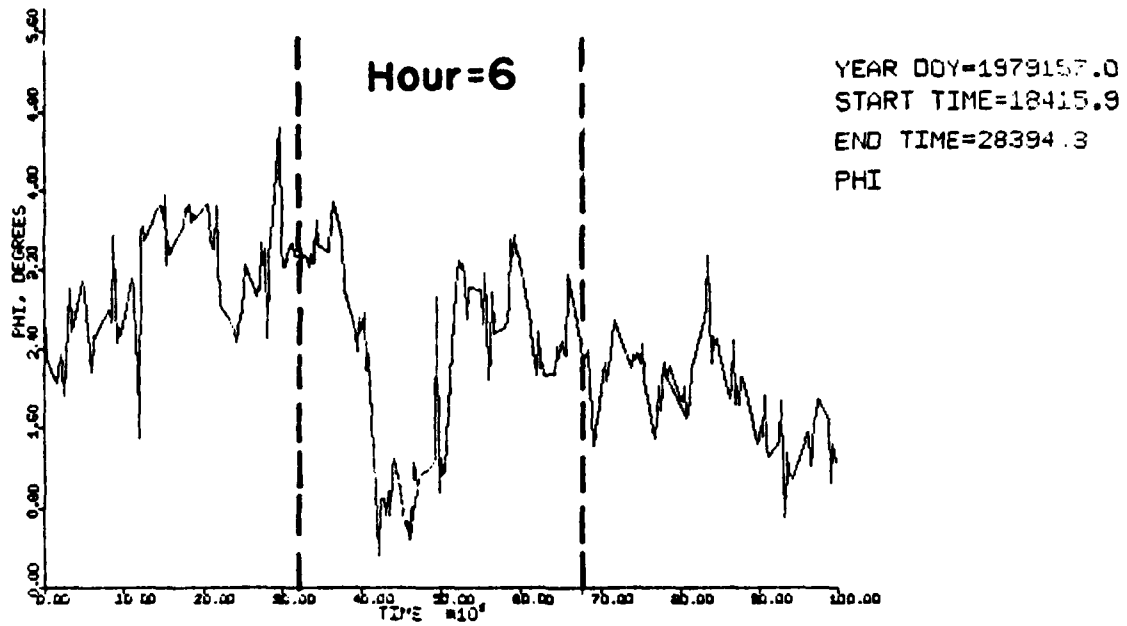


Fig. 14 (g)

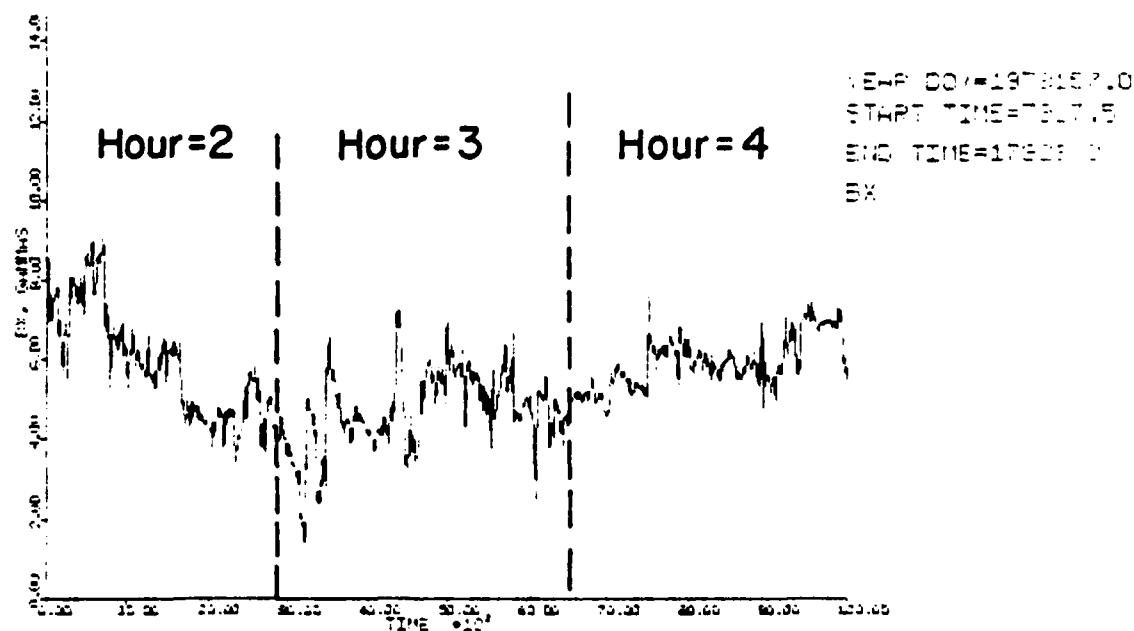
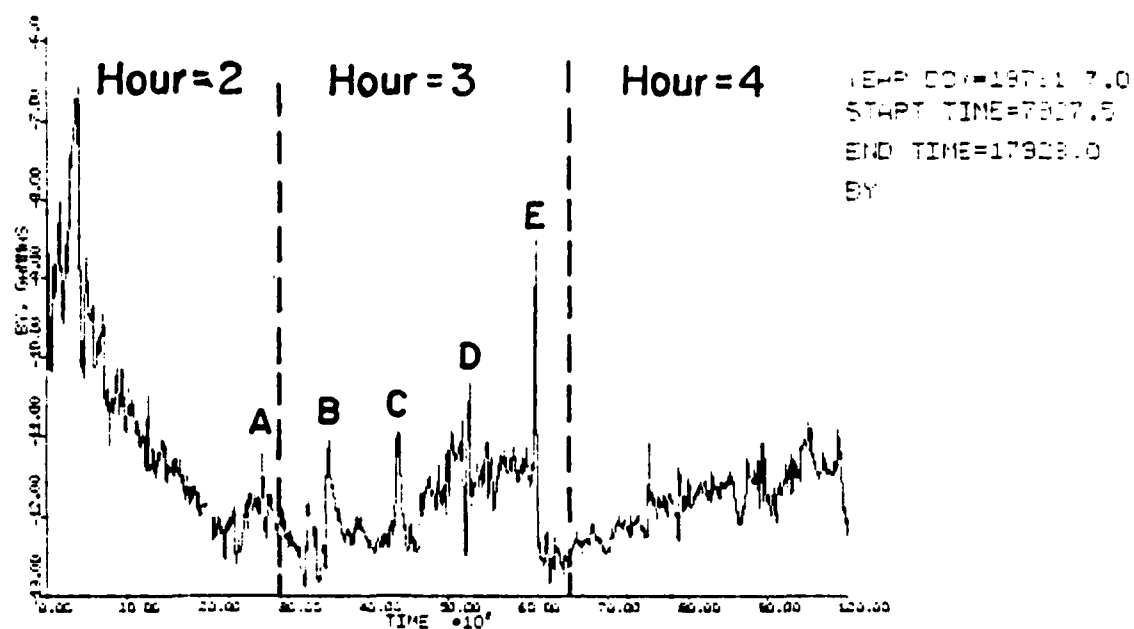


Fig. 15 (a)

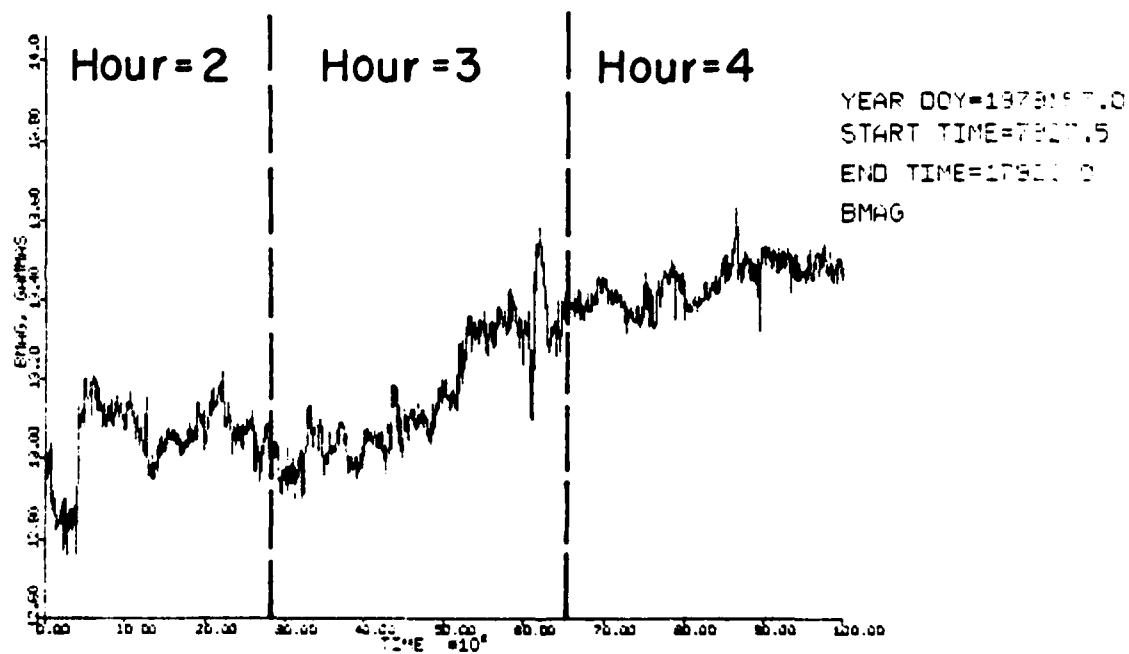
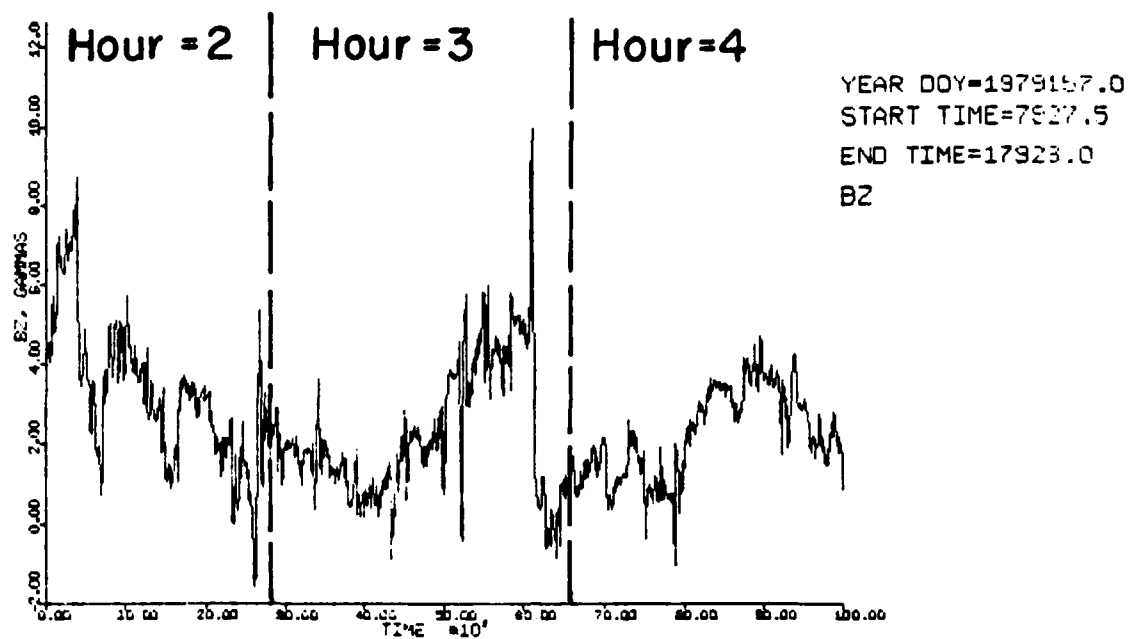


Fig. 15 (b)

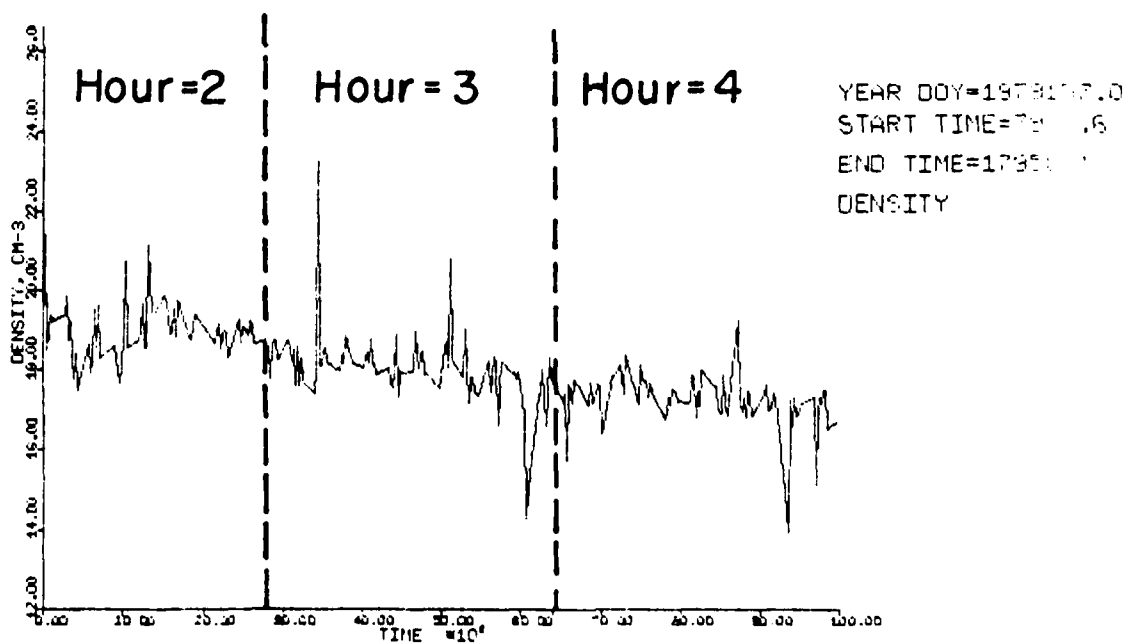
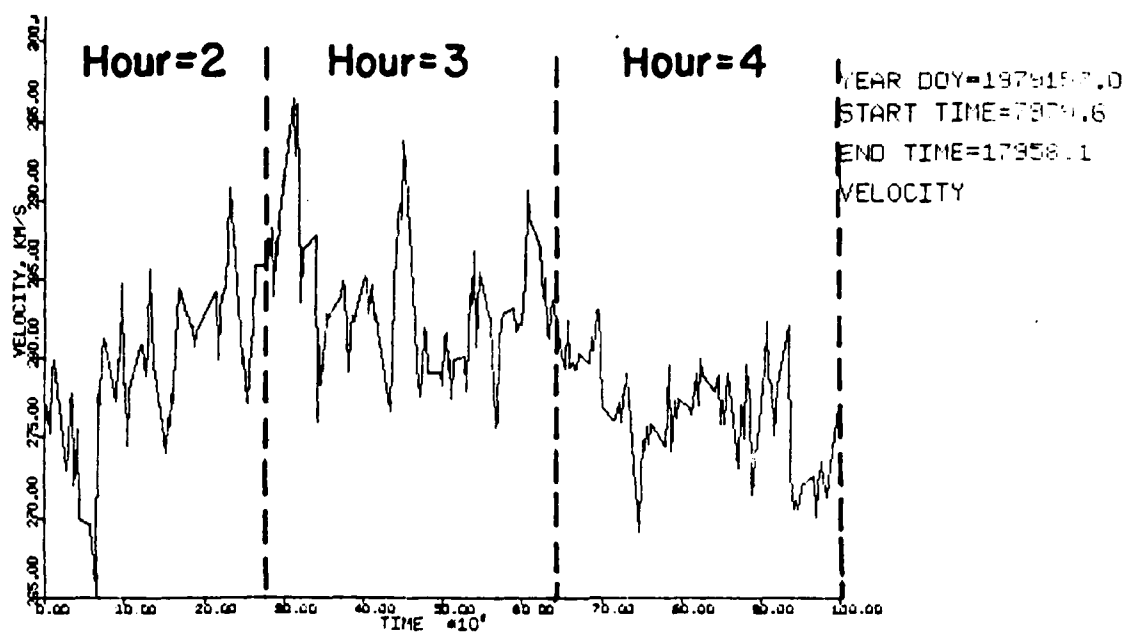
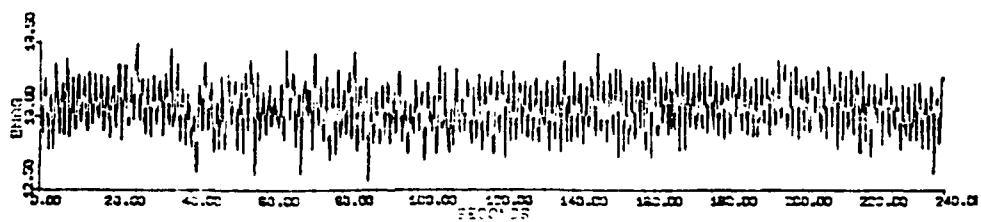
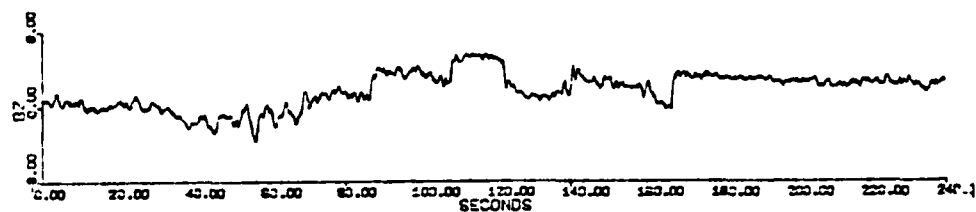
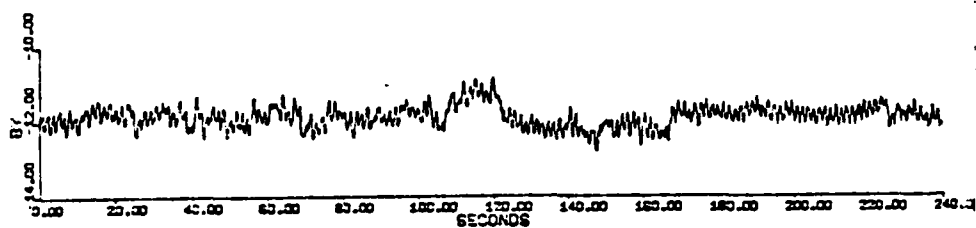
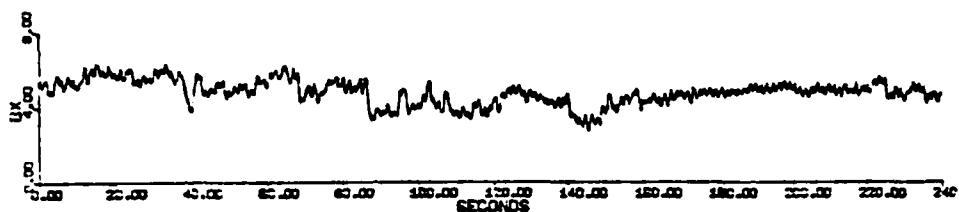


Fig. 15 (c)

FIG. 10 (a)

T0=10502.



TC-11310.0

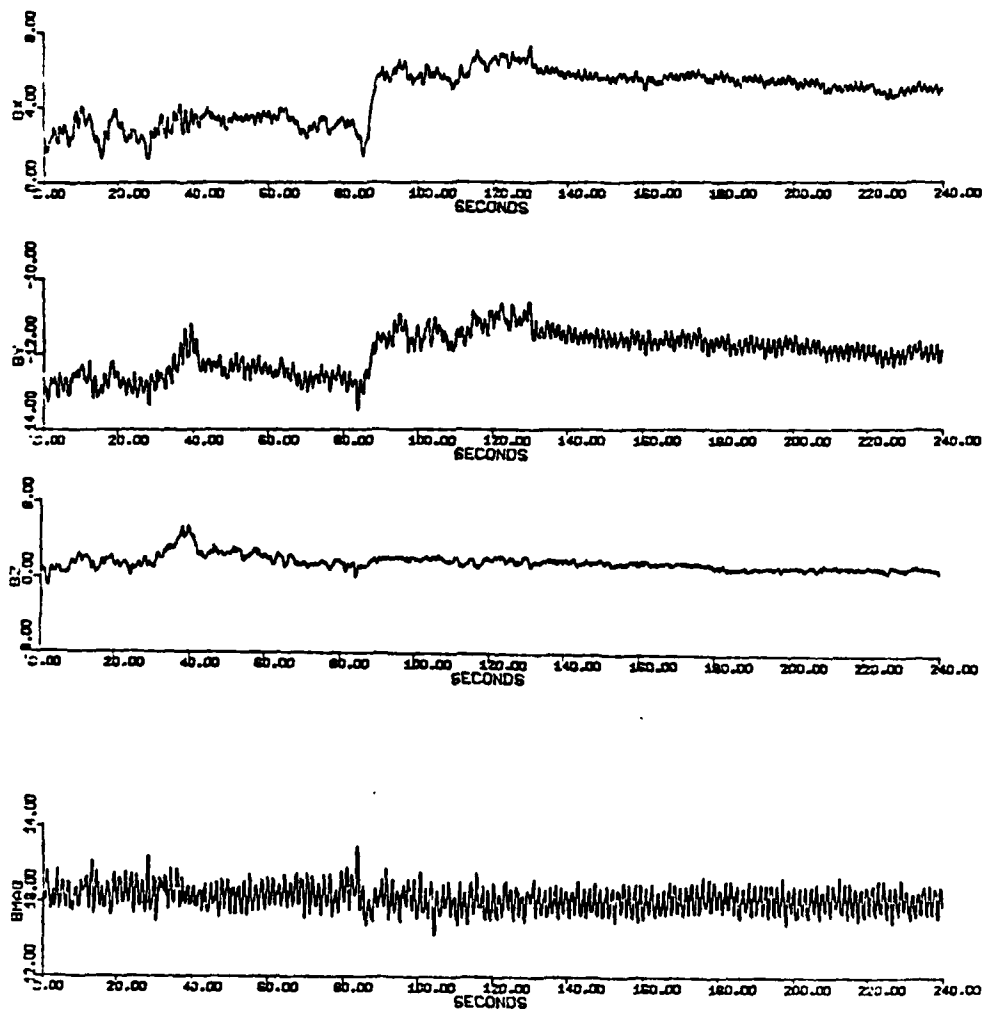
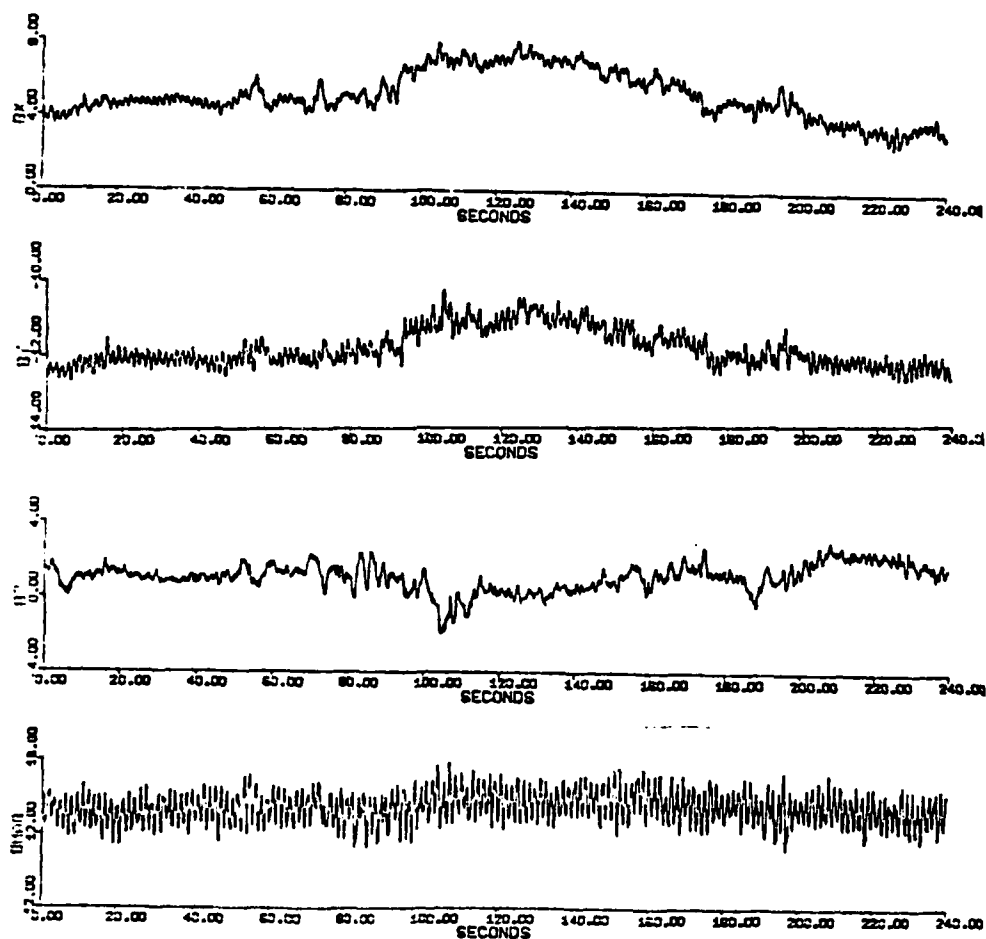


Fig. 16 (b)

Fig. 16 (c)

T0=12181.



T0=13077.2

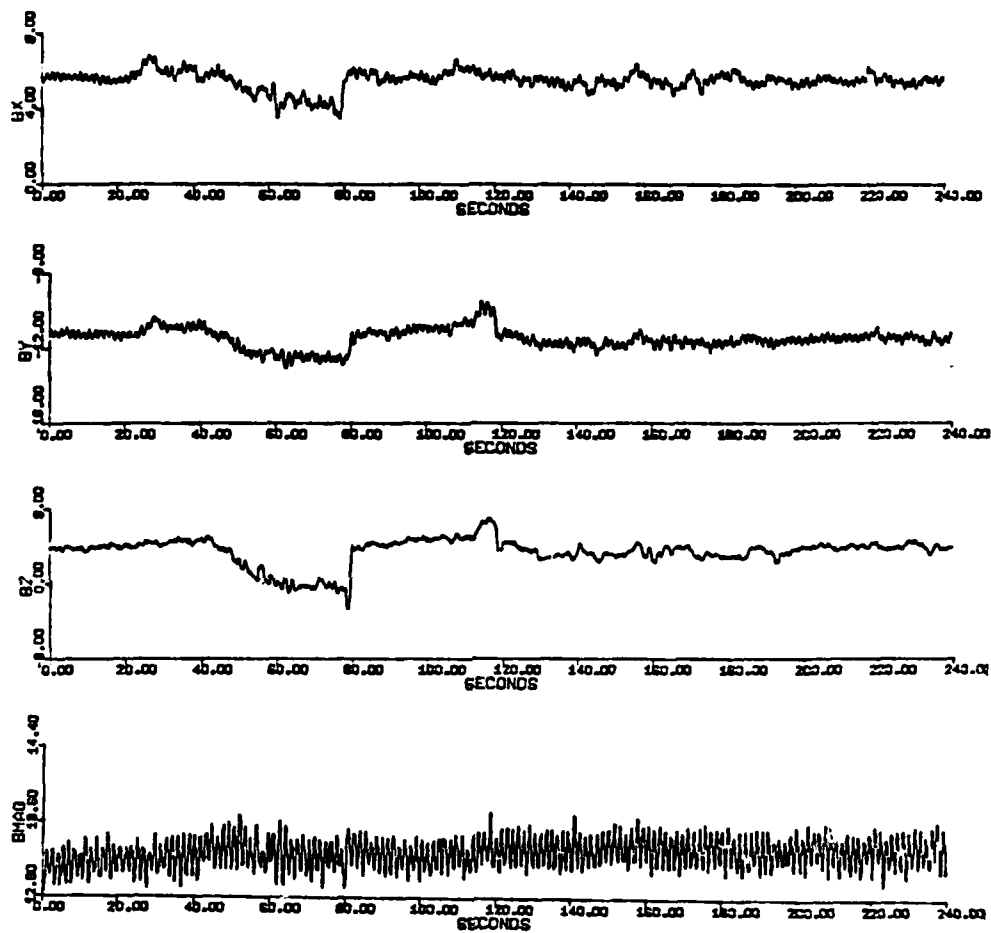


Fig. 16 (d)

T0=13900.9

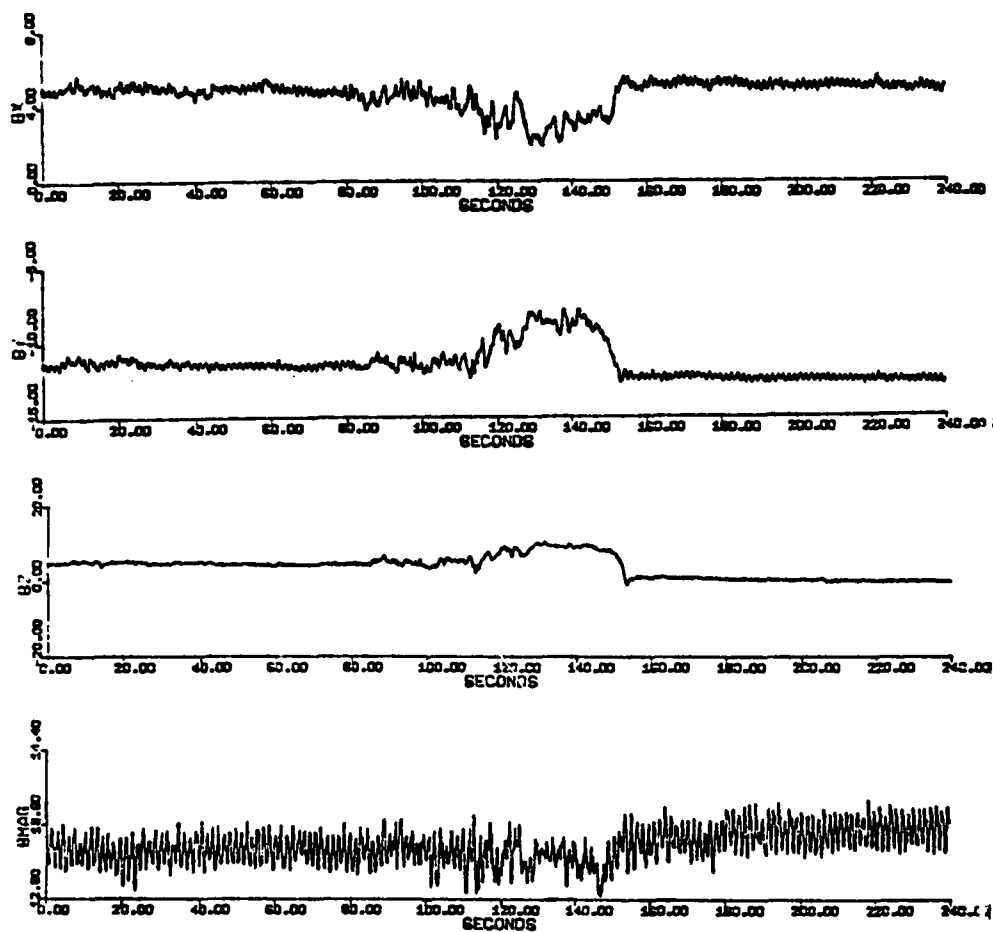


Fig. 16 (e)

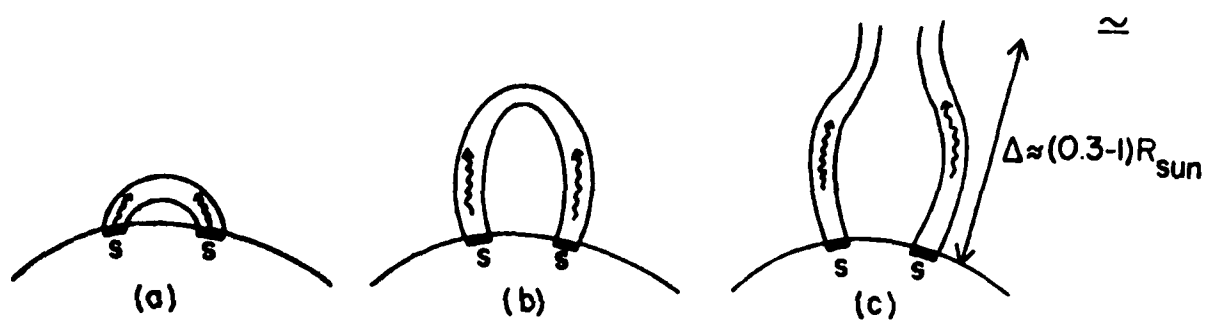


Fig. 17

END

FILMED

6-83

DTIC